Estimation of effective soil hydraulic parameters for water management studies in semi-arid zones

Integral use of modelling, remote sensing and parameter estimation

Promotor: Prof. dr. ir. R.A. Feddes
Hoogleraar in de bodemnatuurkunde, agrohydrologie en het grondwaterbeheer, Wageningen Universiteit

Co-promotor: Prof. dr. W.G.M. Bastiaanssen
Deeltijd Hoogleraar in Toepassingen van Remote Sensing voor het Waterbeheer, ITC-Enschede

Dr. ir. J.C. van Dam
Universitair docent in de Bodemnatuurkunde en agrohydrologie, Wageningen Universiteit

Samenstelling promotiecommissie:
Prof. dr. ir. H. Savenije , Technische Universiteit, Delft
Prof. dr. ir. A. Leijnse, Wageningen Universiteit
Dr. ir. J.A. de Vos, Alterra, Wageningen Universiteit en Researchcentrum
Dr. ir. W. Wolters, Alterra-ILRI, Wageningen Universiteit en Researchcentrum

Estimation of effective soil hydraulic parameters for water management studies in semi-arid zones

Integral use of modelling, remote sensing and parameter estimation

Raj Kumar Jhorar

Proefschrift
ter verkrijging van de graad van doctor
op gezag van de rector magnificus
van Wageningen Universiteit
Prof. dr. ir. L. Speelman
in het openbaar te verdedigen
op dinsdag 25 juni 2002
Des namiddags te 1600 uur in de Aula, Wageningen

The research reported in this thesis was supported by the Wageningen University (WU) through a 'sandwich' PhD fellowship. The costs involved in the analysis of remote sensing data and the extended period of fellowship was met from the WATPRO project of the Department of Water Resources, WU. Their financial support is gratefully acknowledged.

ISBN 90-5808-644-5

Raj Kumar Jhorar
Department of Soil and Water Engineering,
Chaudhary Charan Singh Haryana Agricultural University
Hisar- 125 004, India
Email: jhorar@yahoo.com

Estimation of effective soil hydraulic parameters for water management studies in semi-arid zones: integral use of modelling, remote sensing and parameter estimation/Jhorar, R.K. Doctoral Thesis, Wageningen University – with references- with summaries in English and Dutch.

This work is dedicated to
my father, Sahab Ram Jhorar,
who could not see his dream come true.

Abstract

Jhorar, R.K. 2002. *Estimation of effective soil hydraulic parameters for water management studies in semi-arid zones: integral use of modelling, remote sensing and parameter estimation*. Doctoral thesis, Wageningen University, The Netherlands.

The meaningful application of water management simulation models at regional scale for the analysis of alternate water management scenarios is often hindered by the lack of required input data. Especially information on relevant soil hydraulic parameters is required for the successful application of these models. The focus of this study is the development of a technique to determine effective regional soil hydraulic parameters by making integral use of simulation models, remote sensing information and parameter estimation procedures. The Sirsa Irrigation Circle, covering an area of 0.48 million ha, located in the Bhakra Irrigation system in the North West India is used as a case study.

Forward and backward simulations with the SWAP model for *homogeneous* soil profiles proved that actual evapotranspiration (ET_a) rates can be used to inversely identify effective soil hydraulic parameters. ET_a rates from fully developed crops during water stress periods are most suitable for this purpose. Frequent measurement on ET_a rates is desired not only to precisely estimate the soil hydraulic parameters but also to reduce the undesirable correlation between different fitting parameters.

Forward and backward simulations for seven *heterogeneous* soil profiles showed that for practical applications, effective soil hydraulic parameters can sufficiently describe the hydraulic behaviour for such profiles. However, if actual soil evaporation and transpiration are to be simulated separately and interpreted independently, an empirical formulation of soil evaporation is very important if the surface soil layers have deviating soil hydraulic properties. The effective soil hydraulic parameters for heterogeneous soils can be determined using information on ET_a rates provided general information on soil texture is known.

Twenty three NOAA AVHRR satellite images were used to produce ET_a maps of the Sirsa Irrigation Circle. The ET_a rates were then used to inversely identify the soil hydraulic parameters for the distributed irrigation water management model FRAME. The inversely identified soil hydraulic parameters were in good agreement with the expected values but could not be validated due to absence of such information at the scale of model application.

Information on remotely sensed ET_a rates and field observation on groundwater levels was also used to estimate actual groundwater use in the study area. Observations on groundwater heads for five years was then used to inversely identify the drainable porosity of the aquifer. Subsequently the model results were validated against observed groundwater heads for nine years and overall good agreement was obtained.

After calibration, the FRAME model was used to analyse irrigation water management at regional scale. Three alternate water management scenarios involving partial reduction in canal water supply and increased groundwater extraction were simulated. Effects of alternate water management scenarios on crop ET_a and groundwater level depths were predicted. It was observed that in the study area where groundwater levels are rising reduction in canal water supply by 25 % during rainy season is unlikely to have any adverse effect on the development of soil salinity. Reduction in ET_a due to decreased canal water supply can be partly compensated for by the increase in groundwater use.

Key words: evapotranspiration, effective soil hydraulic parameters, remote sensing, regional water management, groundwater use, Bhakra Irrigation System, India.

Acknowledgements

The work reported in this thesis was made possible in the present shape with the support and contribution from many individuals to whom I feel indebted and wish to express my gratitude.

First of all, I would like to pay my kind regards to my promotor, Prof. R.A. Feddes and thank him for his inspiring guidance, valuable support during the whole research period and the faith he shown in me. I whole heartedly appreciate his intellectual thoughts and the way he put them in simple and straight forward arguments and suggestions, more importantly always with a smiling face. I feel proud of the honour I got of working under the guidance of Prof. Feddes. He gave all due attention to the work despite the heavy demands he already had due to being head of the department dealing with the most important natural resource of the planet, more so for the Netherlands.

I gratefully acknowledge my gratitude to my co-promotor, Prof. W.G.M. Bastiaanssen for his help, motivation and valuable guidance. I appreciate him for his critical reading and comments on the drafts of different chapters. His supervision, suggestions and remarks have helped significantly to shape the work.

I acknowledge my indebtedness to my co-promotor Dr. Jos van Dam for his valuable comments, specific suggestions and prompt help during all the stages of this study. His easy accessibility and willingness to help made my life comfortable while working on parameter optimisations. Jos not only helped me on the technical aspects of the work but also provided much needed financial assistance at his command.

I would like to render my special gratitude to Robert Smit for the help and support he provided on every aspect of my life in Wageningen. He generously created time in his agenda to discuss various aspects of the work. He was always there to help me out on personal as well as educational matters. Robert is one of the few persons whom I did not hesitate to meet without the typical Dutch appointment. Unfortunately, words fall short when I try to reciprocate honestly to all that he has done for me. If I would ever be asked to list individuals without whose support this work would not have been possible, my answer would be- Robert. I also thankfully acknowledge the hospitality extended by Robert and his wife Nahla in the form of vegetarian dinner for uncountable number of times. Thanks a lot.

I respectfully acknowledge the moral and scientific support received from Koen Roest. In fact I always looked at him as my guardian in Holland. His moral support gave me necessary confidence during my stays in Wageningen and I sincerely acknowledge its value. I also thank Dethmer Boels for the support I received from him. Whenever I had any doubt on different processes incorporated in the model FRAME, he explained from the basics to the final adoptions in the model.

There is only one part in this thesis (evapotranspiration estimates from remote sensing) which I cannot reproduce (as yet) on my own. The task of translating the digital numbers recorded by remote sensing satellites to the evapotranspiration data was done by Edwin Noordman. Thanks a lot Edwin for this task. Your data gave me the opportunity to face the reality, otherwise I was happily working with forward and backward simulations.

I thankfully acknowledge the authorities of Chaudhary Charan Singh Haryana Agricultural University for allowing me to use this unique opportunity of the Wageningen University sandwich programme. I thank my senior colleagues especially Prof. M.C. Agarwal, Prof. R.S. Malik, Prof. Ranvir Kumar, Prof. Joginder Singh, Prof. Rajinder Singh, Dr. Satyendra Kumar and Dr. M.K. Garg for the moral support received during this period. I am also thankful to my friend M.J. Kaledhonkar and my students, especially Ranvir Khatri and Virender Sehrawat, for the help provided during this study.

During my both stays in Wageningen, I enjoyed the friendly atmosphere in the Department of Water Resources. I like to acknowledge the pleasant company of Dr. Mehdi Homaee, Mr. Jan Schalk, Prof. J. Ben Asher and Miss Anuraga Jain. Away from the office, I also enjoyed the company of many Indian friends in and around Wageningen. Though it is not impossible to mention all of them by name, but I fear that if I forget anyone's name, he or she would not like it. For example, if I forget the name of Arun, he will be unhappy and so would be Ajay, Basav, Shital, Pankaj, Vrushali, Nitin, Bhanu, Sre Prakash, D.K. Singh and Sreeramulu. All of them were very kind to me. I also spent few evening hours in Wageningen at the hotel WIR in the pleasant company of Dr. S.K. Gupta, Dr. D.P. Sharma, Dr. K.N. Singh, Dr. S.K. Luthra and Er. A. Srinivasulu. Thanks a lot.

I also sincerely appreciate the secretarial staff of the Department, Mrs. H. van Werven and Mrs. Annemarie Hofs for their prompt help on different administrative matters. Thanks are also due to Piet Warmerdam for his support in coordinating financial matters and Bram Kuyper for his prompt help on computer related matters. I also thankfully acknowledge the staff Department for Education and Student Affairs, particularly C.M.M. van Heijst for the help provided during my struggle with the Dutch Embassy in New Delhi to get a visa. Though, finally it was the Dutch Embassy who won the battle and caused a delay of six months in completing this work.

The role played by my family during the whole work cannot be disputed. I express my deepest gratefulness to my mother, uncle, aunt, brothers and sister for their continuous moral support and encouragement during my endeavour to complete this work. I could not have completed this work without their kindness and help. Specially, I thank my daughter Mansi for providing a pleasant environment while working at home. I am deeply indebted to her for the time I could not spend with her, particularly during my both the stays in Wageningen. During finalisation of this thesis, it was not possible for me to be at home on her birthday and little Mansi helped me by postponing her birthday (!) by a month (that is what she told me on phone).

It is impossible to list in full all the individuals whose support benefited this study. Whether mentioned by name or not, please accept my whole hearted thanks for your part in the successful completion of the present work.

It is just impossible to acknowledge by any words the long term contribution of my late father, who always motivated me for higher study. Though I have completed this job but have no joy without the company of my father. He was very happy when I joined the PhD program therefore, I dedicate this thesis to my father.

Contents

1	**Introduction**	**1**
	1.1 General background	1
	1.2 Problem identification	4
	1.3 Objectives and outline of the thesis	7
2	**Description of the Sirsa Irrigation Circle**	**11**
	2.1 Location and climate	11
	2.2 Topography and soil types	11
	2.3 Irrigation system	13
	2.4 Groundwater quality	14
	2.5 Crops and cropping patterns	15
	2.6 Water management related issues	15
3	**Computational tools**	**19**
	3.1 On-farm agrohydrological model SWAP	19
	3.2 Distributed irrigation water management model FRAME	24
	3.3 Parameter estimation program PEST	37
4	**Inversely estimating soil hydraulic functions for *homogeneous* soils using evapotranspiration rates**	**41**
	4.1 Introduction	41
	4.2 Forward simulations with SWAP and parameter estimation procedure	43
	4.3 Evaluation criteria for inversely estimated parameters	46
	4.4 Sampling strategy and sensitivity of T_a to VG model parameters	47
	4.5 Performance of inversely identified soil hydraulic parameters	51
	4.6 General discussion	59
	4.7 Conclusions	60
5	**Calibration of effective soil hydraulic parameters for *heterogeneous* soil profiles**	**63**
	5.1 Introduction	63
	5.2 Data set on heterogeneous soil profiles	64
	5.3 Forward simulations with SWAP and parameter estimation procedure	67
	5.4 Performance of inversely identified parameters for *individual* soil profiles	69
	5.5 Performance of inversely identified *area effective* soil profile	75
	5.6 General discussion	79
	5.7 Conclusions	81
6	**Calibration of the regional model FRAME using remotely sensed evapotranspiration rates and groundwater heads**	**83**
	6.1 Introduction	83
	6.2 Schematisation of the Sirsa Irrigation Circle area and input data	85
	6.3 Calibration strategy	89
	6.4 Sensitivity of model parameters to ET_a	91
	6.5 Prior analysis of calibration strategy	93
	6.6 Calibration of selected model parameters using ET_{RS} rates	95
	6.7 Calibration of selected model parameters using groundwater heads	104
	6.8 General discussion	108
	6.9 Conclusions	109

7 Scenario analysis of irrigation water management at regional scale 111
7.1 Introduction 111
7.2 Reference situation and alternative scenarios 112
7.3 Effect of alternative strategies on crop evapotranspiration 114
7.4 Effect of alternative strategies on soil salinity 116
7.5 Effect of alternative strategies on groundwater levels 119
7.6 General discussion 121
7.7 Conclusions 123

8 Summary and conclusions 125

Samenvatting en conclusies 133
References 141
List of symbols 151
Curriculum vitae 157

Chapter 1

Introduction

1.1 General background

Water resources development has been an effective vehicle in ushering the green revolution that India witnessed in the post independence era. The role of irrigation can be judged from the fact that, except in rare and limited areas, there has been no green revolution in India on unirrigated land. Presently, irrigated agriculture contributes nearly 60 % of the total agriculture output. However, continuous population growth coupled with increasing constraints on water resource development puts an enormous pressure on Indian agriculture. The total water available in the country remains more or less fixed according to the natural hydrologic cycle. The per capita water availability is reducing progressively due to increasing population (Fig. 1.1). Prospects for finding new major sources of water are relatively dim (*Navalawala*, 1995). Water management experts increasingly agree that the most effective long term strategy for dealing with water scarcity is the improved productivity of existing water resources (*IWMI*, 2000) i.e. harvest more food from less water resources.

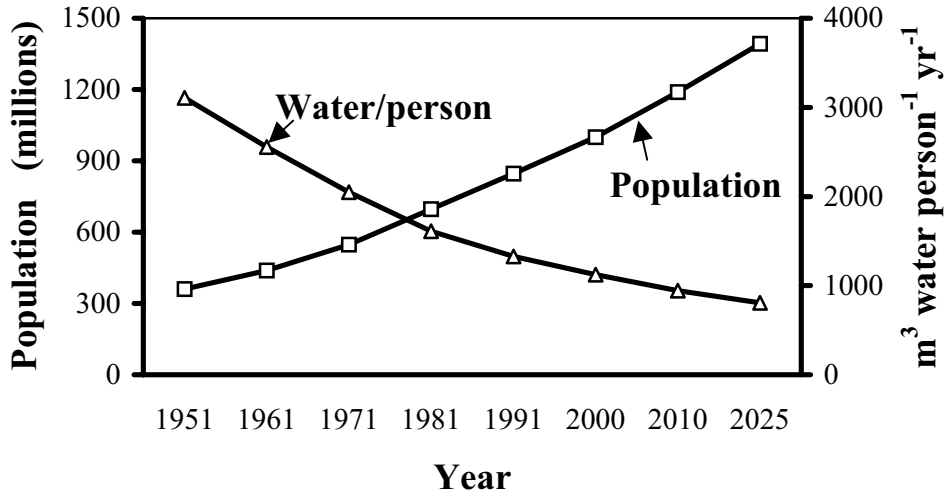

Figure 1.1. Population growth and per capita water availability in India. The water availability figures are based on a potentially utilizable amount (*Navalawala*, 1999a) of 1122 billion m^3.

The performance of an irrigation system can be evaluated from various points of view and a wide spectrum of indicators (*Molden*, 1997). But, irrigation *efficiency* is the most commonly used term to describe how well water is being used (*Israelsen*, 1950). It is generally held that irrigation efficiency in canal irrigated regions in India is very low (30 to 40 %: *Navalawala*, 1999a; *Singh*, 2000b). This implies that there is a huge potential for water saving from the existing irrigation projects. However, it may not be realised in the real world. The reported low efficiency figures are based on the notion that water not being used at first place is a loss. In fact, some of the *unused water is reused elsewhere through groundwater development*. That is why the basin efficiency of most irrigation projects is fairly high: 70 to 80 % (*Chaudhary*, 1997). Higher irrigation efficiency at basin level does not mean that no changes in existing water management strategy are required. Water should, however, be saved in irrigated areas that looses water to locations from which it cannot be recovered in the usable form such as from saline depressions, oceans and poor quality groundwater bearing formations.

Introduction of irrigation coupled with other management practices has resulted in substantial increase in crop productivity (yield per ha) . The productivity in case of food grain crops increased from 0.5 ton ha^{-1} in 1951 to 1.7 ton ha^{-1} in 2000. However, the productivity is lower than what has been achieved elsewhere in the world. For example, while being the second largest producer of wheat and rice, India lags far behind in the crop productivity (Fig. 1.2). The productivity also varies considerably among the Indian States. In the year 1991, the yield of paddy was of the order of 3.2 to 3.4 ton ha^{-1} in Punjab and Tamil Nadu, the yield in Madhya Pradesh, Maharashtra and Bihar was in the range of 1.6, 1.7 and 1.4 ton ha^{-1}, respectively. While yield depends on agro-climatic and soil conditions, there is ample scope for increasing the yield of crops in the country. Under conditions of emerging water scarcity, a primary strategy is to increase the water productivity (yield per m^3) as well.

Notwithstanding that irrigation development in the country has strengthened the nations economy to large extent, it has also caused in some regions waterlogging, soil salinity and alkalinity. Extensive tracts of land, once highly productive, have been rendered woefully infertile. It is reported that about 10 % of the irrigated land is already affected by salinisation (*Tyagi*, 1996).

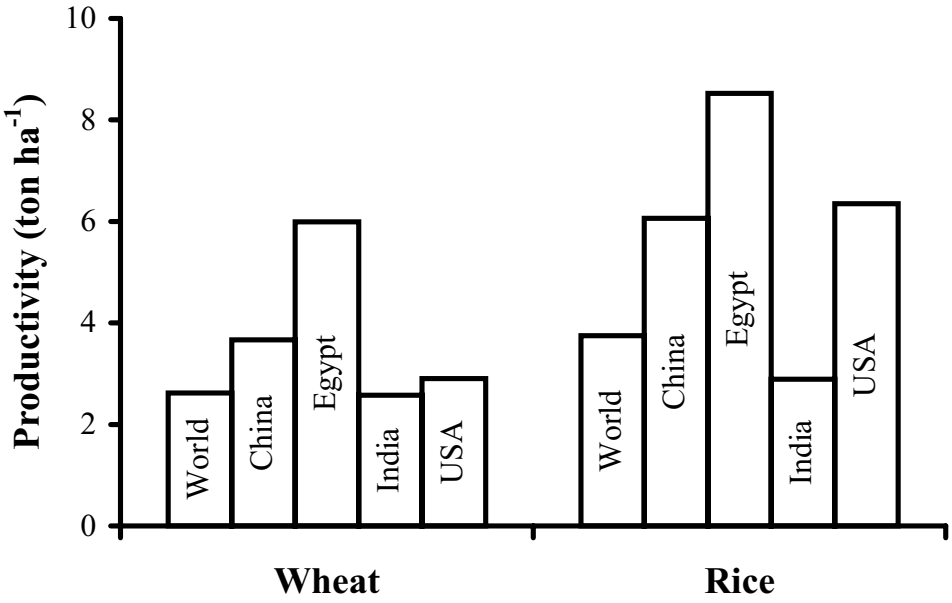

Figure 1.2. Productivity (crop yield ha^{-1}) of wheat and rice in some selected countries vis a vis the world average productivity (based on http://www.nic.in/agricoop/statistics/wprod2.htm : verified on June 17, 2001)

Problems such as waterlogging and soil salinization, though severe, generally are reversible (*Jensen*, 1996). Assuming that the emerging hydro-salinity problems in irrigated areas are consequences of adopted water management practices and poor natural drainage conditions (*Tyagi*, 1996), irrigated agriculture can be environmentally sustained provided basic principles of good water management and salt control are recognised. Some of the reasons for the problems of waterlogging and soil salinity are: increasing water application by irrigation, low irrigation efficiency and poor natural drainage conditions. Therefore, improved water management can play an important role in maintaining the productivity of irrigated agriculture.

The government has taken various policy and programme initiatives to control the problem of water logging and soil salinity. These include emphasis on improved water management practices, promoting conjunctive use of surface and groundwater, adoption of drip and sprinkler irrigation system, construction/improvement of drainage systems and reclamation of waterlogged and saline lands. *Development of an efficient and sustainable water management strategy in the coming years is going to be crucial in achieving the anticipated agricultural production while maintaining soil health.*

To summarise, irrigated agriculture in India has the following characteristic features: constant water resources, rising demands, low crop productivity, continued mismanagement, advent of water scarcity and deteriorating environment. Therefore, *there is a need to identify appropriate water management strategies for on-farm as well as regional level to solve the problems*. No single water management strategy can be equally efficient and optimum at all locations owing to spatial variability in agro-geohydrological conditions. Alternative water management options need to be examined for their short term as well as long term impacts on agricultural production both at local and regional level. This will also require a thorough analysis of the existing and projected water management practices. Therefore, there is a need to develop appropriate techniques to study alternative water management options, preferably before their actual implementation.

1.2 Problem identification

Proper water management cannot be accomplished without an understanding of the effects of human interventions on the hydrological processes and their interactions. The key to evaluate different options lies in the assessment of the resulting water and salt balance for the area under consideration. Traditionally, plot experiments are conducted to identify appropriate water management technology. However, specific recommendations emanating from experimental work, generally have relevance to the conditions under which experiments are conducted. Such recommendations cannot be applied directly at district or state level, where different conditions in soil type, groundwater depth, salinity levels, potential evapotranspiration and rainfall exist. Further such experiments, besides being too expensive are practically impossible to conduct at regional level due to lack of suitable field measurement techniques to quantify different water balance components at that scale. This does not mean that field experiments are irrelevant. Detailed local knowledge and analysis is required under all conditions.

New extrapolation techniques are required to prepare guidelines for on-farm and regional water management for areas where field experiments could not be conducted. *Simulation models offer an attractive alternative to study the effect of proposed water management strategies for situations where experiments could not be conducted.* Though modelling is a

representation of the real world with a certain level of simplification, several explicit alternative policies can be simulated for one or more crop seasons and predicted water and salt balance components/ crop yields can be compared to select the appropriate policy. However, application of the hydrological models at regional scale is limited by the non-availability of key hydrological parameters (*Stewart et al*., 1996). As a result, the potential practical application of modelling studies still remains unutilised.

There is always a justifiable fear of losing the role of heterogeneity of the hydrological parameters when hydrological models are applied at larger scale. This is because these models are basically process based i.e. they describe only the time aspects of the process regardless spatial variations. This is partly solved by applying these models in a distributed manner. The application of water management simulation models in a distributed manner attempts to include the effect of spatial variability of soil characteristics by making use of a network of grid points in space. Owing to computational and practical limitations, each grid point represents a sub-area generally varying from a few hectares to several hundred hectares. Fundamental to the use of the distributed models for water management analysis is that the use of representative soil hydraulic parameters for the sub-areas is adequate in representing the heterogeneity of water balance components at that scale. Distributed models loose much of their strengths and advantages to lumped models when their distributed parameters can not be identified (*Griensven and Bauwens*, 2001). This requires that the sub-area representative soil hydraulic parameters must be defined at the model grid scale. However, the usual scale of measurement of the soil parameters is much smaller, varying from a few centimetres to a maximum of about 2 m (*Binley et al*., 1989). This requires some kind of aggregation to convert the point measured soil parameters to representative parameters at the model grid scale.

Efforts have been made by different international organisations to develop appropriate databases of soil hydraulic properties (*Leij et al*., 1996; *Wösten et al*., 1999). However, there is a general lack of available soil hydraulic data bases for simulation model applications to Indian conditions. Considering the paucity of data bases, the scientific meeting cum workshop on Sustainable Irrigation in Saline Environment (*Tyagi et al.,* 1993) recommended that appropriate parameter estimation procedures should be developed to support water and solute transport models.

Indirect methods such as pedotransfer functions (PTFs) (*Saxton et al*., 1986) and scaling techniques (*Raats*, 1990) are often suggested to derive area representative soil hydraulic parameters (*Kabat et al.*, 1997; *Batjes*, 1996). PTFs relate the soil hydraulic characteristics to more easily available soil properties (*Wösten and van Genuchten*, 1988) through regression equations. In principle, PTFs must be derived from large profile data sets (*Reynolds et al.*, 2000) and are applicable for similar conditions only (*Burke et al*., 1997). In fact, PTFs does not exist without direct methods since only measurements create the required database (*Wösten et al.*, 1995). Another frequently used technique to account for spatial variability is scaling (*Kabat et al*., 1997). In the scaling procedure, a mean curve is fitted though the scaled hydraulic data (*Clausnitzer et al.*, 1992). To capture all possible variability in the soil hydraulic parameters, intensive direct field measurements are required. Direct measurement of these soil hydraulic properties is often extremely difficult, time consuming and expensive (V*an Genuchten and Leij*, 1992). It may not be feasible to obtain enough direct measurements across an area to adequately reflect the soil spatial heterogeneity. This restricts the practical applicability of these techniques to derive area representative soil hydraulic parameters. There appears as yet, no simple way to predict a field *effective* set of soil hydraulic parameters on the basis of the sample measurements of soil parameters (*Smith and Diekkrüger*, 1996).

As an alternative to the scaling or aggregation problem, indirect estimation of effective soil hydraulic parameters by inverse modelling has been suggested (*Feddes et al*., 1993b). Rapid increase of processor calculation speed, development of effective optimization algorithms and availability of areal fluxes from remote sensing techniques have created the possibility to determine area *effective* soil hydraulic parameters of distributed hydrological models by inverse techniques (*Schmugge et al*., 1992; *Burke et al.*, 1998; *Feddes et al.*, 1993a). However, successful application of the inverse modelling technique requires an adequate physical description of the system being simulated. Any error in the physical-mathematical model concept, including the interrelated processes, will affect the '*effective*' parameters. Therefore, inversely estimated parameters are *effective* only within the employed modelling concept. Nevertheless, in the past few years, applications of the inverse method to estimate soil hydraulic parameters have increased rapidly (*see Hopmans and Simunek,* 1999). Assuming that a given physical-mathematical model concept is an acceptable representation of the real system, the inverse approach would result in more representative parameter estimates. This is due to the fact that the inverse approach is based on experimental data that

convey explicit information about the combined heterogeneous system behaviour (*Wildenschild and Jensen*, 1999).

Fundamental to the inverse approach is availability of data to calibrate the effective parameter values at the desired scale of application. The inverse approach requires that one or more of the hydrological responses of the sub-areas to be known under the given state of conditions. Again most of the direct measurement techniques in hydrology are at point scale. Areal integration of point measurements have the same limitations as pointed out for soil parameters. In this context, a great deal of effort have been put into remote sensing as a source of distributed hydrologically useful information (e.g. soil moisture, evapotranspiration, crop water stress). Remote sensing can be used to observe hydrological variables for area of metres up to the complete globe. This gives remote sensing the potential to provide information which cannot easily be obtained by ground based techniques. Since ground surveys have restricted possibility for sampling, the possibility of remote sensing and statistical procedures (e.g. inverse modelling) to retrieve the model specific soil hydraulic parameters needs to be better explored. Therefore, *to develop optimum water management plans, there is a need to integrate advanced techniques such as soil water flow and salt transport modelling, remote sensing and optimisation procedures*.

An attempt is made in this study to derive effective soil hydraulic parameters using an inverse modelling approach. Data from the Sirsa Irrigation Circle, a part of the command area of Bhakra Irrigation System, located in Haryana, Northwest India is used in this study. The water management related problems in the study area are typical for an irrigation command in arid and semi-arid regions i.e. rising/falling groundwater levels and emergence of waterlogging and soil salinity problems.

1.3 Objectives and outline of the thesis

The main objective of this study *is to develop a procedure to identify effective soil hydraulic parameters for distributed irrigation water management modelling using remote sensing and optimisation procedures.*

The specific objectives of this study are:

- To test the feasibility of estimating effective soil hydraulic parameters using actual evapotranspiration rates.
- To integrate simulation model, remote sensing and optimisation procedures for the calibration of a distributed irrigation water management model under limited soil hydraulic data availability.
- To study alternative water management strategies using the distributed irrigation water management model for improved water management planning in the study area.

Chapter 2 describes some salient features of the study area i.e. Sirsa Irrigation Circle, in Haryana, India. The location, specific topographical features and climatic conditions of the study area are described. A brief overview of the working of the Bhakra irrigation system along with common water management related issues, are highlighted.

In Chapter 3 a brief description of different computational tools used in the study is presented. First the theoretical background and relevant processes as adopted in the Soil-Water-Atmosphere and Plant SWAP simulation model are described. Next the distributed irrigation water management model FRAME is described. Thereafter, a brief description of the model independent parameter estimation program PEST is presented.

Chapter 4 deals with the estimation of effective soil hydraulic functions for soils using actual evapotranspiration ET_a rates. Simulated ET_a response for three uniform soils is presented to demonstrate that different soils act differently in their ET_a response. The most appropriate sampling strategy for ET_a rates is identified and finally the ability of inversely estimated effective soil hydraulic functions to predict different water balance components of practical interest, is presented.

Chapter 5 deals with the application of the inverse methodology to identify effective soil hydraulic functions of heterogeneous soil profiles. The ability of inversely estimated effective soil hydraulic functions to predict different water balance components for individual heterogeneous soil profiles as well as for regional level is demonstrated.

Chapter 6, deals with the calibration of the distributed irrigation water management model FRAME. The model is calibrated against evapotranspiration rates estimated from NOAA images and in-situ measurements on groundwater heads. The Sirsa Irrigation Circle described in Chapter 2 is used as a case study.

Chapter 7 deals with the analysis of irrigation water management at regional scale. Performance of alternative water management strategies, namely, changes in canal water supply and conjunctive use of canal water and groundwater are studied through the model FRAME calibrated in Chapter 6.

Finally, a summary and conclusions of the study are given in Chapter 8.

Chapter 2

Description of the Sirsa Irrigation Circle

2.1 Location and climate

The study area Sirsa Irrigation Circle is located in the western part of Haryana, India (Fig. 2.1). It is situated between latitude 29.1° to 30.0° North and longitude 74.2° to 75.3° East and covers an area of 0.48 million ha. The area is bounded by the State of Punjab in the north and north east and by the State of Rajasthan in the west and south. The climate of the area is characterised by its dryness and extremes of temperature and scanty rainfall. The area receives an annual average rainfall of 310 mm and has an annual reference evapotranspiration of 1720 mm. Rainfall is highly erratic both in quantity and distribution. About 80 % of the annual normal rainfall is received during the monsoon period, July to September. The mean daily maximum temperature during May and June, which is the hottest period, varies from 41 to 46 °C . On individual days, the maximum temperature during the hot period may rise up to about 49 °C. January is generally the coldest month with the mean daily maximum at 21 °C and the mean daily minimum at 5 °C. In the study area, a year may be divided into four distinct seasons: the dry season from March to June, hot monsoon (rainy) season from July to September, post-monsoon season from October to November and cold season from December to February. Dust storms occur often during the hot and dry season. Occasional fogs affects the area in the cold season.

2.2 Topography and soil types

The terrain of the Sirsa Irrigation Circle is classified into three major types: old alluvial plains, recent alluvial plains and aeolian plains with sand dunes. The old alluvial plain is a vast surface of flat to rolling terrain and extends from northern boundary of the area towards south. The southern most part of the Sirsa Irrigation Circle is covered by the aeolian plain

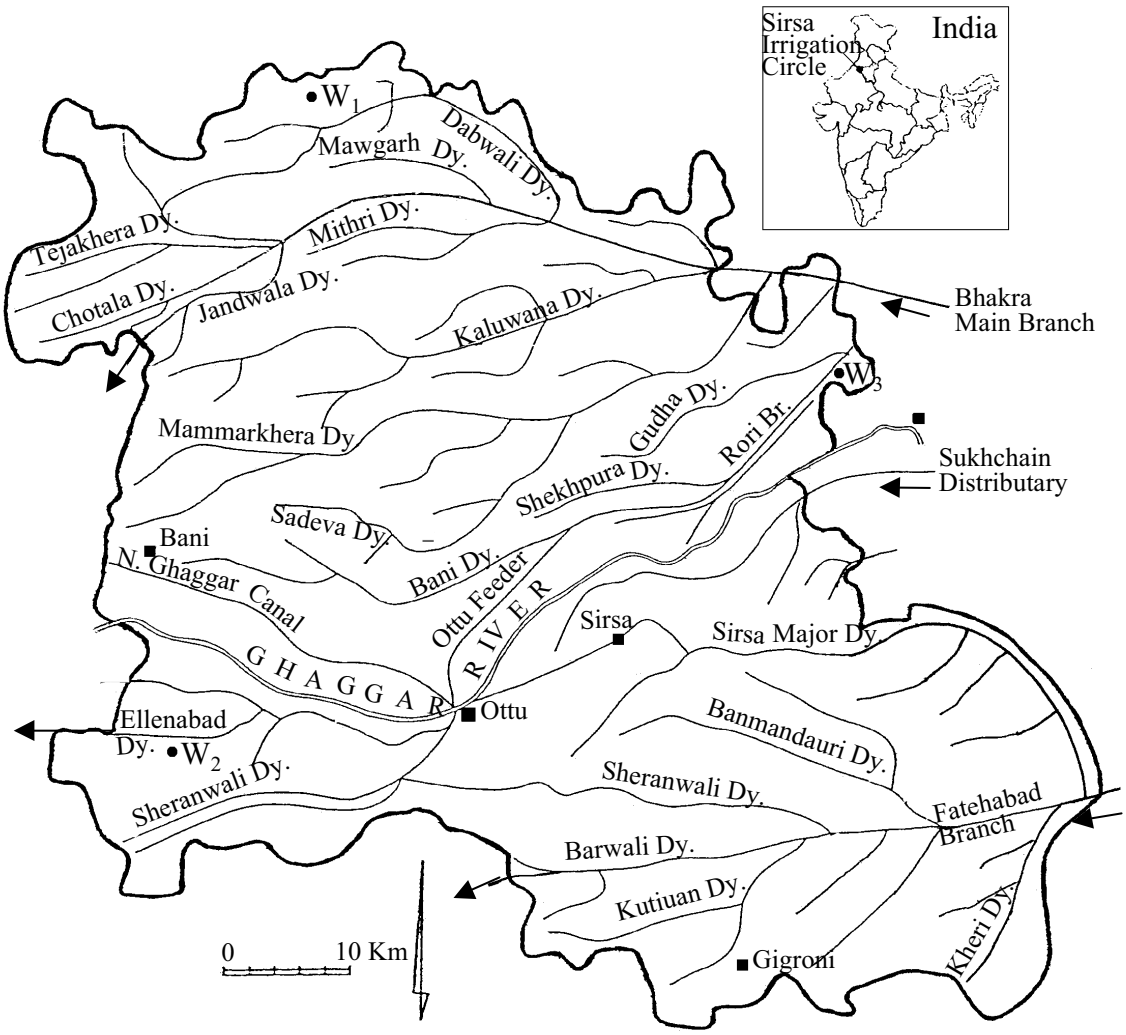

Figure 2.1 Location of the Sirsa Irrigation Circle showing the canal network

with sand dunes. A narrow belt between the old alluvial plains and aeolian plains, along the Ghaggar river, is covered by the recent alluvial plains. The soil texture generally varies from loamy sand to sandy loam with some sandy soils occurring in patches. The soil texture in the belt along Ghaggar river varies from silt loam to silty clay loam.

2.3 Irrigation system

The Sirsa Irrigation Circle is a part of Bhakra Irrigation System and is served by an extensive network of canals (Fig. 2.1). Irrigation Circle is an administrative unit within the management of Irrigation Department. The Sirsa irrigation circle covers Sirsa district and part of Fatehabad district. The irrigation water originates from the Gobind Sagar Storage Reservoir located across the river Sutlej in the State of Himachal Pradesh. The irrigation system consists of a large network of canals consisting of varying carrying capacity. Broadly speaking, the system consists of main canals, branch canals, distributaries, minors and water courses. The Sirsa Irrigation Circle is covered by three main canals. Bhakra Main Line serves in the north, Sukhchain distributary in the central part and Fatehabad branch in the south. Tails of these canals supplied water to the adjoining areas of the state of Rajasthan. A seasonal river Ghaggar flows from the eastern to the western direction draining through the central part of the Sirsa Irrigation Circle. The Ghaggar river originates from the Siwalik hills on the outer Himalayan ranges. During monsoon, water from the Ghaggar river is partly diverted for irrigation.

The Bhakra project was designed to distribute a limited supply of water to the greatest number of farmers possible over a large area (*Sakthivadivel et al.*, 1999). Because of the limited available water supply, irrigation water is not continuously available to different parts of the irrigation command. Water is rotated among a group of canals following a procedure known as *rostering*. The period of *rostering* is 24 days. Typically an irrigation command area has three distributaries in a group, say A, B and C. During the first 8 days of a rotation, distributary A has first priority, receives fully supply of water, distributary B has second priority, receives water depending on the availability and distributary C has last priority and is scheduled not to receive water unless the supply to the region is excessive. During the next 8 days of rotation, distributary C moves to first priority, distributary A to second and distributary B to third. During the last 8 days of rotation, the priority order changes again.

The distribution of water among the farmers is at the water course level. The allocation is based on one week fixed rotational system called '*warabandi*'. Water from a water course is allocated to the individual farmer for a specified period in proportion to his land holding. In this way, every farmers is ensured a uniform volumetric water allocation per hectare per week. This system of water distribution has the advantage of higher equity, ease in operation and less management problems. The disadvantage is that the farmer's entitlement of water is

proportional to his landholding size without consideration of his soil type and crop water requirements. During their turn, the farmers distribute the water on their fields. The amount of water applied to each field is decided by the farmer. Mostly, farmers use the surface flooding method to irrigate their fields. *Irrigation water charges to farmers are fixed, based on type of crop and area actually irrigated with surface water. This means the farmers have to pay less if they irrigate less area with the same amount. It may appear that this could lead to over irrigation and wasteful use of water* (*Agarwal and Roest*, 1996). *However, prevailing water charges are very low and, as such, they have no influence on farmers' management decisions* (*Navalawala*, 1999b).

2.4 Groundwater quality

Keeping in view the potential salinity hazard of irrigation water, the groundwater in Haryana has been classified into three broad categories: good (EC_{gw} < 2 dS m^{-1}), marginal (EC_{gw} 2-6 dS m^{-1}) and poor (EC_{gw} > 6 dS m^{-1}), where EC_{gw} is the electrical conductivity of groundwater. The groundwater quality on both sides of the of the Ghaggar river was generally good, resulting in installation of numerous tubewells in the belt along the river. The deep groundwater quality in the northern and extreme southern part of the Sirsa irrigation circle was quite poor. However, over the years, a relatively better quality water layer has been developed over the saline groundwater prompting the farmers to install shallow tubewells. Generally speaking, the shallow groundwater has a better quality than the deep groundwater. According to a groundwater quality map of Haryana, prepared by Haryana State Minor Irrigation and Tubewells Corporation (HSMITC), in year 2001, the shallow groundwater quality was good in about 28 %, marginal in 64 % and poor in 8 % of the Sirsa district. On the other hand deep groundwater quality was good in 20 %, marginal in 16 % and poor in 64 % of the area.

Groundwater use is implemented in two ways. The HSMITC operates deep direct irrigation and augmentation tubewells and farmers operate shallow tubewells. The augmentation tubewells supplies water to canals. A major portion of groundwater use takes place through farmers owned shallow tubewells.

2.5 Crops and cropping pattern

Two distinct crop growing seasons can be identified in the study area: the winter growing season called *rabi*, lasts from October to April and the summer growing season called *kharif,* lasts from April to October. Wheat in the *rabi* season and cotton in the *kharif* season are the principle crops in the area. Other important crops are oil seeds, paddy, gram (chickpea) and fodder. At present, cotton-wheat is the most dominant crop rotation in the study area. About 87 % of the total cropped area receives irrigation. The crop yields in the study area are generally at par with the state average yields in Haryana.

2.6 Water management related issues

Successful crop production without supplemental irrigation even in the rainy season is hardly possible in the study area. As a result, development and utilisation of irrigation facilities got top priority. However, in the process of exploiting various water resources by technical means, certain imbalances and anomalies have emerged. The major issues related to water management in the Sirsa Irrigation Circle are: rising groundwater levels in the poor and marginal quality groundwater zones due to water losses from the irrigation system, waterlogging risks (groundwater depth < 3.0 m) in a few pockets, associated with secondary soil salinization, declining groundwater levels in the good quality groundwater zones due to overexploitation and shortage of water to irrigate all agricultural crops.

The groundwater level in the area is monitored during the pre- and post-monsoon periods (June and October) through a grid of open wells and piezometric tubes spread throughout the area. Leakage losses from the canal irrigation system led to rise in groundwater levels particularly in areas underlain with marginal to poor quality groundwater (Well W_1, Fig. 2.2). Another problem of quite opposite nature was experienced in the good groundwater quality zone along the Ghaggar river. Over-exploitation of groundwater resulted in declining groundwater levels (well W_2, Fig. 2.2). In some of the areas the groundwater depths were within 3.0 m from the soil surface (well W_3, Fig. 2.2). About 13 % of the total area of Sirsa district was under less than 3.0 m depth during October 1998 (Table 2.1).

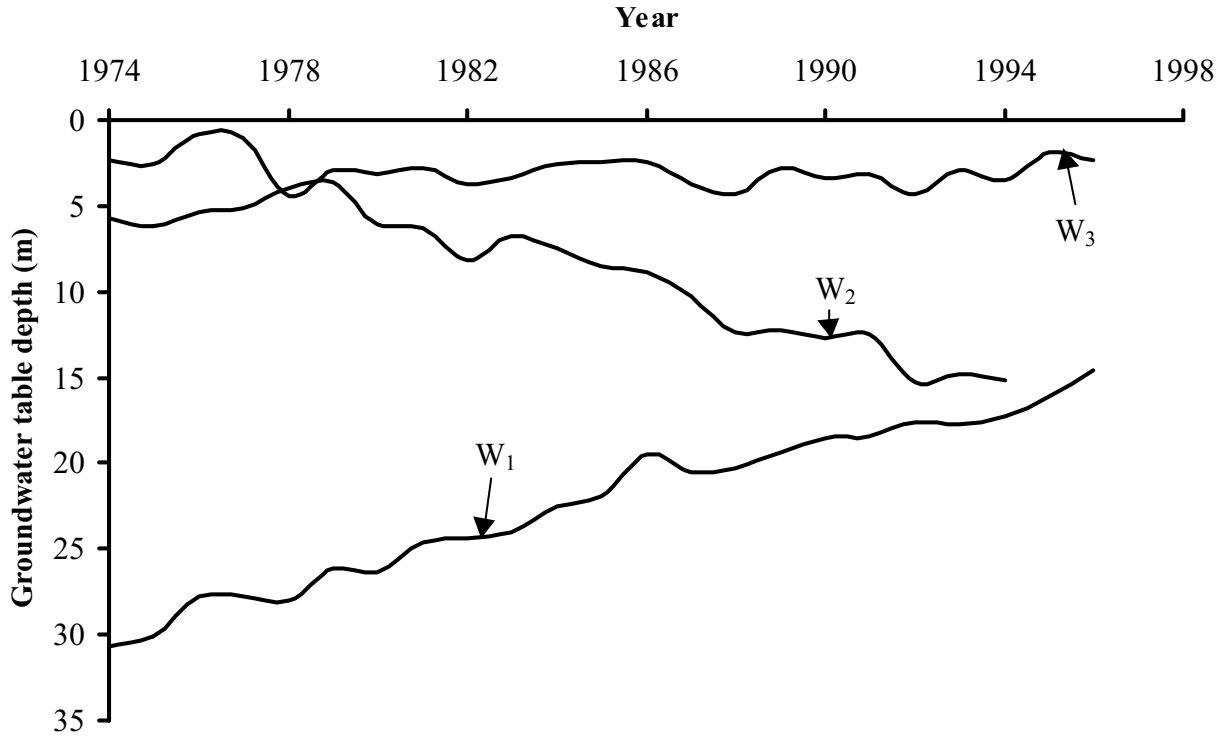

Figure 2.2. Depth of groundwater below the soil surface at different locations in the Sirsa Irrigation Circle. The location of wells W_1, W_2 and W_3 is shown in Fig. 2.1. The well W_1 is located in the area having saline groundwater, well W_2 is located in the area having good quality groundwater and well W_3 is located in the area facing waterlogging problems

Table 2.1. Percentage area of the Sirsa district under different groundwater depth in June and October (*Singh*, 2000a)

Groundwater depth, m	1996		1998	
	June	October	June	October
0-1.5	0.61	2.32	0.86	2.89
1.5-3.0	2.81	7.38	7.67	9.43
>3.0	96.58	90.30	91.47	87.68

Lack of saline groundwater exploitation, addition of excess water through the irrigation system, occasional heavy rainfall events and absence of sufficient drainage facilities aggravate the problems of groundwater level rise.

The long term groundwater level trend shows that the average rate of rise in groundwater levels between 1974-84 was 0.63 m yr^{-1}, while the same for 1974-94 and 1974-98 was 0.41 and 0.36 m yr^{-1}, respectively. This shows that over the years the rate of rise in groundwater levels has decreased. However, the groundwater level is still rising in many parts of the area.

The stage of stagnation or even decline in productivity of major crops appears to have reached in the area (*Yadav*, 1998). In this context, it is important to note that sharp increase in wheat and rice yields was the main contributing factor to the green revolution. The present level of crop productivity in the area (wheat 3.9 ton ha^{-1} and rice 3.3 ton ha^{-1}) are much lower than the attainable productivity level (Fig. 1.2).

By nature, the study area is in a disadvantageous position with regard to rainfall and groundwater quality. According to an estimate of *Dhindwal and Kumar* (2000), there is not enough water to meet all demands with present efficiencies. *It is vital to exploit the full potential of conjunctive use of surface and groundwater as a solution to the problem of inflexible canal water supply, rising groundwater levels and stagnating production.*

Chapter 3

Computational Tools

This chapter contains the main features of different computational tools used in the present study. These include the on-farm agrohydrological model SWAP, the distributed irrigation water management model FRAME and the parameter estimation program PEST.

3.1 On-farm agrohydrological model SWAP

The Soil-Water-Atmosphere-Plant (SWAP) model describes one dimensional water flow, solute transport and heat flow in top soils. SWAP is an extended version of the agrohydrological model SWATR (Soil Water Actual Transpiration Rate) developed by *Feddes et al.*, 1978. Fig. 3.1 schematizes the hydrological processes incorporated in SWAP. The main flow processes are assumed to occur in vertical direction allowing a one-dimensional model structure. When a region with variability in horizontal direction has to be analyzed, the model should be applied either at each location separately (*Droogers et al.*, 2000) or a more or less representative situation should be defined (*Van Dam*, 2000).

The model offers a wide range of possibilities to address practical questions in the field of agricultural water management and environmental protection. SWAP and its previous versions have successfully been applied in many hydrological studies for a variety of climatic and agricultural conditions (*Van Dam*, 2000). Options exists for irrigation scheduling, drainage design, salinity management, leaching of solutes and pesticides and crop growth simulation. In the present study SWAP was used to simulate soil water flow and evapotranspiration fluxes.

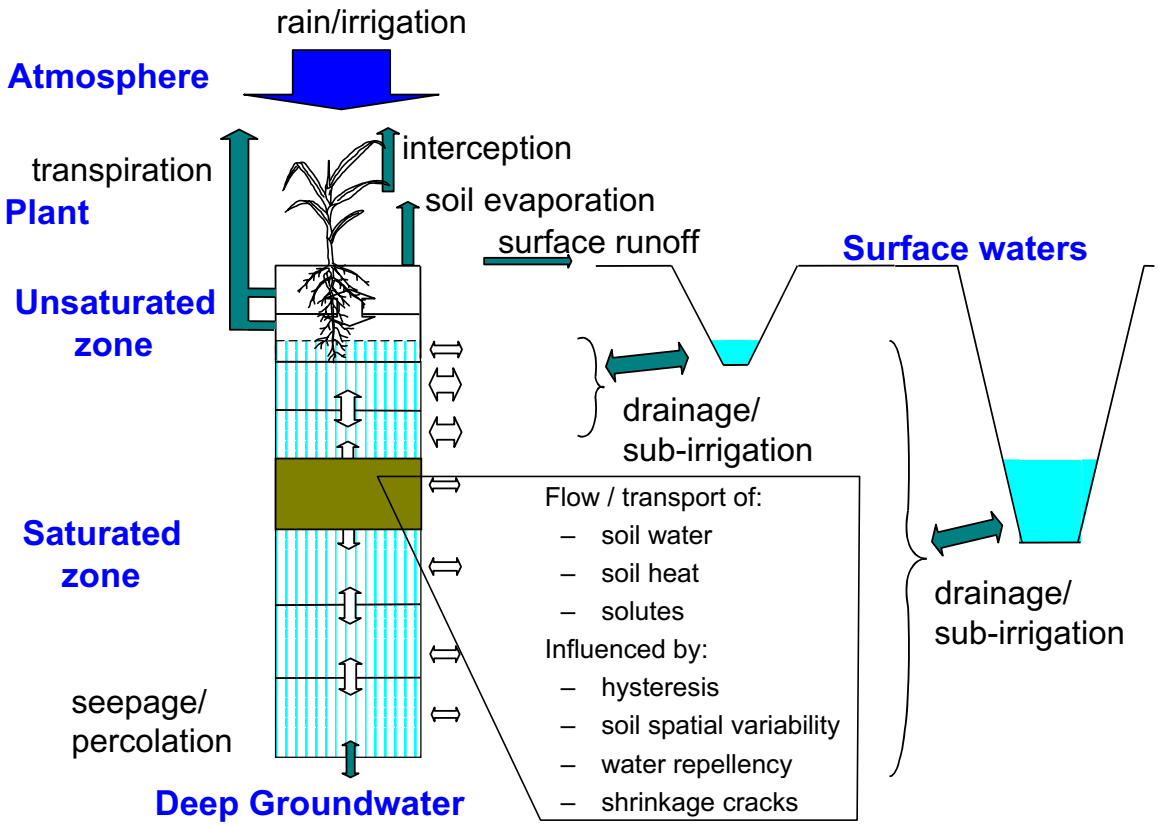

Figure 3.1. Schematization of hydrological processes incorporated in SWAP

Spatial differences of the soil water hydraulic head cause flow of soil water. Darcy's equation is used to quantify these soil water fluxes. For one-dimensional vertical flow, Darcy's equation can be written as:

$$q = -k(h)\frac{\partial(h+z)}{\partial z} \tag{3.1}$$

where q is soil water flux density [L T^{-1}] positive upward, k hydraulic conductivity [L T^{-1}], h soil water pressure head [L] and z the vertical distance [L] taken positively upward .

Water balance considerations of an infinitely small soil volume result in the continuity equation for soil water:

$$\frac{\partial \theta}{\partial t} = -\frac{\partial q}{\partial z} - S_a(z) \tag{3.2}$$

where θ is volumetric water content [-], t time [T] and S_a the actual soil water extraction rate by plant roots [T^{-1}].

Combination of Eqs. 3.1 and 3.2 results in the well known Richards' equation:

$$C(h)\frac{\partial h}{\partial t} = \frac{\partial}{\partial z}\left[k(h)\left(\frac{\partial h}{\partial z} + 1\right)\right] - S_a(z) \tag{3.3}$$

where C is the differential water capacity ($d\theta/dh$) [L^{-1}].

SWAP solves Eq. 3.3 numerically, subject to specified initial and boundary conditions and soil hydraulic functions, which relate θ, h and k. The Richards' equation is solved using an implicit finite difference scheme as described by *Belmans et al.* (1983). This scheme has been adapted such that the solution applies both to the unsaturated and saturated zone and that water balance errors due to non-linearity of the differential water capacity are minimised (*Van Dam and Feddes*, 2000).

The following form of soil hydraulic functions is used (*Van Genuchten*, 1980):

$$\theta = \theta_{res} + [\,\theta_{sat} - \theta_{res}]\,[1 + (\alpha h)^n]^{-m} \tag{3.4}$$

$$k = k_{sat}\, S_e^{\lambda}\,[\,1 - (1 - S_e^{\,1/m})^{\,m}\,]^2 \tag{3.5}$$

where θ_{res} is residual volumetric water content [-] in the very dry range, θ_{sat} saturated volumetric water content [-], α (L^{-1}), n [-], m (=1-1/n) [-] and λ [-] are empirical shape factors, k_{sat} saturated hydraulic conductivity [$L\ T^{-1}$) and S_e is the relative saturation [-], defined as $(\theta - \theta_{res})/(\theta_{sat} - \theta_{res})$.

The upper boundary conditions are determined by the rates of potential evapotranspiration, irrigation and precipitation. Daily meteorological data, consisting of air temperature, solar radiation, wind speed and air humidity, are used to calculate daily potential evapotranspiration ET_p [L T^{-1}] according to the Penman-Monteith equation (*Allen et al.*, 1998).

Under partial canopy coverage ET_p is assumed to be the sum of potential soil evaporation, E_p [L T^{-1}] and potential transpiration, T_p [L T^{-1}]. The partitioning of ET_p into E_p and T_p is established either according to the leaf area index, *LAI* [-] or soil cover fraction, *SC* [-], both as a function of crop development stage. For this study, *SC* was used to partition ET_p into E_p and T_p as:

$$E_p = (1\text{-}SC)\, ET_p \tag{3.6}$$

$$T_p = ET_p - E_p \tag{3.7}$$

In case of a wet soil, actual soil evaporation rate E_a [L T^{-1}] is determined by the atmospheric demand and equals E_p. When the soil dries out, the soil hydraulic conductivity decreases and E_a is controlled by the maximum possible soil water flux E_{max} [L T^{-1}] in the top soil. In SWAP, E_{max} is computed according to Darcy's law and E_a is set equal to the minimum of E_p and E_{max}. However, there is one serious limitation of the E_{max} procedure. The E_{max} depends on the soil hydraulic functions of the top soil compartments. Still it is not clear to which extent the soil hydraulic functions, that usually represent a top layer of a few decimeter, are valid for the top few centimeters of soil, which are subject to splashing rain, dry crust formation, root extension, various cultivation practices (*Van Dam*, 2000), wind and water erosion or sediment deposition. Under such situations, empirical functions may be used to compute soil evaporation rate E_{emp} [L T^{-1}]. SWAP has the option to choose the empirical evaporation functions of *Black et al.* (1969) or *Boesten and Stroosnijder* (1986). SWAP determines E_a by taking the minimum value of E_p, E_{max} and, if selected by the user, E_{emp}.

Reduction of T_p to actual transpiration rate, T_a [L T^{-1}] depends on the root density and soil moisture distribution in the root zone. First T_p is distributed over the rooting depth resulting in assignment of the potential root water extraction rate at different depths, $S_p(z)$ [T^{-1}]. This means that $S_p(z)$, integrated over the rooting depth is equal to T_p. The $S_p(z)$ at a certain depth

is determined by the fraction of the total root length density at that depth. SWAP can handle different distribution of root length density. However, in this thesis, a uniform root density distribution is assumed, leading to the computation of $S_p(z)$ as (*Feddes et al.*, 1978):

$$S_p(z) = \frac{T_p}{D_{root}} \tag{3.8}$$

where D_{root} is the depth [L] of root zone. Stresses due to dry or wet conditions and/or high salinity conditions may cause reduction in water uptake by plant roots so that $S_a(z)$ (Eq. 3.3) is less than $S_p(z)$. In this study, only water stress has been considered. The water stress in SWAP is described by the function proposed by *Feddes et al.* (1978):

$$S_a(z) = \alpha_w(h) S_p(z) \tag{3.9}$$

where α_w is a dimensionless function of h, with a range of 0 to 1, as depicted in Fig. 3.2.

The reduction factor α_w accounts for either too dry or too wet conditions. It is assumed that under conditions wetter than h_1 (oxygen deficiency) and drier than h_4 (wilting point), water uptake is zero. Between h_1 and h_2 and between h_3 and h_4 a linear variation in α_w is assumed. Between h_2 and h_3, water uptake remains optimal. In this way T_a is related to T_p by the factor α_w which in turn is affected by h and thus the soil hydraulic functions. The sink term variables for reduction in root water uptake are crop specific and need to be defined in advance. Limit h_3 also depends on the evaporative demand of the atmosphere (for higher T_p, reduction in water uptake occurs already at more wet conditions than for low T_p, see h_{3h} and h_{3l} in Fig. 3.2). Critical pressure head values of this sink term function for a variety of crops can be derived from available literature (*Taylor and Ashcroft*, 1972; *Doorenbos and Pruitt*, 1977; *Doorenbos and Kassam*, 1979).

In the unsaturated zone water flow occurs mainly in the vertical direction. Once in the saturated zone, water starts to move in a three dimensional pattern, following the prevailing hydraulic head gradients. Therefore the bottom of the one-dimensional SWAP is either the unsaturated zone or in the upper part of the saturated zone. As a result, various boundary conditions may exists at the bottom of the system. A number of options are offered in SWAP

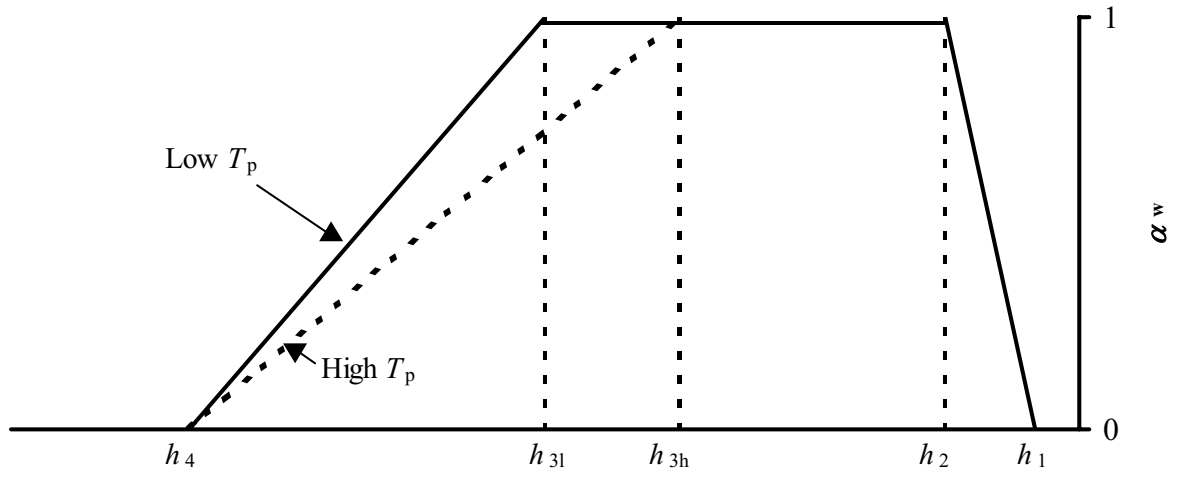

Figure 3.2. Dimensionless sink term variable, α_w, as a function of soil water pressure head h and potential transpiration rate, T_p (after *Feddes et al*., 1978)

to prescribe the bottom boundary conditions. These include groundwater level or pressure head as a function of time, bottom flux as a function of time, bottom flux as a function of groundwater level or, when the groundwater is deep, free drainage. In this study, SWAP was used for deep groundwater conditions. Therefore, free drainage at the bottom of the soil profile was specified as lower boundary condition. In the free drainage case, a zero gradient of the soil water pressure head (unit hydraulic head gradient) at the bottom of the soil profile is assumed (*Van Dam*, 2000). Application of Darcy's law gives for such a case:

$$q = -k(h)\left(\frac{\partial h}{\partial z} + 1\right) = -k(h)(0+1) = -k(h) \qquad (3.10)$$

3.2 Distributed irrigation water management model FRAME

The distributed irrigation water management model, referred to as FRAME (*Boels et al*., 1996), is composed of two model packages, SImulation of Water management in Arid REgions (SIWARE) for canal and on-farm water management (*Boels et al.,* 1989; *Sijtsma et al.*, 1995)

and the Standard Groundwater Model Package (SGMP) for regional groundwater flow (*Boonstra and De Ridder*, 1990). The main objective of linking SIWARE with SGMP is to enable quantification of spatial variations in recharge from the top system to the aquifer and to assess its effect on groundwater levels. Both these models are linked on time step basis (Fig. 3.3). For the first time step, net recharge (the difference between gross recharge and groundwater use) from the top system is computed by SIWARE using initial groundwater levels. Subsequently, the computed net recharge is used by SGMP to determine change in groundwater level over the same period. The groundwater levels computed by SGMP then serve as an input to SIWARE to compute recharge during next time step. The procedure continues till the end of last time step when SGMP computes final groundwater levels. Keeping in view the *rostering* policy (Chapter 2) of water distribution in the study area, the entire year is divided into 16 periods with 15 periods of 24 days each and one period of 5 days to have exactly a calendar year.

***Canal and on-farm water management model SIWARE*:** SIWARE simulates regional water and salt related processes (irrigation, drainage, unsaturated and saturated flow). To facilitate computation of water and salt balance components in a spatially distributed manner, SIWARE requires that the study area be schematized into a number of sub-areas known as calculation units. Each calculation unit is assumed to be uniform with respect to soil parameters, climate, hydrology and water supply conditions. The schematization of calculation units is such that each calculation unit receives continuous water supply from the irrigation system. For the rotational supply system, the boundaries of the calculation units are chosen in such a way that during rotations at least one of the canals feeding the calculation unit has first priority. Under these conditions, the supply to such a calculation unit is continuous. Therefore, the boundaries of the calculation units are dictated by the irrigation system instead of a regular grid. Each calculation unit has heterogeneity in crop cultivation. Each particular crop in a calculation unit is represented by a typical single field plot. Therefore, every calculation unit contains a number of plots, each of them representing a particular crop, including one for fallow land. The computed water balance components of all the typical field plots in a calculation unit with different crops are summed up in a weighted manner to produce representative values for the entire calculation unit. Different water flow processes as simulated using SIWARE for the study area are shown in Fig. 3.4.

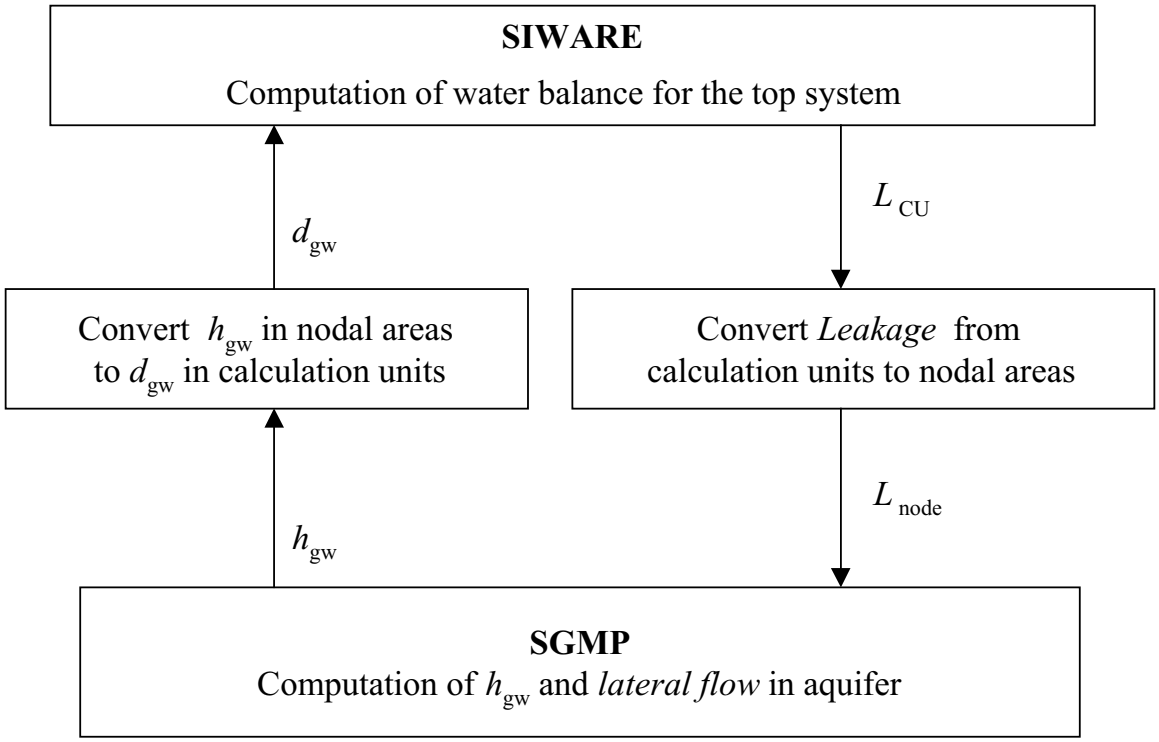

Figure 3.3. Schematic view of link between SIWARE and SGMP. The symbol h_{gw} stands for head of groundwater, d_{gw} for depth of groundwater and L for net recharge/leakage. The schematization of the study area in sub-regions for SIWARE is termed as calculation units (CU) and that for SGMP as nodes.

Simulation starts with the allocation of available water $\boldsymbol{Q}_{CW}$ (canal + river) [L^3] to different main canals ($\boldsymbol{Q}_{CW,\ MCi}$, $\boldsymbol{Q}_{CW,\ MCj}$, $\boldsymbol{Q}_{CW,\ MCk}$). Canal water is then distributed to different calculation units ($\boldsymbol{Q}_{CW,\ CUi}$, $\boldsymbol{Q}_{CW,\ CUj}$, $\boldsymbol{Q}_{CW,\ CUk}$). $\boldsymbol{Q}_{CW,\ CUi}$ allocated to a particular calculation unit is then stored in an internal canal. Water requirements for different crop (WR_{CRi}, WR_{CRj}, WR_{CRk}) in the study area are computed and compared with the $\boldsymbol{Q}_{CW,\ CUi}$ to determine the quantity of groundwater to be pumped ($\boldsymbol{Q}_{TW,\ CUi}$). The actual amount of $\boldsymbol{Q}_{TW,\ CUi}$ is limited by the installed capacity of tubewells in the calculation unit. Sum of $\boldsymbol{Q}_{CW}$ and $\boldsymbol{Q}_{TW}$, $\boldsymbol{Q}$ is considered total water available for crops and is allocated to different crops ($\boldsymbol{Q}_{CRi}$, $\boldsymbol{Q}_{CRj}$, $\boldsymbol{Q}_{CRk}$). Eventually allocated water is applied to fields ($\boldsymbol{Q}_{Fi}$, $\boldsymbol{Q}_{Fj}$, $\boldsymbol{Q}_{Fk}$) through water courses/field channels and actual evapotranspiration is simulated. From the head of the main canals to the fields, losses take place at different levels: main canals ($\boldsymbol{L}_{MCi}$, $\boldsymbol{L}_{MCj}$, $\boldsymbol{L}_{MCk}$), internal canal ($\boldsymbol{L}_{IC,CUi}$), field channels/water courses ($\boldsymbol{L}_{WCi}$, $\boldsymbol{L}_{WCj}$, $\boldsymbol{L}_{WCk}$) and field plots ($\boldsymbol{L}_{Pi}$, $\boldsymbol{L}_{Pj}$, $\boldsymbol{L}_{Pk}$).

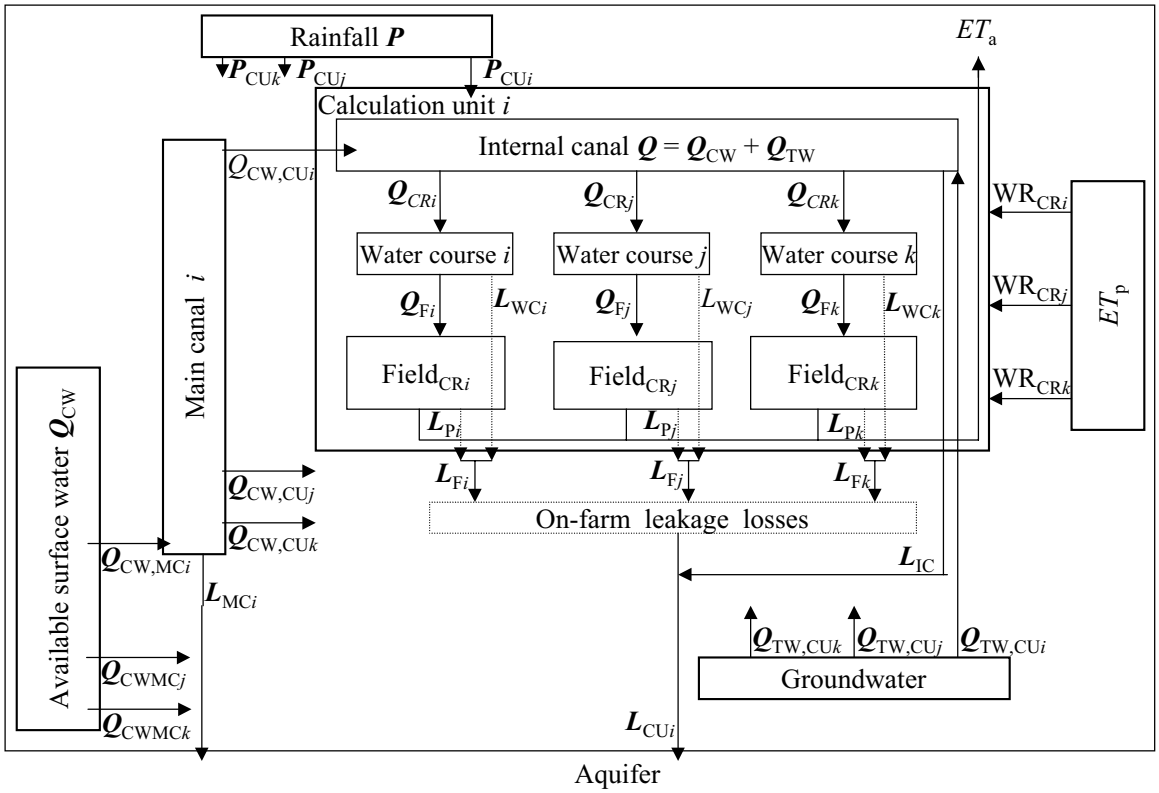

Figure 3.4. Representation of different water flow processes simulated by SIWARE for the Sirsa irrigation circle. The symbol $\boldsymbol{Q}$ stands for available water supply, $\boldsymbol{L}$ for leakage, and WR for water requirements. The subscripts CW denotes surface water (canal water + river water), TW tube-well water, MC main canal, IC internal canal, CU calculation unit, WC- water course, CR- crop and P-field plot

Allocation of water among main canals: The canal irrigation system in the study area is a typical supply based system. Water is supplied to different canals proportional to the irrigation command area and is independent of crop water requirements. For this study, the available annual canal water supply is divided into different time periods according to pre-set time distribution fractions. The time distribution fractions for each of the 16 time periods were computed from the records of daily flows of canal water supply to the study area and is supplied as an input to the model. Available water for different time periods $\boldsymbol{Q}_{CW}$ [L^3] is allocated among intakes of main canals based on the principle of proportionality between $\boldsymbol{Q}_{CW}$ and culturable command area A_{CCA} [L^2] served by each of the main canals.

$$\boldsymbol{Q}_{CW,MCi}(t) = \frac{A_{CCA,MCi}}{\sum_{MCi=1}^{ncnl} A_{CCA,MCi}} \boldsymbol{Q}_{CW}(t) \tag{3.11}$$

where $\boldsymbol{Q}_{\mathrm{CW,\ MC}i}$ is the water supply to main canal i, $A_{\mathrm{CCA,\ MC}i}$ cultural command area served by the main canal i, $\boldsymbol{Q}_{\mathrm{CW}}$ is total available canal water supply and *ncnl* is total number of main canals.

Leakage losses from main canals: Estimation of leakage losses from canals requires that the dimensions of the canal system are known. The design characteristics of various canals in the study area were used to derive empirical relations relating maximum discharge capacity, water depth, bed width and bed slope to the area served (*Kumar and Singh*, 1994). FRAME redesigns different canal sections according to derived relationships. A particular main canal serves a number of calculation units. Each main canal is described by a series of chained sections extending to the points where delivery to a calculation unit is assumed to take place. Starting in the most downstream canal section, the area served by each canal section is calculated by adding all area served. The area served by any branch canal is added to the area served in the upstream nodes of the connected canal. Through this procedure, area served by each canal section is obtained. Leakage losses from each of the defined canal section i is then computed depending on length, wetted area per unit length, depth of flow and radial resistance as:

$$\boldsymbol{L}_{\mathrm{MC}} = \left(\frac{X_{\mathrm{sl}i} A_{\mathrm{w}i} y_i}{R_{\mathrm{r}}} \right) \times t \tag{3.12}$$

where X_{sl} is section length [L], A_{w} wetted area per unit length of section [L], y depth of water [L] in the canal section, R_{r} radial resistance [T] and t is the time [T]. R_{r} is computed from a semi-empirical function derived from the tabulated values of the analytical solution (*Polubarinova-Kochina*, 1962) of the infiltration problem.

Allocation of water among calculation units: Discharge in the irrigation main canal system are reduced due to leakage losses. At each take-off in the water distribution system the available discharge is allocated proportional to the culturable command areas of the branches (Eq. 3.11). Water to different calculation units is allocated according to culturable command area of different calculation units.

Leakage losses from internal canals in calculation units: The conveyance network inside the calculation units are represented by a hypothetical internal canal, with length equal to the

total length of canals present inside the calculation unit, with a certain storage capacity, which is related to the culturable command area of the calculation unit. Any diverted but unused irrigation water is assumed to by-pass the soil and contribute directly to the recharge of the aquifer system. To this purpose, the excess water is diverted to hypothetical depressions where this water infiltrates. The leakage losses from internal canal are estimated similar to that from main canals.

Computation of water requirement: The study area have a number of crops during the *rabi* and *kharif* season. A maximum of 15 crops are included in the model computations: 7 during *rabi* season and 8 during *kharif* season. The small areas under the minor crops were added to the areas of the closest resembling major crops e.g. area under barley was added to area of wheat. ET_p is calculated from local meteorological data and is a tabulated input to the model as a function of crop characteristics (crop heights and soil cover). For each crop the following information must be supplied: planting date, harvesting date, number of irrigations and intervals between them, crop growth development (soil cover, root depth and crop height) and area under different crops and fraction of the reserved area under the crop during different intervals. Depending on the actual crop height and soil cover, potential evapotranspiration ET_p for different crops and irrigation intervals is computed.

Groundwater extraction: As a result of the inadequacy and unreliability of canal water supplies, farmers use groundwater. In the model, groundwater extraction ($\boldsymbol{Q}_{TW}$) is simulated for different calculation units based on available canal water supply $\boldsymbol{Q}_{CW,\ CUi}$, rainfall $\boldsymbol{P}$, crop water requirement WR and installed capacity of tubewells $\boldsymbol{Q}_{TW,\ max}$. Groundwater extraction is set equal to the minimum of *deficit* in water supply (WR - $\boldsymbol{Q}_{CW,\ CUi}$ - $\boldsymbol{P}$) and $\boldsymbol{Q}_{TW,\ max}$ and is given as:

$$\boldsymbol{Q}_{TW} = \min\left(deficit,\ \boldsymbol{Q}_{TW,max}\right) \tag{3.13}$$

Allocation of water to different crops: The distribution of available irrigation water quantity in a particular calculation unit $\boldsymbol{Q}$ [L^3] among different crops in the fields is a decision made by farmers. They decide about the water allocation during periods of unforeseen shortage of irrigation water. In the model, a fraction ε of the total water supplied is distributed in proportion to crop water requirement WR [L^3] and a fraction (1-ε) in proportion with the so

called farmers irrigation preference score value for each crop $fp_{,CRi}$. The higher priority crop receives a larger amount than the lower priority crops. The priority, an input to the model, is mainly based on the relative drought and salt tolerance of the crops. Based on the $fp_{,CRi}$, weighted deficit for each crop WD_{CRi} is calculated as:

$$WD_{CR\,i} = (1-\varepsilon)\boldsymbol{Q}\frac{WR_{CRi}}{\sum_{i}^{n} \mathrm{WR}_{CRi}} fp_{CRi} \tag{3.14}$$

The quantity of water to be allocated to each crop $\boldsymbol{Q}_{CRi}$ is determined as

$$\boldsymbol{Q}_{CR\,i} = \varepsilon\boldsymbol{Q}\frac{WR_{CRi}}{\sum_{i}^{n} \mathrm{WR}_{CRi}} + (1-\varepsilon)\boldsymbol{Q}\frac{WD_{CRi}}{\sum_{i}^{n} WD_{CRi}} \tag{3.15}$$

If the computed $\boldsymbol{Q}_{CRi}$ is greater than WR_{CRi}, the $\boldsymbol{Q}_{CRi}$ is set equal to WR_{CRi} and the excess is allocated among other crops in proportion to their weighted deficit.

On-farm conveyance losses: Water from the internal canal in a particular calculation unit flows to different field plots through water course/field channels. As a consequence leakage losses from these small channels do occur. The discharge capacity of the water course q_0 [L^3 T^{-1}] and leakage loss rate q_s [L^3 T^{-1}] is specified as an input to the model. Knowing q_0, net irrigation time t_n [T] is determined and the leakage losses from water courses $\boldsymbol{L}_{WC}$ [L] are computed as:

$$\boldsymbol{L}_{WC} = t_n \frac{q_s}{X_{pl} \times X_{pw}} \tag{3.16}$$

where X_{pl} is plot length [L] and X_{pw} plot width [L].

Net irrigation water reaching field plots $\boldsymbol{Q}_F$ [L^3] is computed as:

$$\boldsymbol{Q}_F = (q_0 - q_s)t_n \tag{3.17}$$

Field irrigation process: The study area was being irrigated exclusively with the surface irrigation method. In this method of irrigation, water is turned on to the field at one end of the plot, and flows to the other end of the plot. In the model, simulation of on-farm irrigation is carried out by using a water advance function (*Roest et al.*, 1993). Depending on the infiltration capacity of the soil, plot size, land slope and stream size, infiltration opportunity time along the length of field plot is computed. Infiltration opportunity time is used to compute depth of water infiltrated along the length of field plot. A definition sketch of the field irrigation process as simulated in the model is shown in Fig. 3.5

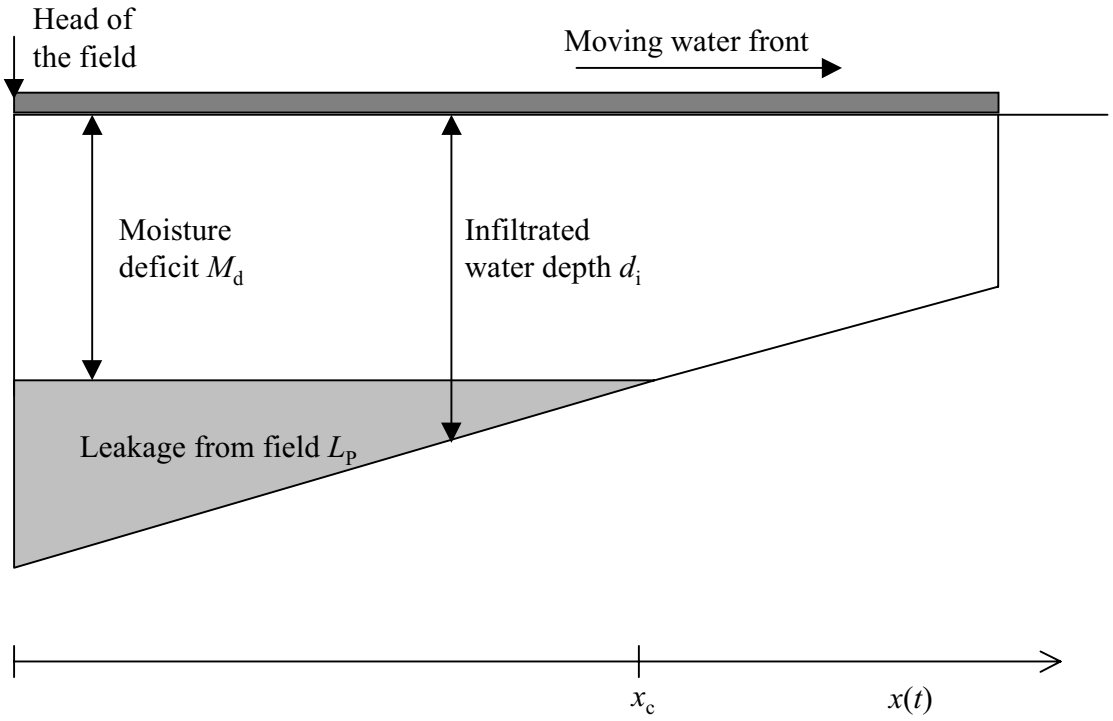

Figure 3.5. Definition sketch of field irrigation and leakage losses (adapted from *Roest et al.*, 1993)

Total leakage losses from field plot $\boldsymbol{L}_{\mathrm{P}}$ [L] is found by integrating the difference between net infiltrated water depth along the plot length d_{i} (x) [L] and soil moisture deficit M_{d} [L]:

$$\boldsymbol{L}_{\mathrm{P}} = \frac{1}{X_{\mathrm{pl}}} \int_{0}^{x_{\mathrm{c}}} \{d_{\mathrm{i}}(x) - M_{\mathrm{d}}\} dx \tag{3.18}$$

where x_{c} is critical distance [L] at which d_{i} is equal to M_{d}.

Actual evapotranspiration: The soil water between field capacity, θ_{fc} and wilting point, θ_{wp}, is considered as total available soil moisture, θ_{TAM} for plants. In addition to water stored in the root zone, 50 % of the water stored in the capillary zone, located below root zone, is considered to be available for plants. The capillary zone accounts for the upward moisture flow from the lower unsaturated wet soil layers to (partly) depleted upper soil layers. Daily actual evapotranspiration ET_{a} is simulated as follows:

$$ET_{\mathrm{a}} = \alpha_{\mathrm{sm}} ET_{\mathrm{p}} \tag{3.19}$$

Value of soil moisture availability factor α_{sm} [-] depends on θ_{TAM} and actual available soil moisture θ_{ASM} for all the layers in the root zone and capillary zone and is given by:

$$\text{if} \quad \theta_{\mathrm{ASM}} \geq \beta\, \theta_{\mathrm{TAM}} \qquad \alpha_{\mathrm{sm}} = 1 \tag{3.20a}$$

$$\text{if} \quad \theta_{\mathrm{ASM}} < \beta\, \theta_{\mathrm{TAM}} \qquad \alpha_{\mathrm{sm}} = \theta_{\mathrm{ASM}} / (\beta\, \theta_{\mathrm{TAM}}) \tag{3.20b}$$

The parameter β depends on crop type (threshold leaf water potential at which stomata close Ψ_{c}, ,bar), soil salinity (osmotic potential Ψ_{o}, bar) and ET_{p} (*Roest et al*., 1993):

$$\beta = \frac{0.51\, ET_{\mathrm{p}}}{(\psi_{\mathrm{c}} + \psi_{\mathrm{o}} - 0.1)} \tag{3.21}$$

Moisture distribution: In the model, the upper limit of water that an unsaturated soil layer can hold is limited to specified θ_{fc}. The time dependency of vertical moisture distribution due to rainfall or net irrigation depth I_n is neglected in the model. Rain water is assumed to refill layers only after filling preceding layers up to field capacity θ_{fc}. Soil moisture distribution after irrigation is formulated in such a way that the two-dimensional infiltration mechanism is accounted for (Fig. 3.5). Net soil moisture recharge I_n is computed as the value of water applied to the plot reduced with leakage losses. If I_n is equal to or exceed the sum of the moisture deficit in different layers, all layers are assumed to reach θ_{fc}. If I_n is less than the sum of the moisture deficit in different layers then I_n is distributed among these layers proportional to the relative of actual moisture deficit for each layer as:

$$\theta(i) = \theta_{t0}(i) + \frac{\theta_{fc} - \theta_{t0}(i)}{\sum_{i=1}^{n} (\theta_{fc} - \theta_{t0}(i)) z_i} I_n \tag{3.22}$$

where θ is moisture content after irrigation, θ_{t0} moisture content before irrigation, z_i thickness [L] of layer i and n is the number of unsaturated layers.

Salt distribution: Salt transport through the boundary of each soil layer is assumed to take place with the mass transport of water. Two different situations are considered for salt transport: downwards movement due to irrigation/rainfall and upward movement due to evapotranspiration and capillary flow. Assuming complete and instantaneous mixing in each soil layer, the transport and conservation equation is formulated as:

$$\frac{d(\theta.z.c)_i}{dt} = \sum (f_{in} c_{in})_i - \sum (f_{out} c_{out})_i \tag{3.23}$$

where z is layer thickness [L], c is salt concentration [M L^{-3}], f water flux [L T^{-1}] and subsrcipt 'in' stands for incoming flux, 'out' for outgoing flux and i for layer number.

Net recharge computation: The net recharge from the top system to the aquifer is the major linking factor between SIWARE and SGMP. Based on L_P from field plots, L_{WC} from water

courses and deep percolation due to rainfall, SIWARE computes hypothetical groundwater head, called shallow groundwater head $h_{shallow}$. The groundwater head h_{gw} as simulated in SGMP nodes is used to compute groundwater head in CUs, called deep groundwater head h_{deep}. The leakage $\boldsymbol{L}_F$ [L] from hypothetical shallow groundwater to the actual groundwater in then computed as:

$$\boldsymbol{L}_F = \frac{h_{shallow} - h_{deep}}{R_{cc}} t \tag{3.24}$$

where R_{cc} is the resistance [T] against vertical flow from shallow to deep groundwater levels and t is the time [T].

The net water losses from calculation unit $\boldsymbol{L}_{CU}$ to aquifer is computed as:

$$\boldsymbol{L}_{CU} = \boldsymbol{L}_F + \boldsymbol{L}_{IC} - \frac{\boldsymbol{Q}_{TW}}{A_{CU}} \tag{3.25}$$

where A_{CU} is area [L^2] of calculation unit.

Transfer functions, using matrix of fractional areas, convert $\boldsymbol{L}_{CU}$ to the leakage from calculation units to nodes $\boldsymbol{L}_{CU,\,node}$. Leakage from main canals to groundwater nodes $\boldsymbol{L}_{MC,\,node}$ (= $\boldsymbol{L}_{MC}$/Area of node) is directly assigned to underlying nodes. Likewise leakage from river to groundwater nodes $\boldsymbol{L}_{R,\,node}$ is also directly assigned to underlying nodes. The net recharge to nodes $\boldsymbol{L}_{net}$ is computed as

$$\boldsymbol{L}_{net} = \boldsymbol{L}_{CU,node} + \boldsymbol{L}_{MC,node} + \boldsymbol{L}_{R,node} \tag{3.26}$$

The net recharge determines to a large extent the groundwater level tendency in an area. When it is too large, a rising tendency may be expected resulting eventually in waterlogging problems. The net recharge can also be negative, for instance when $\boldsymbol{Q}_{TW}$ is very large and may cause a decline in groundwater level .

Crop rotation: In practice, a crop rotation is a result of many factors including harvest date of preceding crop and sowing date of proceeding crop, previous irrigation history of particular field plot (especially for rain-fed crops), need to grow certain area of certain crops for optimising farmers income, control of soil salinity or control of disease. Different crop

rotations may occur in the same calculation unit e.g. wheat-cotton, oilseed-cotton, pearlmillet-cotton etc. In the model, a score value is assigned for a certain crop to be grown after another crop. A high score value means that most probably the considered crop will be grown after the crop for which it has such a high preference. When a crop is to be grown after a number of preceding crops, initial salinity and moisture conditions depends on the conditions at the end of the growing season of preceding crops. In the model, however, only one standard plot is considered, that represents the average conditions of the preceding crops. Initial conditions on this plot are, for this reason, weighted average of end conditions on the standard plots of preceding crops. For example, let cotton in a particular calculation unit has to occupy 100 ha area and it has preference, in decreasing order, for wheat (let area under wheat is 70 ha) and oilseed (let area under oilseed 50 ha). In this case cotton will take 70 ha of wheat field and 30 ha of oilseed. Since only one standard plot is defined for cotton, the initial conditions for the plot allocated to cotton will be weighted average of the end conditions for the plots of wheat (70 %) and oilseed (30 %).

In the model, planting or sowing starts on a single day, while in reality this occurs during a certain period. The area increases gradually. The model allows for a gradual increase of cropped area after the planting or sowing date. In the model, harvesting of a particular crop takes place in a single day for the complete area.

***Groundwater model package SGMP*:** SGMP is a numerical program package for the simulation of two-dimensional groundwater flow in unconfined, confined and semi-confined aquifer conditions. However, *for the present study, only unconfined aquifer conditions are assumed.* SGMP is based on Darcy's law and the equation of conservation of mass. Combination of these two equations results in a partial differential equation for unsteady flow:

$$\frac{\partial}{\partial x}\left(KH\frac{\partial h}{\partial x}\right)+\frac{\partial}{\partial y}\left(KH\frac{\partial h}{\partial y}\right)=-N \tag{3.27}$$

where K is saturated hydraulic conductivity of the aquifer [L T^{-1}], H saturated thickness [L] of the aquifer, h hydraulic head [L] in the aquifer and N sink [L T^{-1}] term.

For unconfined aquifers N is defined as:

$$N = L_{\text{net}} - S_{\text{y}} \frac{\partial h}{\partial t} \tag{3.28}$$

where L_{net} is net recharge [L T^{-1}], S_{y} is specific yield [-] of the aquifer. Neglecting the effects of elasticity of aquifer material and fluid in unconfined aquifers, S_{y} may be considered to equal to the effective porosity or drainable pore space.

Eq. 3.27 is solved through an implicit finite difference technique (*Richtmeyer and Morton*, 1967). This requires that the space (study area) be divided into small intervals. The sub areas thus formed are called nodal areas. It is assumed that all recharge and abstraction in a nodal area occurs at the node (central point of a nodal area). To each node a certain value of S_{y} is assigned, which is constant and representative for that nodal area. Different K values can be assigned to the sides between nodal areas, thus allowing anisotropic conditions. The model computes groundwater heads and groundwater flow between different nodes. The groundwater heads are computed based on recharge and abstraction rate occurring at each node. In the present case these are calculated with SIWARE. The movement in the horizontal direction is calculated from the heads in the nodes. In order to couple SGMP with SIWARE, SGMP is split into two parts i.e. SGMP1 and SGMP2.

SGMP1 is a pre-processing program for the integrated model. It is executed at the start of a simulation run with the integrated model. The data required are the time independent parameters like geometry of the nodal network and the geohydrological parameters. Based on the initial groundwater depth data, SGMP1 calculates the aquifer thickness data and the corresponding transmissivity data to be used by SGMP2. Aquifer thickness based on initial groundwater depth data implies an unconfined aquifer.

SGMP2 is the actual groundwater model that performs the calculations for saturated groundwater flow. It is repeatedly executed for each time step in a simulation run with the integrated model. In addition to the pre-processed data obtained from SGMP1, it requires nodal net recharge values. The nodal net recharge values are computed from the water balance components simulated in SIWARE (Eq. 3.26). The output of SGMP2 includes groundwater heads at all the nodes, change in storage and horizontal groundwater flow between different

nodes. It is assumed that neither recharge nor discharge take place through the base of the aquifer system. The nodes at the boundary are provided with known groundwater heads.

3.3 Parameter estimation program PEST

PEST (Parameter ESTimation) is a non-linear parameter estimation program which can easily be linked via templates to any model (*Doherty et al.*, 1995). PEST runs the particular model, compares the model results with target values (e.g. observations), adjusts selected parameters using an optimization algorithm, and runs the model again (Fig. 3.6). This continues until the difference between the model results and observations, or the number of iterations, meet a pre-set criterion.

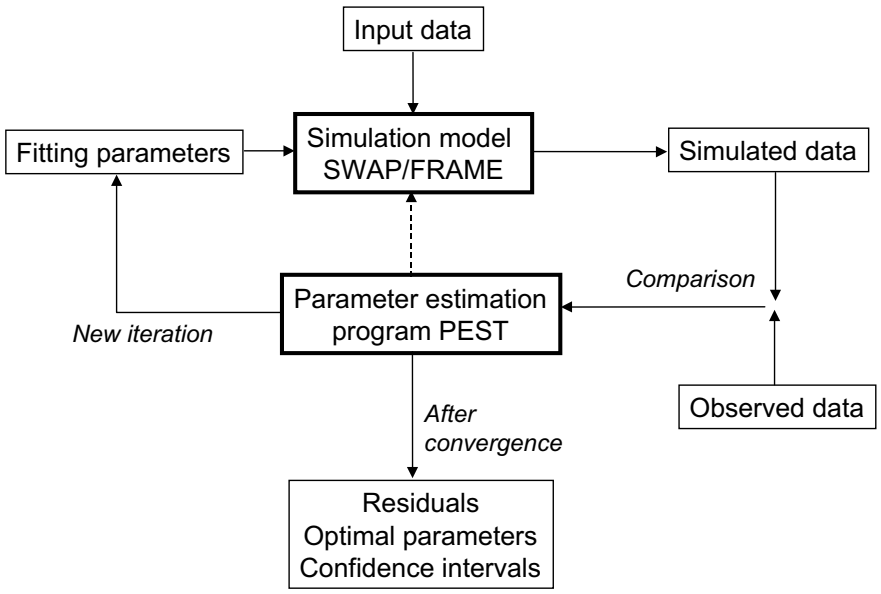

Figure 3.6. Overview of the parameter estimation procedure employed using PEST and the simulation models SWAP and FRAME

The inverse parameter estimation is a non-linear optimization problem, where a vector **b** containing the unknown parameters of the constitutive relationship is estimated by minimizing an objective function. An objective function quantifies the differences between

model results and observations. Assuming that model errors are zero, the difference between observation and corresponding prediction may be designated as observations error. If the observation error follow a multivariate normal distribution with zero mean, no correlation, and constant variance for each measurement type, maximization of the probability of reproducing the observed data leads to weighted least squares objective function Φ (*Bard*, 1974; *Kool* and *Parker*, 1988; *Press et al*., 1989; *Doherty et al*, 1995):

$$\Phi(\mathbf{b}) = \sum_{j=1}^{m}\left[\sum_{i=1}^{n_j}\left(w_{ij}\left(y_j^*(t_i) - y_j(t_i,\mathbf{b})\right)\right)^2\right] \tag{3.29}$$

where **b** is the vector with fitting parameters, *m* represents the different sets of measurements, n_j is the number of measurements in a particular measurement, $y_j^*(t_i)$ denotes the observation of type j at time t_i, $y_j(t_i, \mathbf{b})$ is the corresponding model prediction and w_{ij} is the weight associated with a particular kind of measurement at a particular point and accounts for the role of data type and data point in the objective function. It appears that there are many possible ways to choose the weighting factors and their choice can affect the optimized parameter set (*Weiss and Smith*, 1998). Better guidelines are needed to provide the rationale for selecting proper weighting factors (*Hopmans and Šimůnek*, 1999). In case of random observation errors only, according to maximum likelihood the weighting factor w_j should be equal to the inverse of the standard deviation of the observation error of observation type j. The use of standard deviation as weighting factor also effectively accounts for measurements unit differences between observation types. *Gribb* (1996) weighted each different data type by the inverse of the mean values, which can be thought of as an approximation to weighting by the inverse of the variance.

The objective function is a non linear function of **b**, so that minimization calculations must be carried out iteratively until pre-defined convergence criteria are satisfied. Inverse problems in which more computation intensive simulation models are used, require an efficient optimization algorithm to arrive at the optimal parameter set with a limited number of model calls. The optimization algorithm used by PEST is derived from Gauss-Marquardt-Levenberg, which starts with searching mainly along the steepest gradient of the objective function surface and gradually switches to a direction based on a second order approximation of the objective function surface (*Marquardt*, 1963; *Press et al.*, 1989; *Doherthy et al.*, 1995).

Experiences in soil water flow modelling show that the Gauss-Marquardt-Levenberg method is very efficient in optimization, in the sense of a minimum amount of model calls (*Cooley*, 1985; *Clausnitzer* and *Hopmans*, 1995; *Finsterle* and *Pruess*, 1995; *Olsthoorn*, 1998). In case of a large number of parameters as compared to the number and quality of observations, the response surface of the objective function may not show a dominant global minimum, but instead a scatter of local, equally sized minima. In such a case, the Gauss-Marquardt-Levenberg optimization search may end up in a local minimum, due to its initial descending along the steepest gradient and its switching to a second order approximation of the objective function surface near a minimum. PEST program partly circumvents local minima by evaluating the objective function with a number of Marquardt values (*Doherthy et al.*, 1995). Still it is recommended to repeat optimization runs with different initial parameter values, in order to check the uniqueness of the results.

Chapter 4

Inversely estimating soil hydraulic functions for *homogeneous* soils using evapotranspiration rates[1]

4.1 Introduction

Soil water flow in physical-mathematical models is often described by the Richards' equation. Application of unsaturated soil water flow theory requires that the relationships between soil water pressure head h, hydraulic conductivity k, and volumetric soil water content θ are known. The relationships between h and θ and k and θ are described respectively by the water retention curve and the hydraulic conductivity function. These are usually referred to as soil hydraulic functions. The evaluation of the soil water balance of the unsaturated zone using simulation models relies strongly on an appropriate characterisation of the $h(\theta)$ and $k(\theta)$ relationships (*Xevi et al.,* 1996). Therefore, reliable estimates of site and region specific soil hydraulic functions is very crucial to a meaningful application of these models. However, obtaining estimates of these functions can be an onerous task. Our ability to mathematically model water movement in the subsurface seems to be well ahead of our ability to accurately quantify the flow and transport properties of the soils (*Wessolek et al.,* 1994).

Laboratory as well as field methods have been developed for the measurement of $h(\theta)$ and $k(\theta)$ relationships (*Dirksen*, 1991) but not a single method has been developed that performs well in a wide range of circumstances and for all soil types. During the past decade many investigators have proposed estimating simultaneously the $h(\theta)$ and $k(\theta)$ relationships from a transient flow experiment by employing the inverse problem methodology (see *Romano and Santini*, 1999).

Inverse methods use non-linear parameter estimation procedures to derive the soil hydraulic functions from a measured flow event, either in the laboratory or in the field. Certain functions for the hydraulic properties are assumed and the parameters in these functions are estimated by using an optimisation procedure, which minimises the discrepancies between the observed and simulated responses of the system. Inverse modelling has been applied to determine soil

[1] Adapted version of Jhorar, R.K., W.G.M. Bastiaanssen, R.A. Feddes and J.C. van Dam. 2002. Inversely estimating soil hydraulic functions using evapotranspiration fluxes. Journal of Hydrology, 258: 198-213.

hydraulic function for laboratory scale problems (*Kool et al.,* 1987; *Van Dam et al.*, 1994) by fitting a solution of Richards' equation to observations of transient outflow. Unfortunately, laboratory fitted functions are often non-representative when used for field scale model applications. Once a complex variable like actual evapotranspiration ET_a can be derived for a given area from remote sensing measurements, ET_a at known boundary conditions can be used inversely to identify the so called '*effective'* soil hydraulic functions (*Feddes et al*., 1993a, b).

Recently estimates of surface soil moisture (*Schmugge et al*., 1992) and ET_a rates (*Rosema*, 1990) for larger flow domains have become available using remotely detectable quantities. Attempts have been made to inversely assess soil hydraulic functions using observations on soil moisture obtained through passive microwave remote sensing techniques (*Burke et al*., 1997, 1998). Unfortunately, the passive microwave approach refers to only the top few centimetres (~ 5 cm) of the soil profile. For many application studies involving field as well as regional water management, knowledge of soil hydraulic properties for the entire root zone is required. The ET_a under unstressed conditions is determined mainly by the atmospheric demand. However, under non-optimal soil moisture conditions, ET_a reflects the integrated effect of moisture distribution over the root zone which, in turn, depends on the soil hydraulic properties, the root distribution and the drought and salt tolerance of the crop. ET_a can be measured with several field methods. The concept of surface energy balance determinations from satellites has been widely studied during the past few years (*Moran and Jackson*, 1991; *Bastiaanssen et al*., 1998). In fact, energy balance for the surface boundary layer is one of the most widely used methods for ET_a estimation (*Tan and Shih*, 1997).

The objective of this study is to investigate the potential of inverse modelling of ET_a and actual transpiration T_a to derive '*effective'* soil hydraulic functions for irrigated soils under arid (Indian) regions having deep groundwater level conditions. Inverse results have been examined for three soil types. Issues that are addressed include: effect of a number of unknown parameters of the selected soil hydraulic function model, effect of measurement frequency of ET_a estimates, and effect of random errors in the ET_a rates on the hydrological behaviour of fitted soil hydraulic functions. Fitted soil hydraulic parameters do not necessarily have a physical meaning. Therefore, hydrological behaviour of fitted soil hydraulic functions have been examined with the simulation model SWAP (*Feddes et al*., 1978; *Van Dam et al.*, 1997) to assess the applicability and reliability of using ET_a rates to inversely estimate soil hydraulic functions.

The potential of deriving *effective* soil hydraulic functions by inverse modelling of ET_a and T_a rates is examined by forward as well as backward simulation of soil water flow by means of the simulation model SWAP. The basic features of SWAP are described in Chapter 3. Forward simulations are carried out to generate hypothetical ET_a rates as if these were available from independent measurements. Two objective functions are defined to test their suitability during optimizations. Backward simulations are carried out to estimate different parameters of the soil hydraulic function model proposed by *Van Genuchten* (1980).

4.2 Forward simulations with SWAP and parameter estimation procedure

***Forward simulations**:* Forward SWAP simulations were carried out for three soil types, designated as S1, S2 and S3 (Table 4.1), for deep groundwater level situations by specifying free drainage of the soil profile as the lower boundary condition. The soil S1 (94% sand, 5% clay), S2 (83% sand, 6% clay) and S3 (46% sand, 30% clay) typically represent a sand, loamy sand and sandy clay loam soil of the USDA classification.

Table 4.1. Van Genuchten model parameters for the three soil types used for forward SWAP simulations

Soil code*	θ_{sat}	θ_{res}	α (cm^{-1})	n	λ	k_{sat} (cm d^{-1})
S1	0.413	0.006	0.0200	2.37	0.500	350
S2	0.473	0.010	0.0130	1.74	0.500	250
S3	0.524	0.010	0.0243	1.53	0.638	55

* S1, S2 and S3 respectively represents a sand, loamy sand and sandy clay loam soil according to the USDA soil textural classification

The *Van Genuchten* (VG) model parameters for the three soil types, are based on an earlier SWAP calibration against $\theta(z,t)$ observed during field experiments at Hisar and Sirsa, India (*Bastiaanssen et al.*, 1996). Under most field conditions, root-zone soil profiles usually consists of hydraulically different soil layers whose sequence strongly influences different processes acting in the root zone viz., infiltration, redistribution, soil water storage etc. Before

a new technique can be applied under such more complex situation, it is important to examine its conceptual feasibility. Accordingly, in this Chapter only uniform soil profiles are considered to examine the possibility of inversely identifying effective soil hydraulic functions using ET_a rates. As a follow up of this study (Chapter 5), the feasibility of proposed technique has been examined for heterogeneous soil profiles.

All simulations start from the assumed date of sowing (June 26) of cotton. Soil matric pressure head corresponding to h = -200 cm (pF 2.3) was specified as initial condition for all the soils. Meteorological data from the Haryana Agricultural University Hisar (India), representing an arid climate, were used. The sink term variables required for reduction in ET_a due to moisture stress according to Fig. 3.2 (h_1 = -10 cm; h_2= -25 cm; h_{3h}= -400 cm, h_{3l} = -800 cm and h_4=-16000 cm) used are those calibrated for a cotton crop grown in a field experiment at Sirsa, India (*Bastiaanssen et al*., 1996). Simulations cover the growing season of cotton crop for 160 days. Five post sown irrigations, each 60 mm, are specified at Day 51, 72, 97, 118 and 143. Day 1 represents the day of sowing.

Daily SWAP outputs of T_a and E_a between Day 100 and 160 were summarised in a time series and sampled to provide ET_a and T_a rates for the inverse modelling exercise. The sampling period was selected such that the crop is fully developed and under actual conditions the ET_a rates will be affected by maximum depth of soil profile.

Parameter estimation procedure: Assuming that for any time t_i , $ET_a(t_i)$ and $T_a(t_i)$, can be obtained independently (in this chapter forward model simulations were used), these data can be employed as input data for the numerical inversion problem. Let $ET_a(b,t_i)$ and $T_a(b,t_i)$ be the numerically calculated values of ET_a and T_a, respectively, corresponding to a trial vector of parameter values $\{\boldsymbol{b}\}$, where $\{\boldsymbol{b}\}$ is the n-dimensional vector containing the parameters that are optimised simultaneously. The inverse problem then is to find an optimum combination of parameters $\{\boldsymbol{b}^o\}$ that minimises either of the following objective functions:

$$\Phi(b) = \Sigma \{w_i[ET_a(t_i) - ET_a(t_i, \boldsymbol{b})]\}^2 \quad (4.1)$$

$$\Phi(b) = \Sigma \{w_i[T_a(t_i) - T_a(t_i, \boldsymbol{b})]\}^2 \quad (4.2)$$

where w_i is a weighting function. The Eqs. 4.1 and 4.2 are, hereafter, referred as *ET* -based and *T* -based objective functions, respectively. The model independent Parameter ESTimation program PEST (*Doherty et al*., 1995) was used to determine $\{\boldsymbol{b}^o\}$. It adjusts the model parameters until the fit between model outputs and observations is optimised in the weighted least square sense. PEST does this by taking control of the model and running it as many times as is necessary in order to determine the optimal set of adjustable parameters. A brief description of PEST is included in Chapter 3.

The parameter estimation procedure was examined for all the three soils in Table 4.1 with deep groundwater level conditions. The data set on ET_a and T_a for the selected days of the SWAP model output as generated with the forward simulations constituted input to the objective functions (Eqs. 4.1 and 4.2) of the inverse problem. In practice such data on ET_a could be acquired from advanced field measurement techniques or from satellite images. The data on T_a were considered anticipating their availability in future, for instance by suitably partitioning remotely sensed ET_a into E_a and T_a. Rather sparse sampling strategy was chosen to represent the constraints on independent ET_a measurements. One of the scenarios investigated for improving the accuracy of soil hydraulic parameter estimations was more frequent sampling of ET_a and T_a rates.

A standard inverse method require that the inverse problem be well posed and well conditioned, so that the solution exists and is unique and stable (*Romano and Santini*, 1999). General information on ill-posedeness and parameter identifiability can be found in *Hopmans and Simunek* (1999). In general, parameter identifiability can be improved by reducing the number of optimized parameters. A number of parameter estimation runs were carried out with different combinations of VG model parameters (Table 4.2) to explore the possibility as to which parameters can be estimated using ET_a or T_a rates.

For parameter set-1, all the VG model parameters are allowed to be optimised. Realising that at least two parameters (θ_{sat} and k_{sat}) of the VG model have a clear physical meaning and can be obtained from field measurements, the parameter set-2 was designed by setting θ_{sat} and k_{sat} at the known values of Table 4.1. It is important to note that, k_{sat} varies strongly between soil types (*Clapp and Hornberger*, 1978; *Cosby et al.*, 1984; *Wosten et al.*, 1995) and also with the

scale (*Quintard and Whitaker,* 1988; *Stam et al.*, 1989). The Darcy parameterization prescribes a linear relationship between the flux density and the hydraulic potential gradient. Unlike the unsaturated conductivity, the k_{sat} does not depend on flux density or the soil water potential. In the case of k_{sat}, the averaging in both horizontal and vertical directions can be done without explicit a priori knowledge of the small scale solutions of the soil water fluxes. In principle, large scale vertical k_{sat} of multi-layer profiles can be determined as harmonic mean in the vertical direction of the arithmetic mean of small scale conductivity in the horizontal (spatial) direction (*Kabat et al.*, 1997). The parameter set-3 was designed to estimate only the $h(\theta)$ relationship by setting k_{sat} and λ at known values. For parameter set-4, an additional parameter θ_{res} was also set at known values, as θ_{res} represents the residual moisture content which for many soils can be assigned a value near to zero (*Russo*, 1988). A uniform initial guess of different VG model parameters was specified for all the three soils. The initial values of VG model parameters as specified during backward simulations were: $\theta_{sat} = 0.4$; $\theta_{res} = 0.0$; $\alpha = 0.01$ cm^{-1}; $n = 2.5$; $\lambda = 0.5$ and $k_{sat} = 200$ cm d^{-1}.

Table 4.2. Summary of different soil hydraulic VG model parameter sets used for backward simulations.

Parameter set	Description
Set-1	All parameters optimised
Set-2	All parameters, except θ_{sat} and k_{sat} optimised
Set-3	All parameters except k_{sat} and λ optimised
Set-4	Only α, n and θ_{sat} optimised

4.3 Evaluation criteria for inversely estimated parameters

Traditionally, reliability of estimated parameters is evaluated based on statistical properties (e.g. bias, standard deviation) of fitted values (*Wagner and Gorelick*, 1986). However, these parameter estimates may be meaningless if the model fails to reliably reproduce salient features of particular interest. The ultimate objective of this study is to derive soil hydraulic functions appropriate to develop and test alternative water management practices in an irrigation context. A water budget for unsaturated zone consists of principal inflows and outflows for depth of

interest and the resulting change in water storage ΔW. For irrigated arid and semi-arid regions with deep groundwater level, the principal inflows are rainfall P and irrigation I and the principal outflows are ET_a and deep percolation Q_{deep}. The water balance [L] for such areas can be described by:

$$\Delta W = P + I - ET_a - Q_{deep} \tag{4.3}$$

where Q_{deep} is taken positive downward.

Fundamental to the adopted inverse procedure is that VG model parameters are fitted in such a way that the ability of the model to reproduce ET_a (or T_a) rates is optimised. It is well recognised that the fitted parameters may not have a physical meaning. A possible correlation between them means that many combinations of the parameters could fit the data (in this case ET_a or T_a rates) equally well (*Snow and Bond*, 1998), so casting doubt on the values of simultaneously optimised parameters. Therefore, it is important to know how fitted VG model parameters will reproduce other water balance components such as ΔW and Q_{deep}. Accordingly, this study do not intend to derive precise parameter values, rather an attempt is made to derive effective soil hydraulic functions which can be reliably used for simple water balance computations. It may also be potentially incorrect to use inversely estimated parameters to conditions different than those present in the original inversion experiment (*Hollenbeck and Jensen*, 1998). Therefore, the performance of fitted soil hydraulic functions was evaluated by studying the overall hydrological consequences of these functions for a different irrigation regime than that was used during parameter optimisation.

4.4 Sampling strategy and sensitivity of T_a to VG model parameters

***Sampling strategy*:** Examination of temporal ET_a behaviour for different soils has an important significance in the present investigation. It is required for two specific purposes: whether, under similar conditions, different soils act differently and if so, to decide appropriate crop period which is suitable to inversely identify soil hydraulic functions. The time series of simulated ET_a/ET_p, E_a/E_p and T_a/T_p for cotton crop on the three soils (Table 4.1) under deep groundwater

level condition is depicted in Fig. 4.1a – 4.1c. The five peaks in the simulated ET_a rates are the result of specification of five irrigation events during the growing season. Although the same initial and boundary conditions were specified, the simulated ET_a, E_a and T_a behaviour for all the three soils is quite different except immediately after an irrigation event when soil moisture conditions are sufficient to meet nearly potential demand. Note the ET_a, E_a and T_a behaviour after Day 100, particularly during the intervening period of different irrigation events i.e between Day 107-117 (irrigation being at Day 97 and 118) and between Day 130-142 (irrigation being at Day 118 and 143). This suggests that during moisture stress period, which is often encountered in the arid regions, these fluxes have the potential to be utilized for the inverse problem. However, E_a, like surface soil moisture, is usually controlled by only the top few centimetres of soil. Any parameter estimated by utilising E_a alone would represent the soil hydraulic functions of only top few centimetres of the soil. Moreover, applicability of the Richards' equation for top few centimetres of soil is also questionable due to the effects of splashing rain, dry crust formation and cultivation practices on the soil hydraulic functions. Note the difference between ET_a (Fig. 4.1a) and T_a (Fig. 4.1c) behaviour for the period covering day 143-160. During this period it is difficult to identify soil type based on ET_a behaviour, but the T_a behaviour is quite different for the three soils. This suggests that the use of T_a rates may be more appropriate to identify soil hydraulic functions.

The following conclusions regarding sampling strategy may be drawn at this stage. Either T_a rates are used for the inverse mode or crop period is selected in such a way that the ET_a component is mainly due to T_a, which happens when the crops are fully developed i.e. fully covering the soil. Therefore, T_a and ET_a data for the present inverse problem (Eqs. 4.1 and 4.2) are sampled from the period covering 100 days after sowing.

Sensitivity of T_a to VG model parameters: Having established that different soils act differently with respect to ET_a rates, the next logical step is to study the sensitivity of these fluxes to different parameters of the selected expression (Eqs. 3.4 and 3.5) of soil hydraulic functions. Considering the problems associated with the simulation of E_a under actual field conditions, the sensitivity of simulated T_a to θ_{res}, θ_{sat} α, n, k_{sat} and λ is studied by varying each parameter in turn. The root mean square error (RMSE) between the reference and modelled T_a for the selected sampling period (Day 100-160) is presented in Fig 4.2.

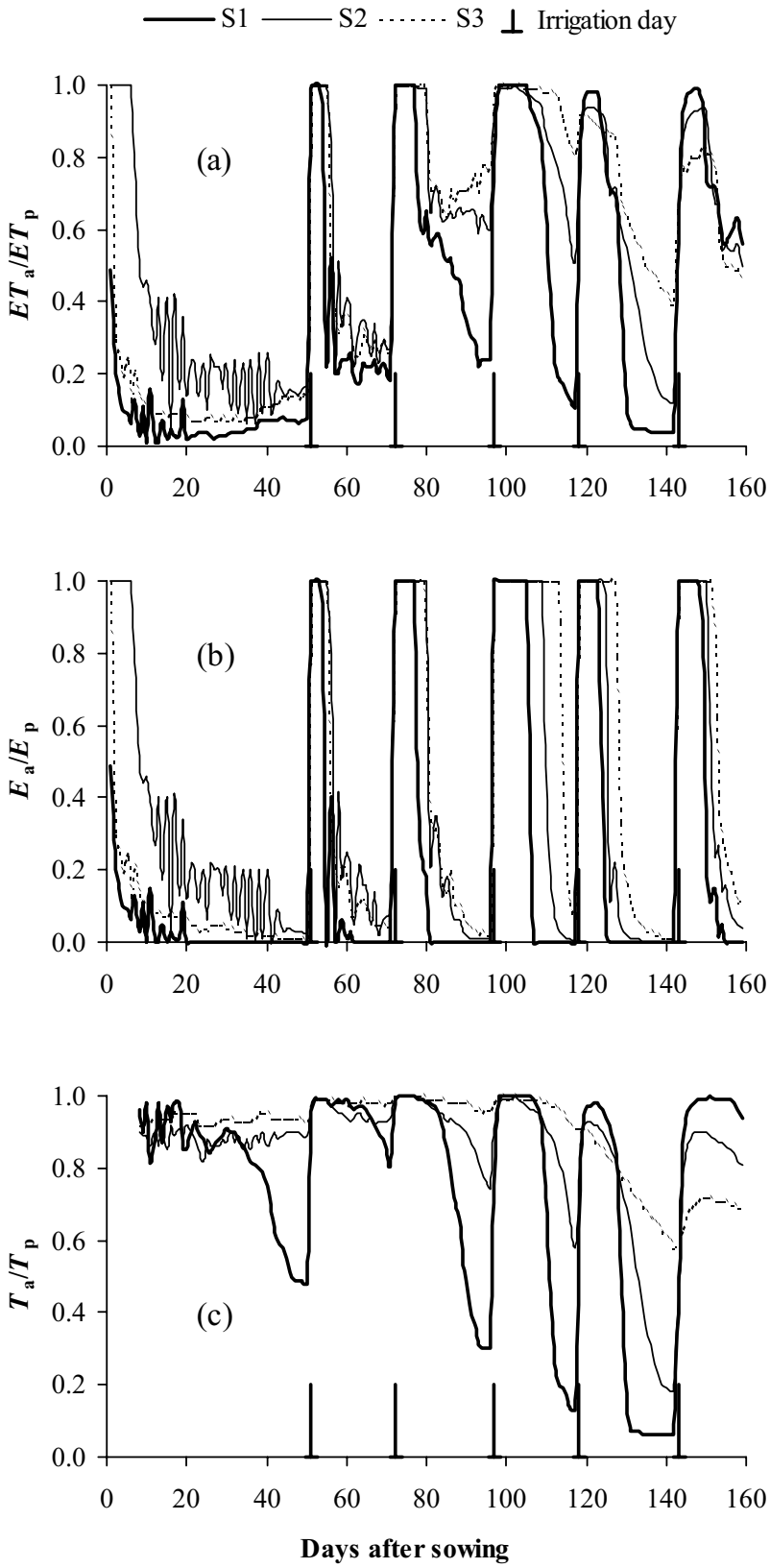

Figure. 4.1. Results of forward SWAP simulations for the three soil types as in Table 4.1. (a) relative evapotranspiration (ET_a/ET_p), (b) relative soil evaporation (E_a/E_p) and (c) relative transpiration (T_a/T_p) for cotton crop under deep groundwater conditions

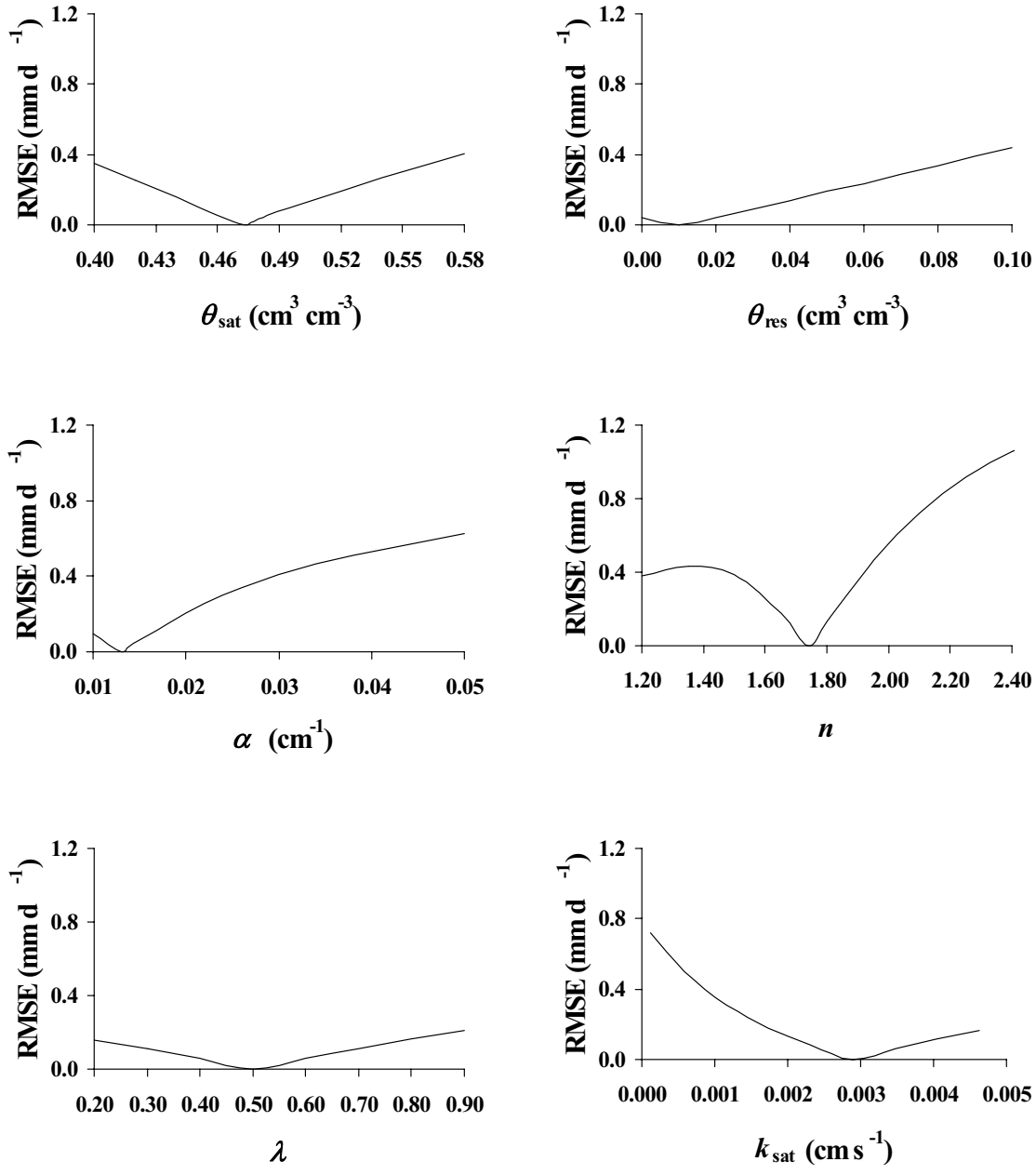

Figure 4.2 The root mean square error (RMSE) of the simulated transpiration as a function of the VG model parameters

The reference parameter set for this sensitivity analysis is that of loamy sand soil (Soil S2, Table 4.1). The range over which the parameters were varied was set according to the three soil types considered in the forward simulations. T_a is sensitive to all the VG model parameters with maximum sensitivity to parameter '*n*' and minimum to parameter 'λ'. This sensitivity analysis indicates the possibility of estimation the VG model parameters using ET_a rates.

4.5 Performance of inversely identified soil hydraulic parameters

No error in ET_a: The adopted parameter estimation methodology was tested, using exact (forward simulated) ET_a and T_a observations. First, ET_a and T_a rates for seven selected days (t=115, 125, 130, 135, 140,150,159) were used as input to the objective functions (Eqs. 4.1 and 4.2). It was only possible to exactly fit parameter set-4 (see Table 4.2 for details about different parameter sets) for loamy sand and sandy clay loam soils, when T- based objective function (Eq. 4.2) was used. Next, the number of observations were increased to 12 by including five more ET_a and T_a rates for t = 100, 105, 110, 120 and 145 day. With this increased frequency of observations, the parameter set-4 was fitted exactly for all the three soils when either ET- or T-based objective functions were used. This increased frequency of observations could not exactly fit other parameter sets. However, the bias, defined as the difference between actual value and fitted value, for different VG model parameters got reduced with the increased number of observations in the objective function.

As mentioned earlier, the performance of fitted soil hydraulic functions was evaluated by their capability to reproduce the hydrologic behaviour of soils. A verification numerical experiment, therefore, tested the hydrological behaviour of different fitted parameter sets through simulation of seasonal water balance of cotton crop. Care was taken to minimise any discrepancies, resulting due to initial conditions, in the simulated hydrological behaviour, particularly $\boldsymbol{Q}_{deep}$. The initial profile condition specified for each verification experiment was such that for zero flux condition at the soil surface, the $\boldsymbol{Q}_{deep}$ past 150 cm depth was just negligible (≈ 0.009 cm) for a period of 160 days. Thereafter, simulations were performed for cotton crop by specifying 20 cm irrigation on Day 1, and 5 post sown irrigation each of 10 cm (instead of 6 cm during inverse optimisation). Seasonal simulated water balance components ($\boldsymbol{ET}_a$, ΔW and $\boldsymbol{Q}_{deep}$) for the reference and fitted soil hydraulic functions are presented in Figs. 4.3-4.5. The figures shows the effect of ET- or T- based objective function, frequency of observations and different parameter set on the hydrological behaviour of fitted soil hydraulic functions. Not much difference is observed in the simulated $\boldsymbol{ET}_a$ (Fig. 4.3) and ΔW (Fig. 4.4). However, considering simulated $\boldsymbol{Q}_{deep}$ (Fig. 4.5), the T-based objective function performs better than ET-based objective function, particularly for soil S1, when the number of input observations on ET_a rates are 7.

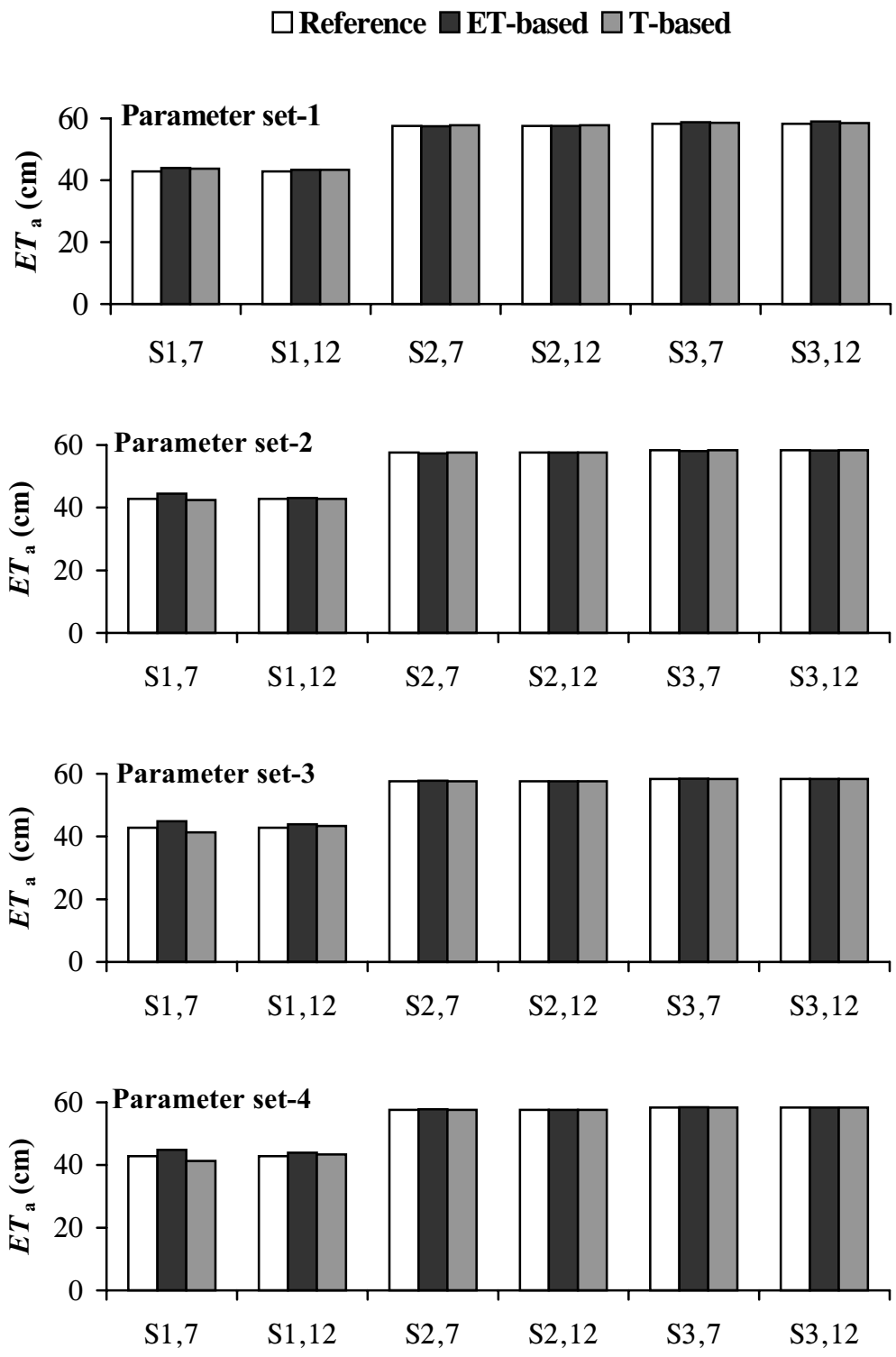

Figure 4.3. Simulated *evapotranspiration* (ET_a) for reference as well as inversely estimated soil hydraulic functions using *ET-based* and *T-based objective function* for S1, S2 and S3 soils. For different parameter sets (1, 2, 3 and 4) see Table 4.2. The digits 7 and 12 indicates the number of observations.

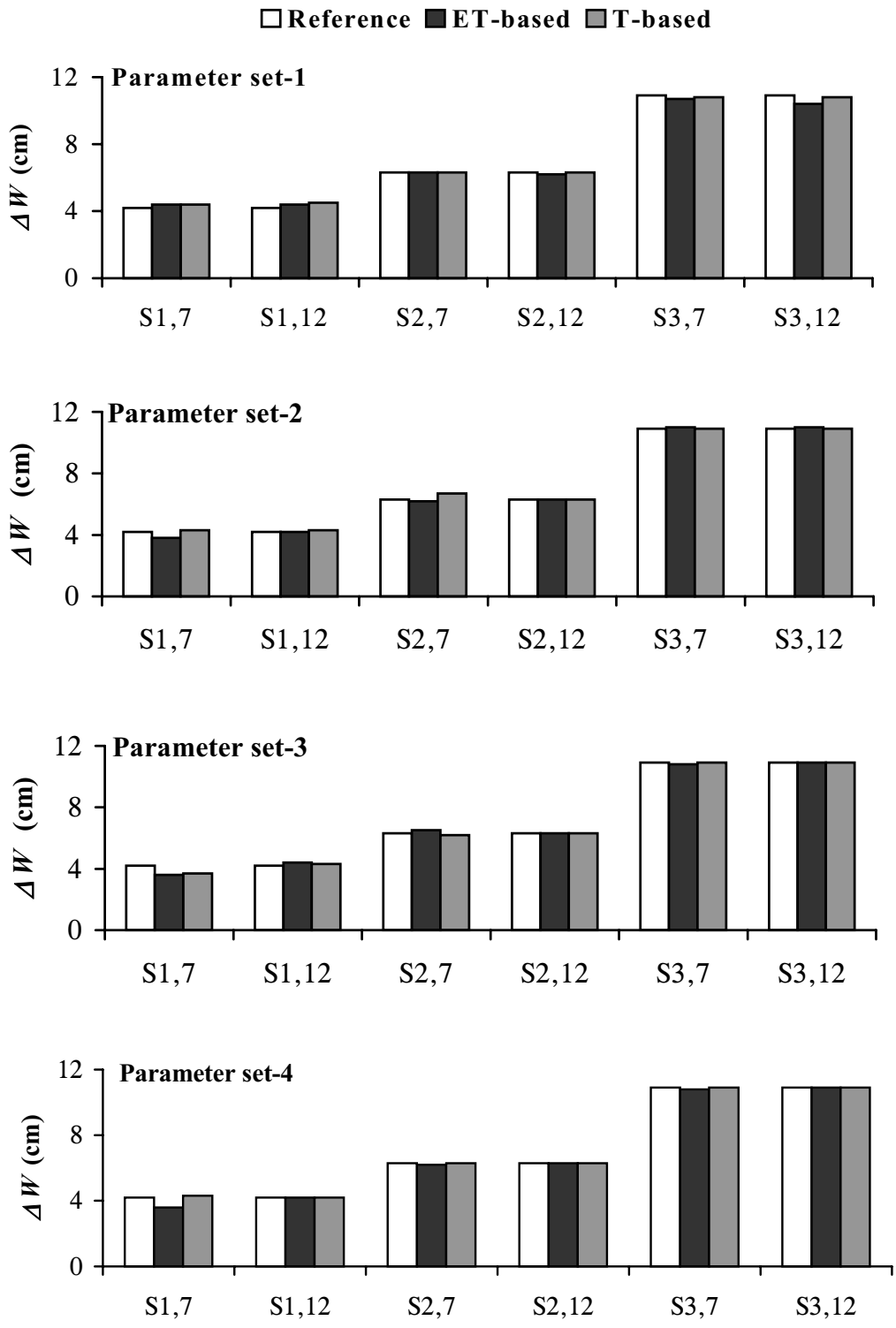

Figure 4.4. Same as Fig. 4.3 but for *change in soil moisture storage* ΔW over 150 cm depth between day 1 and day 160.

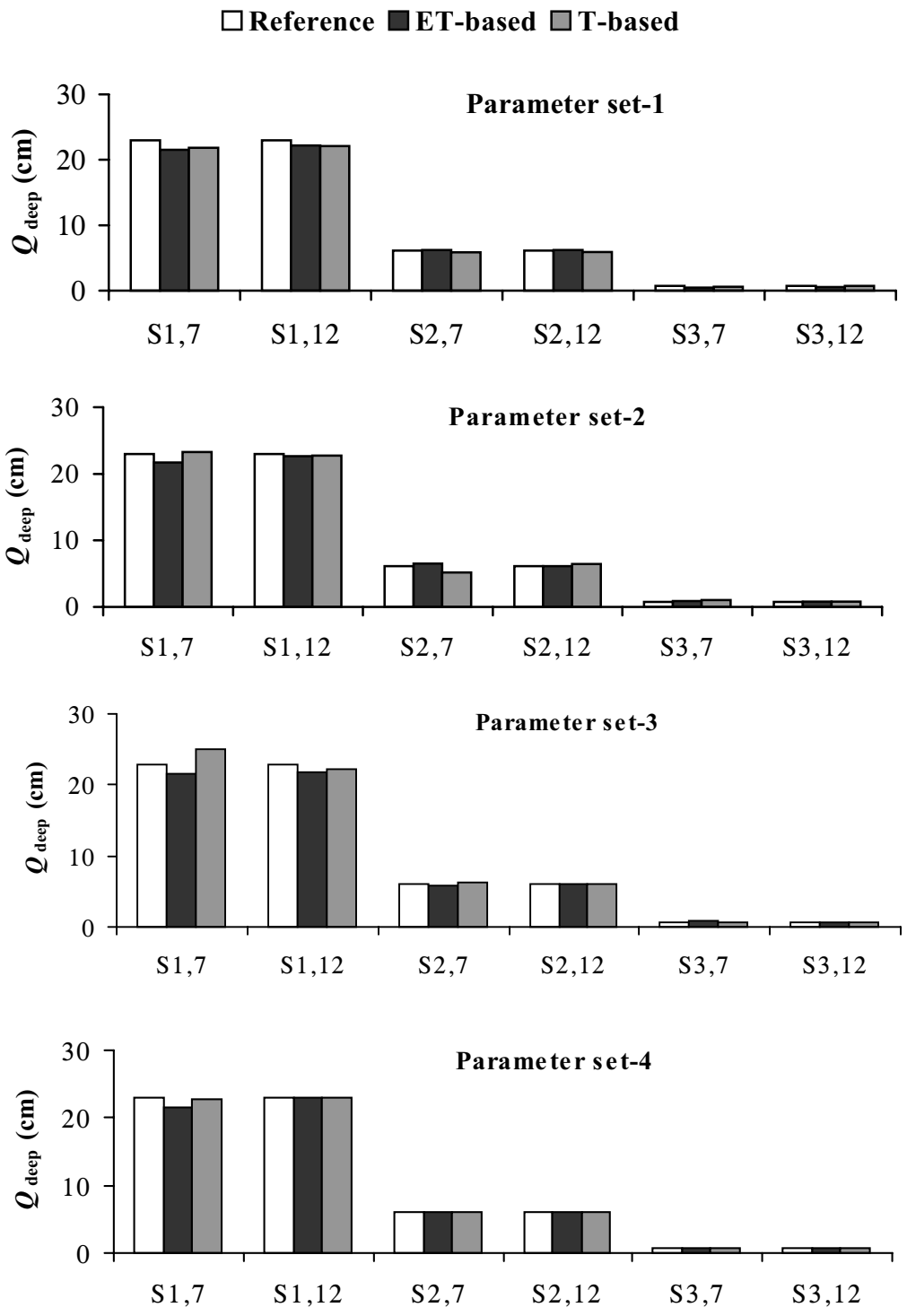

Figure 4.5. Same as Fig. 4.3 but for simulated *deep percolation* (Q_{deep}) at 150 cm depth.

When the frequency of observations was increased from 7 to 12, the simulated hydrological behaviour ($\boldsymbol{ET_a}$, $\boldsymbol{\Delta W}$ and $\boldsymbol{Q}_{deep}$) of fitted soil hydraulic functions tended to become closer to that of the reference set and both the forms of objective function performed equally good. This suggests the necessity of more frequent sampling of ET_a rates to inversely identify effective soil hydraulic functions. When the number of observations are 12 or more, information on ET_a is sufficient to solve the inverse problem. This greatly simplifies the data collection for inverse modelling experiments from independent data sources.

Among the different parameter sets, as defined in Table 4.2, the hydrologic behaviour of parameter set 4 was closest to the reference set. In fact, it is the only parameter set which was fitted exactly. This means that if k_{sat} and θ_{res} can be estimated independently, the ET_a rates are most suitable to derive rest of the VG model parameters (i.e. α, n and θ_{sat}).

Encouraged by the favourable effects of increased number of observations, the effect of more intensive sampling was further investigated by including alternate day ET_a rates into the objective function. This sampling strategy resulted in 30 observations of ET_a rates for the period covering Day 100-160. Now the parameter set-1 was also fitted closely. Under ideal conditions such intense measurements may be available, for instance NOAA satellite scans earth daily. However, there may be constraints in realistic situations due to persistent cloud coverage.

Therefore, further analysis deal only with the limited (i.e. 12) number of observations. However, an important implication of frequency of sampling may be noted. Table 4.3 shows the correlation between different VG model parameters as affected by the frequency of observations. The correlation coefficients which are unacceptably large when 7 observations are used, reduces considerably when number of observations are increased to 30. It is important to note that, if two or more parameters are simultaneously estimated, it is desirable that correlation between the optimised parameters should be small. This further stresses the need to have more observations of ET_a rates from independent measurements to inversely identify soil hydraulic functions.

Table 4.3. Correlation coefficients for different VG model parameters as affected by the number of observation

Parameter	α	n	θ_{res}	θ_{sat}	K_{sat}	λ
	Number of observations = 7					
α	1.00					
n	$7.7*10^{-14}$	1.00				
θ_r	0.92	0.32	1.00			
θ_s	0.96	0.23	0.99	1.00		
k_s	0.94	0.26	0.99	0.99	1.00	
λ	0.95	0.24	0.99	0.99	0.99	1.00
	Number of observations = 30					
α	1.00					
n	0.20	1.00				
θ_r	0.62	0.01	1.00			
θ_s	0.39	0.82	0.27	1.00		
k_s	0.27	0.17	0.34	0.11	1.00	
λ	0.75	0.21	0.42	0.27	0.26	1.00

Two conclusions can be drawn at this stage. When the number of independent observations on ET_a rates are sufficient, there is no specific advantage of utilising T_a rates in the objective function meaning that ET_a rates are sufficient to solve proposed inverse problem. The increased frequency of observations improves the precision of parameter estimation and the hydrological behaviour of different parameter sets.

Effect of random error in ET_a: In reality, exact correspondence between model predictions and observed data never occur, partly due to simplifications inherent in the parametric model as well as to the measurement errors (*Kool et. al*., 1987). Further, errors in observations may make the inverse procedure ill posed (*Hollenbeck and Jensen,* 1998). The effect of random error in the input data (ET_a rates) on the fitted functions was considered to show the accuracy required in the measurement/estimation of ET_a rates for the proposed parameter estimation procedure.

Two different levels of random error (10% and 20%) were added in the no error ET_a rates. The ET_a rates with error, ET_{ae}, were calculated as:

$$ET_{ae} = ET_a (1+ n_{0,1}*p) \tag{4.4}$$

where $n_{0,1}$ represents a number drawn at random from a normally distributed population with a mean of 0 and a variance of 1. Random numbers greater than 1 and less than –1 were set equal to 1 and –1, respectively, to control error level. p represents relative error. To simulate measurement errors of 10 % and 20 %, p was set to 0.10 and 0.20, respectively. At each error level, 10 series of ET_{ae} rates were generated, each consisting of 12 data points, to incorporate any variation that might occur at a given error level. Thereafter, the inverse procedure was repeated for all the three soils. Two options were studied for the assignment of weights w_i to different observations. First, equal weights (w_i = 1.0) were assigned to each observation. Another option tried was assignment of weight, w_i, inversely proportional to the magnitude of the observation (i.e. $w_i = 1/ET_{ae}$). Assignment of weight in this way implies that every observation have equal contribution to the objective function, irrespective of its magnitude. This is particularly important for erroneous data. The second option resulted into better results. The simulation results, with weight assigned inversely proportional to the magnitude of the observation, are discussed further.

For each of the four parameter sets, the inverse problem was solved repetitively, each time with a different realization of random measurement error incorporated into the exact ET_a rates. There were 10 repetitions of parameter inversion each for both the error levels. Each repetition yielded a single realization of parameter estimates. Hydrological behaviour of each of the fitted parameter set was then quantified. The resulting water balance components were then used to evaluate the statistical properties of the simulated hydrological behaviour of fitted parameters by averaging different water balance components over all the 10 realisations of parameter estimates. The statistical properties for different water balance components are the bias B and 99 % confidence interval CI, which measure systematic and random error, respectively. The B of the *kth* water balance component is the absolute difference between the mean expected value of the component $\boldsymbol{E}[x_k]$ and the true value of the component x_k.

$$B = \left| \boldsymbol{E}\left[x_k\right] - x_k \right| \tag{4.5}$$

The 99 % CI for estimate $\boldsymbol{E}[x_k]$ is given by

$$CI = t_{0.005} \frac{sd(x_k)}{\sqrt{n_{rr}}} \tag{4.6}$$

where $t_{0.005}$ is the value of *t*-distribution associated with the 0.005 probability level, $sd(x_k)$ is the standard deviation of *kth* water balance component estimated by different (=10) realizations and n_{rr} is the number of random realizations.

The results of the statistical analysis are presented in Table 4.4. It is desirable that both *B* and the *CI* of the water balance components be small.

Table 4.4. Statistical properties (mean μ ,bias, *B* and 99% confidence interval *CI*) of estimated water balance components for different parameter sets fitted on perturbed ET_a data. Incorporation of random errors (re) of 10% and 20% to the no-error data set generated the perturbed data. The results are based on 10 generated data sets each having 12 data points

Parameter Set	ET_a (cm)						ΔW (cm)						Q_{deep} (cm)					
	10% re			20% re			10% re			20%re			10% re			20% re		
	μ	B	CI	μ	B	CI	μ	B	CI	μ	B	CI	μ	B	CI	μ	B	CI
	Soil S1																	
Reference	42.8	-	-	42.8	-	-	4.2	-	-	4.2	-	-	23.0	-	-	23.0	-	-
Set 1	43.6	0.8	1.0	43.2	0.4	2.2	4.4	0.2	0.1	4.4	0.2	0.1	22.0	1.0	1.0	22.5	0.5	2.3
Set 2	42.6	0.2	0.9	42.1	0.7	2.6	4.3	0.1	0.2	4.1	0.1	0.2	23.2	0.2	0.8	23.8	0.8	2.6
Set 3	43.2	0.4	1.0	43.1	0.3	2.9	4.3	0.1	0.1	4.1	0.1	0.2	22.5	0.5	1.1	22.8	0.2	3.0
Set 4	42.7	0.1	0.9	42.4	0.4	2.0	4.3	0.1	0.1	4.2	0.0	0.2	23.0	0.0	1.0	23.5	0.5	2.0
	Soil S2																	
Reference	57.6	-	-	57.6	-	-	6.3	-	-	6.3	-	-	6.1	-	-	6.1	-	-
Set 1	57.8	0.2	1.0	57.6	0.0	1.2	6.4	0.1	0.1	6.1	0.2	0.5	5.8	0.3	0.9	6.4	0.3	1.4
Set 2	57.9	0.3	1.0	58.1	0.5	0.8	6.3	0.0	0.1	6.1	0.2	0.2	5.9	0.2	1.0	5.9	0.3	0.8
Set 3	58.0	0.4	0.2	57.6	0.0	0.8	6.3	0.0	0.2	6.0	0.3	0.3	5.7	0.5	0.4	6.4	0.2	0.9
Set 4	57.9	0.3	0.4	58.0	0.4	0.6	6.2	0.1	0.1	6.1	0.2	0.2	5.9	0.2	0.5	5.9	0.2	0.5
	Soil S3																	
Reference	58.3	-	-	58.3	-	-	10.9	-	-	10.9	-	-	0.8	-	-	0.8	-	-
Set 1	56.8	1.5	2.8	56.6	1.7	3.0	8.6	2.3	2.3	10.0	0.9	2.6	4.7	3.9	4.1	3.4	2.6	3.3
Set 2	56.9	1.4	2.2	56.2	2.1	3.2	11.0	0.1	1.0	11.3	0.4	2.0	2.1	1.3	1.4	2.5	1.7	2.6
Set 3	56.9	1.4	2.4	56.4	1.9	2.8	10.6	0.3	1.2	10.9	0.0	2.1	2.6	1.8	1.8	2.7	2.0	2.6
Set 4	56.7	1.6	2.8	55.8	2.5	3.0	11.1	0.2	1.1	11.7	0.8	2.0	2.2	1.4	2.2	2.5	1.8	3.1

The estimates of mean water balance components, bias and *CI* (Table 4.4) indicates that both the systematic and random error increases with increase in random error incorporated in ET_a rates. The results further indicate that the parameter set-4 is fitted most reliably with bias (< 5%) and 99% *CI* (<10%) of different water balance components within acceptable limits. For soil S3,

none of the four fitted parameter set predicted acceptable water balance components, very high bias and 99% *CI*, particularly for $\Delta \boldsymbol{W}$ and $\boldsymbol{Q}_{deep}$ (Table 4.4). This may be due to the fact that soil S3 showed minimum drought stress to ET_a (Fig. 4.1a) under prescribed irrigation regimes. It means that periods with prolonged and severe stress are the most suitable for selecting the satellite overpass dates because the effect of VG model parameters is more pronounced under such situations. Further if the expected error in the ET_a rates are proportional to the magnitude of true value, as incorporated in this Chapter, then selection of severe drought stress periods means less absolute deviation in ET_a rates.

4.6 General discussion

The proposed inverse procedure may invite some criticism, particularly prior knowledge of sink term variable. Though it is beyond the scope of this study to deal with this problem, a simple framework is suggested to solve the same. The sink term variables (h_1-h_4) are crop dependent. For uniform cropping pattern, these can be derived locally from field or laboratory experiments or may be derived from available information. In case of mixed cropping patterns, the following strategy may be adopted. *Kabat et al.* (1997) have demonstrated that scaling techniques may be used to derive effective parameters. From satellite images, pixels representing similar vegetation cover may be grouped. Representative pixels from each group may be selected and effective parameters derived by scaling techniques. With known hydraulic functions for these pixels, ET_a rates may be used to inversely identify sink term variables. The sink term variables determined in this way may then be employed to derive effective hydraulic functions for other pixels belonging to the representative groups. In this way much of the tedious and time consuming work involved in the conventional methods of determining soil hydraulic functions may be avoided.

In this study, similar initial guesses, independent of soil type, for different VG model parameters was assigned. When dealing with an actual system, however, two favourable situations may occur. A few measurements at representative sites may provide not only a better initial guess of θ_{res}, θ_{sat} and k_{sat}, but more importantly, it may provide a narrower allowed range of these parameters as compared to those considered during this study. For example θ_{res} was allowed to change from 0.0-0.1, θ_{sat} from 0.40-0.58 and k_{sat} from 10-500 cm d^{-1}. Alternatively, the pedo-

transfer function approach may be used for obtaining reasonable initial guess of the soil hydraulic parameters to initialise the optimisation procedure (*Burke et al*., 1998).

It must also be noted that during this study the ET_a was affected only by water stress i.e. there was no effect of other stresses such as salinity and pest/diseases. As such the present findings may not be applicable to situations where other stresses are dominant, until and unless properly accounted for during backward simulations. Further studies are needed to test the present approach for spatially variable fields, but if the conclusions hold, a relatively simple method is available to parameterise soil variability at large scales.

The application of the proposed inverse modelling approach to estimate soil hydraulic functions requires that information on timing and amount of rainfall/irrigation is known. This is also a prerequisite for the successful application of any simulation model to study appropriate water management strategies. Thus, it does not demand additional data collection. The findings are applicable only to regions where strong moisture depletion is experienced during the growing season (thereby making soil hydraulic characteristics an important factor affecting ET_a). This is often the case in arid and semi-arid regions having deep groundwater.

4.7 Conclusions

- Provided the root water extraction function is known, ET_a rates can be used to inversely identify effective soil hydraulic functions for arid and semi-arid regions. The *ET*- based fitted functions are suitable to make simple water balance computations required for water management related decisions.

- Simulated temporal ET_a rates for three soil types suggest that moisture stress period of fully developed crops is most appropriate for sampling ET_a rates to solve proposed inverse problem.

- Under ideal conditions (no error in ET_a rates) when number of ET_a data are sufficient, it is possible to inversely identify all the parameters of VG model. However when number of

observations are limited, it is necessary to reduce the number of fitting parameters in order to obtain exact soil hydraulic functions.

- Frequent measurement of ET_a rates is desired not only to precisely estimate soil hydraulic functions by the inverse technique but also to reduce the undesirable correlation between different fitting parameters.

- If the expected errors in the ET_a rates are proportional to the magnitude of the true value of ET_a rates, as incorporated in this chapter, the weight assigned to the observations must be inversely proportional to the magnitude of ET_a rates.

Although the results described in this chapter are promising, they are only applicable to a number of prevailing conditions such as homogeneous soil and crop conditions, free drainage, moisture stress during growing season and root water extraction function known. There are many situations in arid and semi-arid regions where the conditions of free drainage and severe moisture stress are often met. Nevertheless the effect of other conditions such as spatially variable field conditions needs further investigation.

Chapter 5

Calibration of effective soil hydraulic parameters for heterogeneous soil profiles[2]

5.1 Introduction

At most sites, soil hydraulic parameters have large variability not only in horizontal direction but also in the vertical direction. For example, *Ahuja et al.* (1984) observed different scaling factors for saturated hydraulic conductivity and wetting front pressure head at different depths for three silt loam soils. In general, it is not feasible to model the heterogeneity deterministically as this would require too much data and computational effort (*Van Dam and Feddes*, 1996). Alternatively, one could interpret the soil as an equivalent homogeneous medium with average (effective) hydraulic properties that predict the average flow and transport behaviour of the system (*Wildenschild and Jensen*, 1999). For instance, when studying the performance of an irrigation system at the canal command of distributary level, we are not directly interested in details of the internal variability. Therefore, it is very important to determine representative soil hydraulic parameters at the scale of model application that yields to satisfactory water balances. In practice, there are only in-direct methods available to determine representative soil hydraulic parameters at larger scales.

Various attempts have been made to derive *effective* soil hydraulic parameters using the inverse approach (*Feddes et al.*, 1993b; *Wildenschild and Jensen*, 1999; *Jhorar et al.*, 2002). Basically, these studies have been carried out to demonstrate that effective soil hydraulic parameters exist/or can be derived for spatially variable hydraulic parameters. In the studies cited above, the concept of effective parameters has been tested on data representing vertically homogeneous soil profiles. For example, *Feddes et al*. (1993b) derived effective soil hydraulic parameters assuming a hypothetical watershed area consisting of 32 parallel blocks of spatially variable but vertically homogeneous soil profiles. In fact, most of the studies reported to assess the impact of soil heterogeneity on field water balance components, whether using numerical-stochastic experiments (*Kim et al.*, 1997) or laboratory-numerical

[2] Adapted version of Jhorar R.K., J.C. van Dam, W.G.M. Bastiaanssen and R.A. Feddes. 2002. Calibration of effective soil hydraulic parameters for heterogeneous soil profiles. Journal of Hydrology (submitted)

experiments (*Wildenschild and Jensen*, 1999), with rare exceptions (*Li et al.*, 2001), assume vertical soil homogeneity and deal with only horizontal spatial variability. However, natural soils are hardly ever uniform or homogeneous in the vertical direction (*Braun and Kruijne*, 1994).

The fact that soil layering affects field water and solute transport is well known (*Feyen et al.*, 1998). *Li et al.* (2001) demonstrated that the spatial variation of soil textural profile structures has a very strong influence on the field water balance and cautioned that soil hydraulic parameters derived from only a few soil profiles are not representative of the quantitative characteristics of the regional field water balance. It is not yet clear whether effective soil hydraulic parameters can be derived for heterogeneous soil profiles. Therefore, this Chapter *examines the possibility of deriving effective soil hydraulic parameters for heterogeneous soil profiles.*

The possibility of deriving effective soil hydraulic functions of heterogeneous soil profiles, by inverse modelling of actual evapotranspiration rate ET_a and total moisture stored in the root zone W_{rz}, was tested through numerical experiments. Forward simulations were carried out with the simulation model SWAP (*Van Dam et al.*, 1997) for different heterogeneous soil profiles to generate ET_a and W_{rz} as if these were available from independent measurements. Thereafter, the parameters estimation program PEST (*Doherty et al*., 1995) is used to inversely identify different parameters of the soil hydraulic function model proposed by *Van Genuchten* (1980).

5.2 Data set on heterogeneous soil profiles

Laboratory measurements on soil water pressure head h –gravimetric water content pair, bulk density, particle density and saturated hydraulic conductivity as reported by *Sood* (1969) for seven soil profiles (Fig. 5.1) were used. The soil texture class at the surface is mainly sand and ranges from sandy loam to sandy clay loam in deeper horizons. The gravimetric water content was multiplied by the soil bulk density to obtain the volumetric water content, θ.

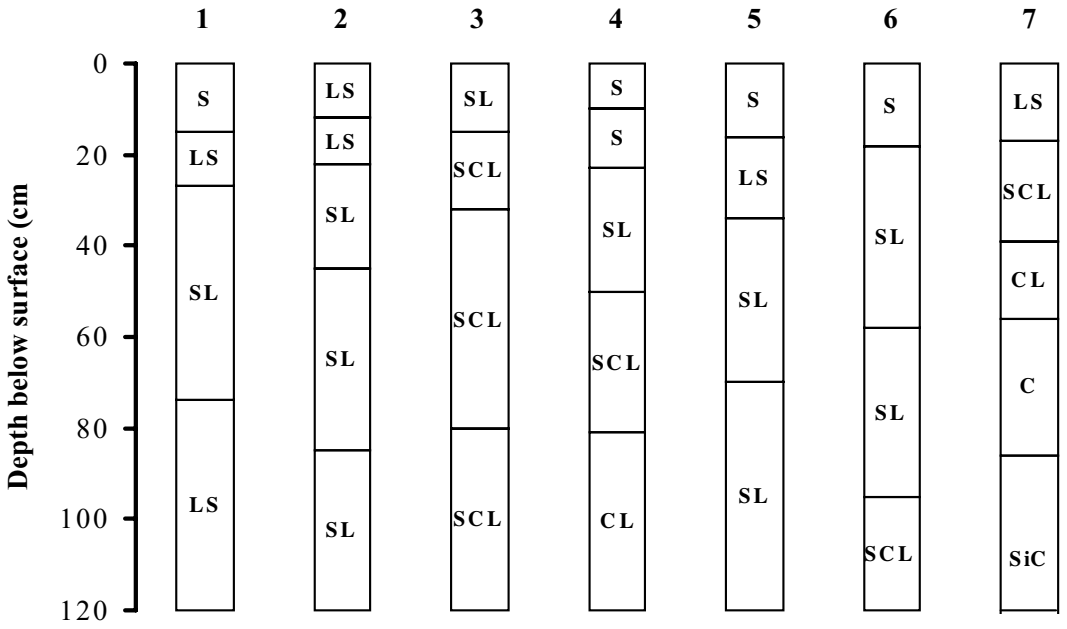

Figure 5.1. Textural information of the seven soil profiles used during forward simulations. The symbol S stands for sand or sandy, Si for Silty, C for clay and L for loam or loamy. Accordingly SL means sandy loam; LS means loamy sand and so on.

The seven sites belong to the command area of Kheri distributary, a part of the Bhakra Irrigation system in Haryana, India. The Kheri distributary commands an area of about 0.023 million ha and is located in the south-eastern part of the Sirsa Irrigation Circle (Fig. 2.1). The majority of the soils in the area are classified as sandy loam, though the surface horizons are mostly sandy in texture and the subsurface horizons vary from loamy sand to silty clay. Further details are reported in *Sood* (1969).

The soil moisture retention function (Eq. 3.4) as proposed by *Van Genuchten* (1980) was fitted to the measured h-θ. Eq. 3.4 was fitted with the parameters estimation program PEST. Similar to *Schaap and Leij* (2000), the following constraints were imposed during the optimisation: $0.0 < \theta_{res} < 0.3$ cm^3 cm^{-3}; $0.6\phi < \theta_{sat} < \phi$ (where ϕ is the total porosity defined as 1-bulk density/particle density); $0.0001 < \alpha < 1.000$ cm^{-1}; $1.0001 < n < 10$. The resulting fitted parameters are given in Table 5.1. The parameters of the hydraulic conductivity function (Eq. 3.5) were not fitted. k_{sat} values were fixed at the measured value of saturated hydraulic conductivity (Table 5.1) and λ was fixed at –1.0 (*Schaap and Leij*, 2000).

Table 5.1. Van Genuchten model parameters for 120 cm soil depth for the seven locations in the Kheri distributary of Bhakra Irrigation system, Haryana, India. Except k_{sat}, all the parameters were fitted as described in section 5.2

Soil depth (cm)	θ_{sat}	θ_{res}	α (cm^{-1})	n	k_{sat} (cm d^{-1})
Site 1					
0-15	0.45	0.03	0.0771	1.66	139.2
15-27	0.46	0.07	0.0564	1.62	119.0
27-74	0.47	0.07	0.0465	1.67	90.5
74-120	0.46	0.08	0.0473	1.74	88.6
Site 2					
0-12	0.45	0.05	0.0330	1.85	80.4
12-22	0.46	0.05	0.0280	1.84	98.4
22-45	0.42	0.10	0.0164	1.98	75.1
45-85	0.41	0.10	0.0118	1.86	72.2
85-120	0.36	0.10	0.0111	1.64	37.7
Site 3					
0-15	0.46	0.03	0.0562	1.85	96.2
15-32	0.41	0.12	0.0166	1.75	53.5
32-80	0.40	0.07	0.0257	1.71	28.8
80-120	0.39	0.13	0.0070	1.70	26.4
Site 4					
0-10	0.43	0.03	0.0559	1.81	184.3
10-23	0.41	0.03	0.0298	2.06	220.8
23-50	0.38	0.08	0.0192	1.70	77.3
50-81	0.38	0.11	0.0149	1.54	26.6
81-120	0.39	0.01	0.0014	1.29	8.4
Site 5					
0-16	0.45	0.04	0.0361	2.07	194.4
16-34	0.44	0.06	0.0275	1.73	139.2
34-70	0.47	0.07	0.0346	1.63	101.3
70-120	0.43	0.08	0.0212	1.65	85.2
Site 6					
0-18	0.45	0.03	0.0667	1.83	162.2
18-58	0.42	0.05	0.0406	1.44	99.6
58-95	0.42	0.09	0.0160	1.54	47.5
95-120	0.37	0.09	0.0059	1.51	19.7
Site 7					
0-17	0.46	0.04	0.0852	1.47	104.5
17-39	0.38	0.00	0.0074	1.22	24.0
39-56	0.33	0.04	0.0009	1.25	24.7
56-86	0.36	0.18	0.0011	1.67	47.3
86-120	0.41	0.00	0.0063	1.21	18.2

5.3 Forward simulations with SWAP and parameter estimation procedure

Forward simulations: Forward SWAP simulation were carried out for a cotton crop for the 7 soil profiles assuming deep groundwater situation by specifying free drainage as the lower boundary condition. All simulations started from the assumed date of sowing (June 26) of cotton. A soil water pressure head corresponding to h = -200 cm (pF 2.3) was specified as initial condition for all the soil profiles. Meteorological data from the Haryana Agricultural University Hisar (India), representing an arid climate, were used. The sink term variables required for reduction in ET_a due to moisture stress (*Feddes et al.,* 1978) were calibrated for a cotton crop grown in a field experiment at Sirsa, India (*Bastiaanssen et al.*, 1996). Simulations cover the growing season of a cotton crop for 160 days. Five post sown irrigations, each 60 mm, were specified at day number 51, 72, 97, 118 and 143, in which day number 1 represents the day of sowing.

First, the inverse approach was applied to identify effective soil hydraulic parameters for the individual soil profiles. Thereafter, an attempt was made to derive *area effective parameters*. To investigate the ability of deriving the area effective soil hydraulic parameters, information on areal fluxes is required. In practice such data can be derived using satellite images. Low resolution satellites such as NOAA-AVHRR and TERRA-MODIS can provide daily ET_a fluxes at a spatial scale of 1 km if the sky is clear. Under Indian conditions, such a spatial scale often involves a mixture of soil and crops.

In accordance with the main aim of this study to test the possibility of defining heterogeneous soil profiles by effective parameters, the effect of crop variability was ignored. The reason for exclusion of crop heterogeneity along with a procedure for its inclusion are further elaborated in the section 5.6 under general discussion. For the present study, it is considered that the whole of the Kheri distributary area may be represented by a collection of n sub-areas. In this case each sub-area is represented by either of the seven soil profiles. Each sub-area occupies a certain fraction of the total area. For each sub-area, the fluxes are known from the forward simulations. The areal measurements on ET_a are then obtained by the following aggregation rule:

$$ET_a^*(t) = \sum_{i=1}^{n} ET_a(i,t)\, F_i \qquad (5.1)$$

where $ET_a^*(t)$ is the estimated areal actual evapotranspiration on day t, n is the number of sub-areas (seven in this case) in the total area, $ET_a(i,t)$ is the corresponding (forward simulated) ET_a for the sub-area i and day t, and F_i is the fraction of total area represented by the sub-area i.

Parameter estimation procedure: The ET_a and W_{rz} observations as generated from forward simulations were employed as input data to the numerical inversion problem. An overview of the parameter estimation procedure is shown in Fig. 3.6. PEST runs the SWAP with an initial guess of the parameters, compares the model results with observations, adjusts selected parameters using an optimization algorithm and runs the model again. The procedure of adjusting selected parameters continues until the difference between the model results and observations or the number of iterations, meets a pre-set criteria.

Let $ET_a(\boldsymbol{b}, t_i)$ and $W_{rz}(\boldsymbol{b}, t_i)$ be the numerically calculated values of ET_a and W_{rz}, respectively, at time t_i corresponding to a trial vector of selected parameter values $\{\boldsymbol{b}\}$, where $\{\boldsymbol{b}\}$ is the n-dimensional vector containing the parameters that are optimized simultaneously. The inverse problem is then to find an optimum combination of parameters $\{\boldsymbol{b}^0\}$ that minimizes the following weighted least square objective function:

$$\Phi(\mathbf{b}) = \sum \left[\left\{ w_i \left(ET_a(t_i) - ET_a(t_i, \mathbf{b}) \right) \right\}^2 + \left\{ v_i \left(W_{rz}(t_i) - W_{rz}(t_i, \mathbf{b}) \right) \right\}^2 \right] \tag{5.2}$$

where w_i and v_i are the weighting factors accounting for data type as well as data point.

The possibility of finding $\{\boldsymbol{b}^0\}$ using only ET_a data (setting v_i =0) as well as using both ET_a and W_{rz} in the objective function was explored. Accordingly Eq. 5.2 will be referred to as ET-based objective function when v_i =0, and ET-θ based objective function when both w_i and v_i are non-zero.

Forward SWAP simulation results on T_a and E_a between Day 100 -160 were used to get ET_a fluxes for the inverse modelling exercise. The modelled moisture content at each node in the 120 cm soil profile was used to calculate the total water stored in the root zone (120 cm). ET_a

or ET_a and W_{rz} observations for twelve selected days (t = 100, 105, 110, 115, 120, 125, 130, 135, 140, 145, 150 and 159) were used as input to the objective function (Eq. 5.2). In the inverse procedure, different sets of soil hydraulic input parameters were selected for optimization. Except for the optimization runs when the effect of initial guess of parameters on the inverse results was investigated, a uniform initial guess of different VG model parameters was specified. The initial values of VG model parameters as specified during inverse optimizations were: $\alpha = 0.01$ cm^{-1}, $n = 1.5$, $\theta_{sat} = 0.40$ cm^3 cm^{-3}, $\theta_{res} = 0.00$ cm^3 cm^{-3}, and $k_{sat} = 100$ cm d^{-1}.

The hydrological behaviour of the fitted parameters was tested through a verification numerical experiment. Water balance components (see Eq. 4.3) were estimated for different irrigation regimes than that specified during inverse optimizations and the performance of fitted soil hydraulic functions was evaluated by their capability to reproduce the hydrological behaviour of soils. Details of the verification experiment are given in Chapter 4.

In the following paragraphs, different water balance components are referred to as 'simulated' for the simulated values based on inversely identified parameters and as 'reference' for the simulated values based on known parameters (forward simulations). Results of inverse procedure are first presented for individual soil profiles and then for the area effective soil profile

5.4 Performance of inversely identified parameters for *individual* soil profiles

Different combinations of measurements data, number of soil layers, E_a simulation and number of optimized parameters (Table 5.2) were selected to study their influence on the hydrological behaviour of the inversely identified soil hydraulic parameters.

In Case 1 the *ET*-based form of the objective function is used. One set of soil hydraulic parameters were optimized for the whole profile at each of the 7 locations. The results of the verification experiment are shown in Fig. 5.2.

Table 5.2. Different cases used during inverse identification of effective soil hydraulic parameters. E_a is simulated as minimum (min) of E_p and E_{max} or E_p, E_{max} and E_{emp} as the case may be. E_{emp} is as calculated with the *Boesten and Stroosnijder* (1986) approach.

Cases	Measurements	Number of soil layers during inversion	E_a simulation Approach	Optimized parameters
1	ET	1	min(E_p, E_{max})	α, n, θ_{res}, θ_{sat}, k_{sat}
2	ET	2	min(E_p, E_{max})	α, n, θ_{res}, θ_{sat}, k_{sat}
3	ET	1	min(E_p, E_{max}, E_{emp})	α, n, θ_{res}, θ_{sat}, k_{sat}
4	ET	1	min(E_p, E_{max}, E_{emp})	Scale factor, θ_{sat}
5	ET	1	min(E_p, E_{max}, E_{emp})	α, θ_{sat}, k_{sat}
6	$ET + W_{rz}$	1	min(E_p, E_{max}, E_{emp})	α, θ_{sat}, k_{sat}

In general, simulated cumulative actual transpiration $\boldsymbol{T_a}$ is within 10 % of the reference $\boldsymbol{T_a}$. However, simulated cumulative actual evaporation $\boldsymbol{E_a}$ and deep percolation $\boldsymbol{Q}_{deep}$ is seriously over and under predicted, compared to the corresponding reference values. At first instance, it could be speculated that it is not possible to define heterogeneous soil profile by a single set of effective parameters. This speculation is partly justified by the fact that, for the 7 profiles, the top 10 to 20 cm layer is dominated by the sand fraction. The textural class varies for sub-surface layers representing medium to heavy soils (Fig. 5.1). The higher sand fraction in the surface layers results in less evaporation during forward simulations. However, when the profile is attempted to be defined by a single set of parameters, these will represent the average conditions of the whole profile (including top 10 to 20 cm). Soil evaporation is mostly determined by the soil moisture content and hydraulic conductivity in the surface layer. This means that there is always a possibility of over estimation of the E_a. To overcome this problem, Case 2 was designed.

In Case 2, an attempt is made to identify two sets of parameters, one for the top 15 cm soil profile and the other for the rest of the profile (15-120 cm). The results of the verification experiment are also shown in Fig. 5.2. Though there is some improvement in the simulated $\boldsymbol{E_a}$ and $\boldsymbol{Q}_{deep}$ for some of the soil profiles, the results are far from satisfactory. Common to

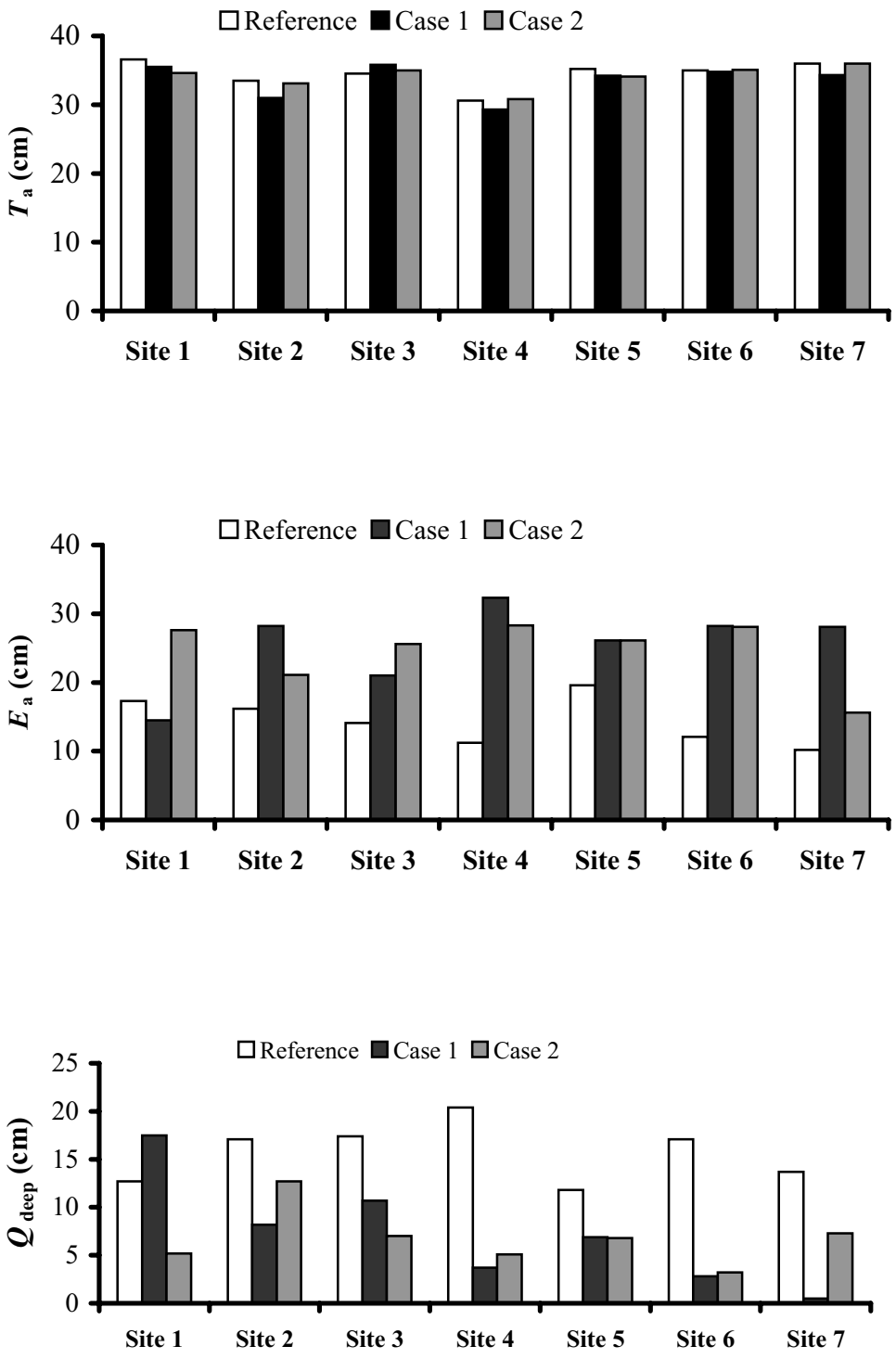

Figure 5.2. Hydrological behaviour of inversely fitted soil hydraulic parameters, for Case 1 and Case 2 (for cases see Table 5.2). Results are based on the verification numerical experiment.

both the cases is that the simulated $\boldsymbol{T_a}$ is predicted reliably while $\boldsymbol{E_a}$ is over-predicted grossly. This means that even when the given soil profile is identified with two sets of parameters, the resulting parameters for the top layer are not representative. In fact, the problem arises due to the dependence of E_a on the soil hydraulic functions of the top layers when it is simulated based on Darcy's flux. To overcome this problem Case 3 was designed. Case 3 is similar to Case 1 but now E_a is simulated according to minimum of E_p, E_{max} or E_{emp}. Accordingly the forward simulations were also repeated to generate appropriate reference set of the water balance components for the changed option for E_a. Under actual field conditions also, the applicability of Darcy flux approach for E_a is questionable (*Van Dam*, 2000). Therefore, the shift in E_a option is a practical assumption as well.

Except for the option of E_a simulation, Case 1 and Case 3 are similar. The results of the verification experiments are shown in Fig. 5.3. There is a considerable improvement in the performance of inversely identified soil hydraulic parameters as compared to Case 1 and Case 2 (Fig. 5.2). However, some over predictions of the simulated $\boldsymbol{E_a}$ are to be noted. This suggests that the identified parameters for top layer are still being influenced by the whole profile behaviour through ET_a as used in the inverse problem. This is due to the fact that E_a is still affected by the soil hydraulic parameters whenever E_{max} governs the evaporation process.

In many application basic information of the soil texture or soil hydraulic functions may be available. In such cases, optimization of scale factor ρ_{scal} and θ_{sat} is probably sufficient to derive suitable soil hydraulic functions (*Van Dam*, 2000). According to the scaling theory, α and k_{sat} at any location are related to ρ_{scal} and their corresponding reference values ($\alpha = \rho_{scal}\alpha_{ref}$; $k_{sat} = \rho^2_{scal}\, k_{sat,\, ref}$). Replacing α_{ref} and $k_{sat,ref}$ by their initial guess α_{guess} and $k_{sat,guess}$, it is possible to optimize both α and k_{sat} by optimizing only ρ_{scal}. Accordingly, in Case 4, scale factor ρ_{scal} and θ_{sat}, are optimized. For this Case, VG model parameters n (= 1.6) and θ_{res} (= 0.05) were fixed during optimization. In practice, these values can be selected based on available information on soil textural class.

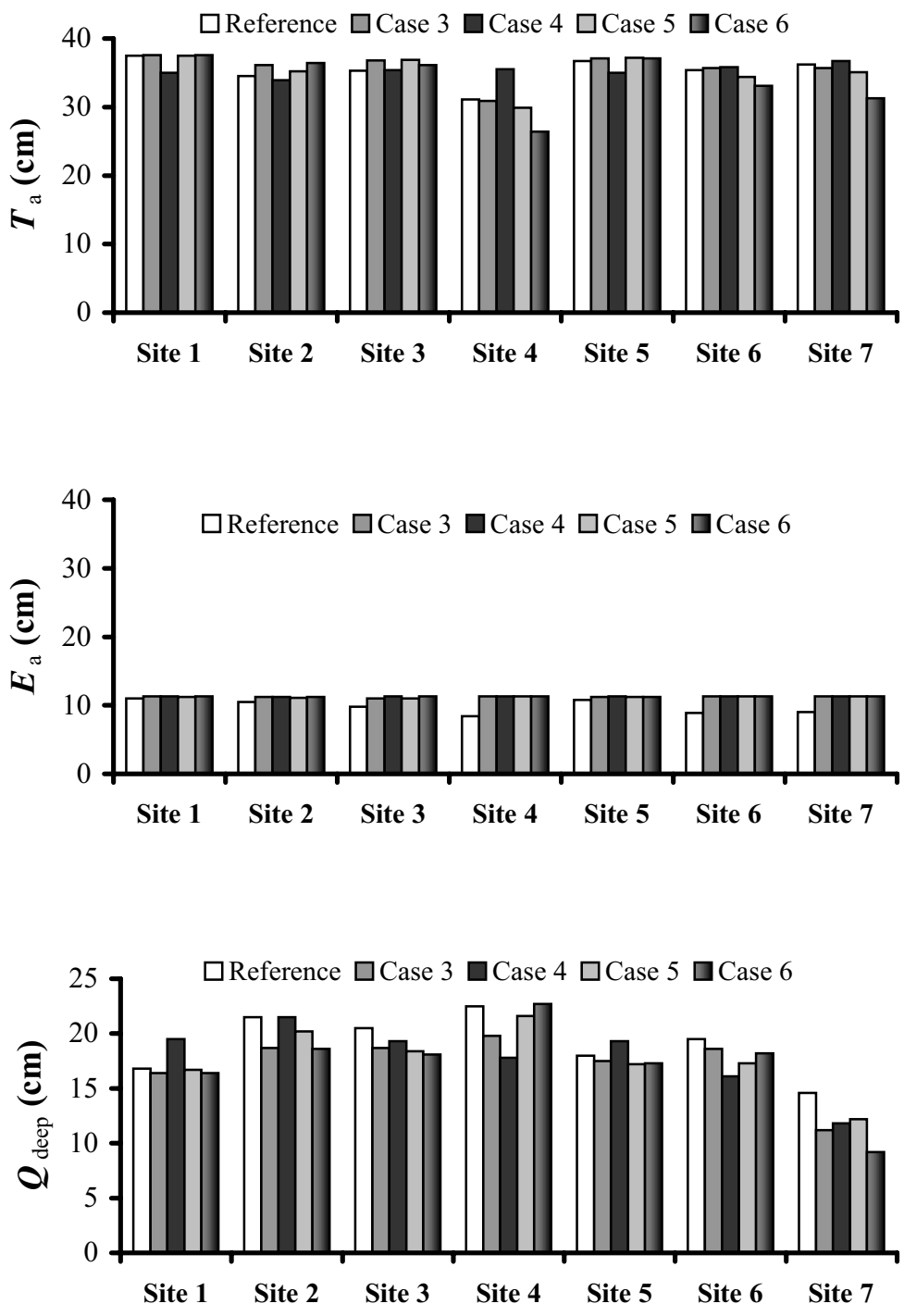

Figure 5.3. Hydrological behaviour of inversely fitted soil hydraulic parameters, for Case 3, 4, 5 and 6 (see Table 5.2 for different cases). Results are based on the verification numerical experiment.

The results of Case 4 (Fig. 5.3) are not consistently better than Case 3. This may be due to fixing of n at one value for all the soil profiles. On the other hand site 4 and 7 have relatively larger clay content in sub-surface layers (Fig. 5.1) and a smaller value of n for these sites would have been more appropriate *(Carsel and Parrish*, 1988; also see Table 5.1). Another reason could be that the scale factor can only modify α and k_{sat} in the same direction ($\alpha = \rho_{scal}\, \alpha_{guess}$; $k_{sat} = \rho^2_{scal}\, k_{sat,\, guess}$). Therefore, a suitable guess of reference α and k_{sat} is very important. Since the ultimate goal is to derive area effective soil hydraulic parameters, these issues are discussed in the next section.

To overcome the limitation of scale factor, Case 5 was designed, wherein both α and k_{sat} along with θ_{sat} are optimized. All the three parameters (α, k_{sat} and θ_{sat}) were determined with much smaller confidence interval than for the Case 3. As can be seen from the results of the verification experiment (Fig. 5.3), Case 5 performs slightly better than Case 3 and Case 4. This further justifies the speculation regarding the limitation of the scale factor as the favourable effect of less number of optimized parameters was not observed when scale factor was optimised. Therefore, it may be concluded that, if textural information is available, it is better to optimize only α, k_{sat} and θ_{sat} rather than optimizing the scale factor or all the VG model parameters. The validity of this conclusion will be further checked while deriving area effective soil hydraulic parameters. The inability of Case 5, to simulate more closer hydrological behaviour for site 7 may be attributed to the fixing of n at a relatively higher value for this site.

Information on different relevant observations which are sensitive to the system parameters being optimized is a desirable feature for the inverse problems. Case 6 was designed considering the potential of satellite remote sensing to provide information on the root zone soil moisture together with ET_a fluxes. In fact it is the only case where the ET-θ based form of the objective function (Eq. 5.2) is used. Addition of W_{rz} in the objective function slightly improved the simulated root zone soil moisture. However, there is no considerable improvement in the hydrological behaviour (Fig. 5.3) of the inversely identified soil hydraulic parameters. This means that use of ET -based objective function is as good as the ET-θ based form of the objective function. Accordingly, only ET-based form of the objective function (Eq. 5.2) will be used to inversely define area effective soil profile.

5.5 Performance of inversely identified *area effective* soil profile

A further analysis of the data on soil profile texture (45 samples) of the Kheri distributary area as reported by *Sood* (1969) showed that the 7 sites respectively represents 0.31, 0.20, 0.04, 0.02, 0.37, 0.04 and 0.02 fraction of the area. Therefore, the above fractions were assigned as the values of F_i in Eq. 5.1 to estimate areal evapotranspiration ET_a^* representing the whole command area of the distributary. A similar approach was followed to derive a reference set of other water balance components for whole the command area. Thereafter, ET_a^* observation for the 12 days was used as input to the objective function to derive area effective soil hydraulic parameters.

Based on the results of the individual soil profiles, Case 3, 4 and 5, of Table 5.2 were used to inversely identify area effective soil hydraulic parameters. In order to examine the uniqueness of the results, the optimization process was repeated with different initial guess of the parameters (α, k_{sat} and θ_{sat}). Again, the performance of the inversely identified area effective parameters was tested through numerical verification experiments. The verification experiment described in the previous sections (hereinafter referred to as wet verification experiment) represents relatively heavier depths of irrigation application. Such irrigation depths are common in the study area due to the use of flood irrigation method on light textured soils. However, another verification experiment (hereinafter referred to as dry verification experiment) was also performed, for relatively shallow depths of irrigation application. In this case a total of 250 mm irrigation against 700 mm in the wet verification experiment was specified. For many applications, it may be sufficient to know only accurate information on seasonal water balance components. However for some specific application, it may be important to have reliable information on temporal variation of different water balance components as well. Therefore, the performance of inversely identified parameters was examined with respect to seasonal as well as temporal hydrological behaviour.

Seasonal water balance components: Table 5.3 shows the mean and coefficient of variation *CV* of seasonal simulated water balance components for the wet verification experiment. The mean value of different water balance components as simulated by different Cases is quite close for the wet verification experiment. The *CV* values are smallest for Case 3 followed by Case 4 and Case 5. In fact for one of the initial guesses, the Case 4 resulted in over prediction of $\boldsymbol{Q}_{deep}$ by more than 15 per cent which is reflected in higher value of *CV* (0.103). On the

other hand, Case 3 and 5, predicted all the water balance components within 10 per cent of the reference set. This means that, reducing the number of parameters by optimizing the scale factor does not produce favourable effects in this study. The smaller *CV* values of different water balance components demonstrate the uniqueness of model predictions with inversely identified parameters.

Table 5.3. Reference and mean value of simulated areal seasonal simulated water balance components (mm) for the *wet verification experiment* for Case 3, Case 4 and Case 5. The results of simulations are based on 5 different initial values of fitting parameters.

Water balance component	Reference	Case 3		Case 4		Case 5	
		Mean	*CV*	Mean	*CV*	Mean	*CV*
$\boldsymbol{E}_a$	106	112	0.000	113	0.000	113	0.004
$\boldsymbol{T}_a$	363	365	0.009	356	0.049	361	0.034
$\boldsymbol{ET}_a$	469	477	0.007	469	0.037	474	0.026
$\boldsymbol{Q}_{deep}$	185	186	0.022	187	0.103	180	0.071
$\Delta \boldsymbol{W}$	46	38	0.029	45	0.052	46	0.024

The *CV* values of the simulated seasonal water balance components for the dry verification experiment are given in Table 5.4. Again, the *CV* values are smallest for Case 3 followed by Case 4 and Case 5. Simulated and reference $\boldsymbol{Q}_{deep}$ and $\Delta \boldsymbol{W}$ is negligible for this verification experiment. The reference and simulated $\boldsymbol{ET}_a$ is quite similar, but $\boldsymbol{E}_a$ is over predicted and $\boldsymbol{T}_a$ is under predicted by different fitted parameters. The deviation between reference and simulated $\boldsymbol{E}_a$ and $\boldsymbol{T}_a$ is minimum for Case 3 followed by Case 4 and Case 5. Even the Case 3 over predicts $\boldsymbol{E}_a$ by 30 per cent and under predicts $\boldsymbol{T}_a$ by 7 per cent. Due to relatively smaller proportion of $\boldsymbol{E}_a$ (28 per cent) into $\boldsymbol{ET}_a$, the over prediction has little effect on the total $\boldsymbol{ET}_a$. A comparison of the mean and *CV* values of $\boldsymbol{ET}_a$ with that of $\boldsymbol{E}_a$ and $\boldsymbol{T}_a$ indicate that prediction of $\boldsymbol{ET}_a$ is much more accurate and reliable than that of separate prediction of $\boldsymbol{E}_a$ and $\boldsymbol{T}_a$.

Temporal water balance components: In order to examine the reliability of inversely identified parameters for temporal hydrological behaviour, the root mean square error RMSE of the daily values of different water balance components were computed. The resulting RMSE values are given in Table 5.5.

Table 5.4. Same as table 5.3 but for the *dry verification experiment.*

Water balance component	Reference	Case 3		Case 4		Case5	
		Mean	*CV*	Mean	*CV*	Mean	*CV*
$\boldsymbol{E_a}$	70	92	0.010	100	0.096	99	0.094
$\boldsymbol{T_a}$	180	167	0.008	152	0.098	154	0.088
$\boldsymbol{ET_a}$	250	258	0.002	252	0.021	253	0.017
$\boldsymbol{Q}_{deep}$	2	1	0.056	1	0.468	1	0.340
$\boldsymbol{\Delta W}$	2	1	0.000	3	1.013	4	1.009

Table 5.5. Root mean square error RMSE (mm d^{-1}) and mean (mm d^{-1}) value of areal daily simulated water balance components for Case 3, Case 4 and Case 5. The results are based on simulation period of 160 days for a typical optimization.

Water balance component	Reference	Case 3		Case 4		Case 5	
		Mean	RMSE	Mean	RMSE	Mean	RMSE
	Wet verification experiment						
E_a	0.66	0.70	0.066	0.70	0.080	0.70	0.080
T_a	2.27	2.25	0.096	2.07	0.374	2.20	0.117
ET_a	2.93	2.95	0.095	2.77	0.317	2.91	0.091
Q_{deep}	1.16	1.20	3.153	1.35	1.980	1.18	0.955
	Dry verification experiment						
E_a	0.44	0.58	0.207	0.69	0.313	0.66	0.283
T_a	1.13	1.03	0.133	0.85	0.486	0.90	0.348
ET_a	1.57	1.61	0.180	1.54	0.359	1.56	0.258
Q_{deep}	0.01	0.00	0.011	0.01	0.013	0.01	0.010

The RMSE values (Table 5.5) are based on the entire simulation period of 160 days. The RMSE values follow more or less a similar trend as that of *CV* of cumulative water balance components except for daily Q_{deep}. The RMSE values of the simulated daily ET_a are in the acceptable range. Surprisingly, Case 3 has a very high RMSE value (3.2 mm d^{-1}) for simulated Q_{deep}. This suggests that if all the VG model parameters are optimized based on ET_a fluxes, the resulting parameters may not reproduce a reliable estimate of temporal Q_{deep}. Reliable prediction of temporal Q_{deep} may be quite important for certain applications e.g. to determine peak drainage coefficient for the design of regional drains.

To further examine the performance of different Cases in reproducing the temporal variation of Q_{deep}, the simulated and reference daily Q_{deep} is also shown in Fig. 5.4. The high RMSE value of simulated Q_{deep} (Table 5.5) is due to the over prediction of Q_{deep} during the period immediately following irrigation, particularly for relatively larger depth of irrigation (20 cm) on day 1. Though there are some over predictions of Q_{deep} by Case 5, during periods immediately following different irrigation events, the overall performance of Case 5 in comparison to case 3 and 4 is noteworthy. This further justifies the earlier conclusion that, if VG model parameters are optimized based on ET_a fluxes, it is more appropriate to optimize α, k_{sat} and θ_{sat} rather than optimizing the scale factor or all the VG model parameters. This also means that some information on the textural soil class of the area under consideration, to assign appropriate value for parameter n and θ_{res}, is an important input to define area effective soil hydraulic parameters using ET_a fluxes.

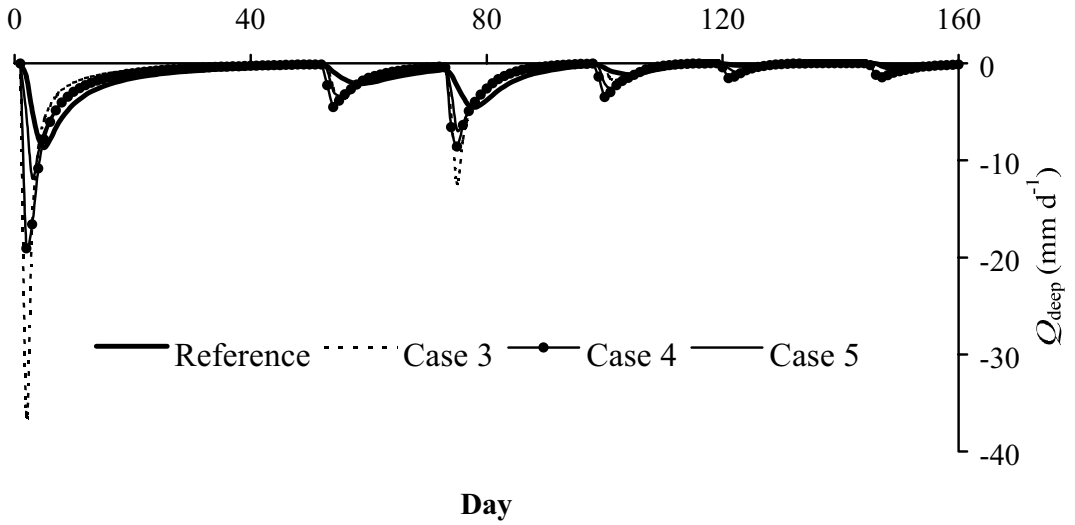

Figure 5.4. Temporal variation of area effective reference and simulated Q_{deep}, at 120 cm depth, for the wet verification experiment using inversely identified soil hydraulic parameters.

Soil water retention curve: Fig. 5.5 shows the area effective soil water retention curve as derived from inverse modelling approach for the best performing case (Case 5). Also shown are the soil water retention characteristics of different layers encountered in the study area. It is important to note that despite a large variation in the soil water retention characteristics of

different soil layers, the identified area effective curve reproduced water balance components quite reasonably well.

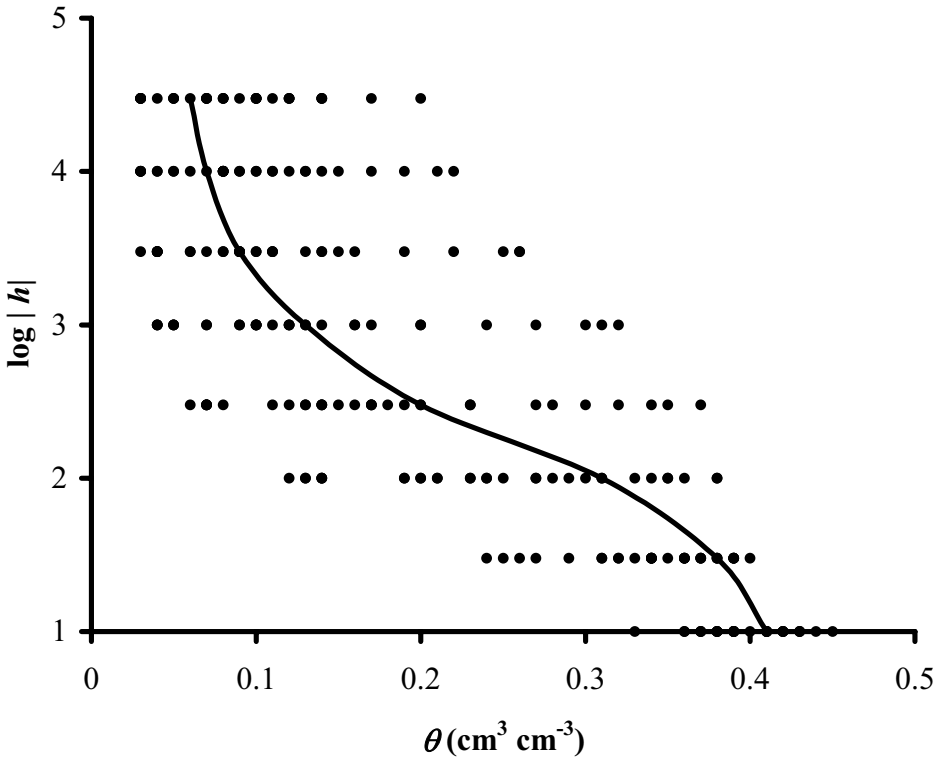

Figure 5.5. Soil water retention characteristics of different layers of 7 profiles used in the study. Also shown is the area effective soil water retention curve as derived from inverse modelling approach (Case 5).

5.6 General Discussion

The results of the present study are based on soil profiles having a relatively high sand fraction in surface layers. The soil evaporation process is mainly governed by the surface layers. Therefore, any alteration of soil hydraulic parameters for the top layer is expected to affect simulated E_a. When the heterogeneous soil profiles are defined by a single homogeneous soil profile, the whole profile effective soil hydraulic parameters are also assigned to the surface layers. In this case, sub-surface soil layers varied greatly in texture. This results in over prediction of E_a by the inversely identified soil hydraulic parameters.

Other conditions may arise in the field situation when surface layers are of relatively heavier texture than sub-surface layers. Under such situations, it may be expected that the effective soil hydraulic parameters derived by the present approach may result in under prediction of the soil evaporation. Therefore, if the surface soil layers have deviating soil hydraulic properties and if T_a and E_a are to be simulated separately and interpreted independently, care must be taken not to give undue attention to absolute values while comparing different scenarios. Alternatively, it may be more appropriate to identify the soil hydraulic parameters of the surface layer independently or an alternative approach must be adopted to simulate E_a. Further, the wide differences in the inverse results when using different approaches of E_a simulation indicate that the simulation of E_a should be given serious attention while attempting to inversely identify soil hydraulic functions for heterogeneous soil conditions. One approach to tackle this problem could be to derive the parameters for the top layer using remotely sensed soil evaporation under bare field conditions as input to the objective function.

The acceptable performance of inversely identified soil hydraulic parameters in predicting the total $\boldsymbol{ET_a}$ and $\boldsymbol{Q}_{deep}$ is encouraging. For irrigated agriculture in arid and semi-arid regions, assessment of water logging risks (directly related to total $\boldsymbol{Q}_{deep}$) is a critical issue. The inversely identified soil hydraulic parameters are sufficient to make simple water balance computation to evaluate the performance of irrigation systems under such regions.

In this study, only the heterogeneity of soil was considered while deriving area effective soil profiles. However, in reality there could also be a mixture of different crops at the scale of model application. It is beyond the scope of this chapter to deal with this problem, as the aim was to know if a mixture of heterogeneous soil profiles can be defined by an overall effective soil profile. However, a simple framework is suggested to account for the crop heterogeneity. Referring to Fig. 3.6, instead of a single simulation run for a given set of parameters (as estimated by each PEST run), the simulation model (in this case SWAP) can be run for a number of crops in the area. The simulated ET_a fluxes for different crops can then be averaged before supplying them as output to the objective function.

5.7 Conclusions

Various problems associated with the assignment of effective soil hydraulic parameters for heterogeneous soil profiles have been addressed. An attempt has been made to derive effective soil hydraulic parameters for a typical area consisting of spatially variable heterogeneous soil profiles. It has been highlighted that the process of deriving effective soil hydraulic parameters for heterogeneous soil profiles is not as straight forwards as for homogeneous soil profiles.

In this study the actual soil evaporation could not be predicted accurately by the inversely identified soil hydraulic parameters due to deviating soil hydraulic properties of surface layers. If actual soil evaporation and transpiration are to be simulated separately and interpreted independently, simulation of soil evaporation should be given serious attention while deriving effective soil hydraulic parameters for field conditions having deviating hydraulic properties of surface layers.

The acceptable performance of inversely identified soil hydraulic parameters in predicting total evapotranspiration and deep percolation is encouraging. It has been shown that, it is *possible to define an area having spatially variable heterogeneous soil profiles by an equivalent single homogeneous soil profile*, which results in reliable water balance computations. The cumulative water balance components could be simulated accurately even when all the VG model parameters were optimized. However, to reproduce acceptable temporal deep percolation loss, it is necessary that general information on soil textural layering is available for the area.

Results as obtained with forward and backward simulations carried out in the present study suggest that if the selected modelling concept is an appropriate representation of the real system, evapotranspiration fluxes, along with general information on soil textural layering, are sufficient to derive area effective soil hydraulic parameters. Despite a large variation in the hypothetically constructed area, it was possible to reproduce a good estimate of relevant water balance components. It means that *even satellite images with poor spatial resolution could be used to identify soil hydraulic parameters at the pixel level*. Heterogeneity of different soil types within the pixel size is not a limitation.

Chapter 6

Calibration of the regional model FRAME using remotely sensed evapotranspiration rates and groundwater heads[3]

6.1 Introduction

In recent years, attempts have been made to use detailed physical models for the diagnosis of irrigation water management practices at regional scale (*Abdel Gawad et al.*, 1990; *Droogers and Kite*, 1999; *D'Urso et al.*, 1999). Agro-hydrological models are effective tools to help planners and managers to compare impacts of different water management policy options. Typically, the processes occurring in the system are represented by parametric functions and relations which are known to reasonably describe the underlying physical system (*Sorooshian and Arfi*, 1982). For small and homogeneous areas, the physics of these models are well understood (*Holman-Dodds et al.*, 1998). However for practical use, the values of vegetation, soil and hydrological parameters are not known *a priori* at the regional scale that the models are applied (*Boyle et al*., 2000). Therefore, reliable estimation of the parameters is required before these models can be applied to solve natural resource problems (*Gupta et al.*, 1998; *Hanson et al.*, 1999).

The parameter identification problem might be ill posed in case of poorly defined model structure, too high correlation between different parameters, too large observation errors for the system response and too large errors in input data. In many cases, parameter uncertainty can be reduced by reducing the number of parameters to be estimated (*Yeh and Soon*, 1981) as well as by using additional system response data during optimization (*Franks et al.*, 1998). Therefore, it is desirable to include as many system responses as possible in the calibration process.

The major aim of an irrigation system is to maintain the crop evapotranspiration ET_a at desired levels. Crop ET_a is an important component/indicator for the evaluation of the

[3] Adapted version of Jhorar, R.K. and M.F.R. Smit. 2002. Calibration of a distributed irrigation water management model using remotely sensed evapotranspiration rates and groundwater heads. Journal of Hydrology (to be submitted)

irrigation system performance (*Bastiaanssen et al.*, 1992). One of the most common negative effects of canal irrigation projects in arid and semi-arid regions is the rise in groundwater levels, leading to problems of waterlogging and secondary soil salinisation. Therefore, the analysis of groundwater level fluctuations as a response to irrigation practices is an important criterion to evaluate the sustainability of irrigated agriculture in arid and semi-arid regions. In summary, ET_a and groundwater level fluctuations are both important factors for the evaluation of irrigation system performance at the regional scale. Therefore it would be worthwhile to incorporate both ET_a rates and groundwater levels in the calibration process of simulation models. In this way, model prediction may be made more accurate, reliable and useful for decision-makers and planners involved in water management.

In an earlier study, a distributed irrigation water management model FRAME (*Boels et al.*, 1996) was used to analyse the performance of an irrigation system for the Sirsa Irrigation Circle, Haryana (India). The model was calibrated (1977-1982) and validated (1982-1990) to reconstruct groundwater dynamics in the study area. The calibration was achieved through manual adjustment of soil hydraulic parameters and aquifer drainable porosity. The model output on ET_a, implicitly assuming that it is correctly simulated, was also used to analyse the effects of the present water management practices. Calibration of a model against an output, of which prediction is utilized for performance or scenario analysis, is important for reliable model application. For instance, *Yan and Han* (1991) and *Wallach et al.* (2001) considered different outputs of their models and showed that estimating parameters using one output may give quite poor results for a different output.

The objective of the present study is *to calibrate the model FRAME using information on both Remotely Sensed evapotranspiraton* ET_{RS} *rates and in-situ measurements of groundwater heads.* The data on ET_{RS} fluxes will be introduced with the primary intent of improving predictions of ET_a through better estimated soil hydraulic parameters. Moreover, the incorporation of more than one set of observational data in the parameter estimation process produces a better conditioned and more stable set of parameter estimates than would occur when using only one data set (*Weiss and Smith*, 1998). The proposed approach of using ET_{RS} data determined from satellites to calibrate FRAME for a region has been applied to the Sirsa Irrigation Circle (Fig. 2.1) in Haryana, Northwest India. A brief description of the study area is included in Chapter 2 and the model FRAME is described in Chapter 3. The distributed irrigation water management model FRAME, is composed of two model packages,

SImulation of Water management in Arid REgions (SIWARE) for canal and on-farm water management and the Standard Groundwater Model Package (SGMP) for regional groundwater flow.

6.2 Schematization of the Sirsa Irrigation Circle area and input data

Schematization of the study area: To facilitate computation of water and salt components in a spatially distributed manner, SIWARE requires the study area to be schematized into a number of sub-areas known as C*alculation Units* (CUs). The Sirsa Irrigation Circle area has been divided into 46 CUs as shown in Fig. 6.1a. Each CU is assumed to be uniform with respect to soil parameters, climate, hydrology and water supply conditions. The schematization of CUs is such that each CU receives continuous water supply from the irrigation system. Depending on the desired accuracy and the availability of geo-hydrological parameters, the SGMP requires that the area is schematized into a nodal network. Although the geo-hydrological parameters at every grid node of the model domain are practically never available, a finer numerical grid is maintained for better system geometry approximation and numerical accuracy and convergence. The nodal network for the study area (Fig. 6.1b) consists of 37 *internal nodes* and 24 *boundary nodes*. Known groundwater heads were specified at the boundary nodes. The model computes groundwater heads for internal nodes and groundwater flow between different nodes. The groundwater heads are computed based on recharge and abstraction rates occurring at each internal node as computed by SIWARE.

Input data:

Rainfall data: Daily rainfall data were available from 9 rain-gauge stations in the study area (Fig. 6.1a). The model requires daily rainfall data for each of the 46 CUs. One approach to representing precipitation over each calculation unit is to interpolate measurements from neighbouring stations using geostatistical methods (*Isaak and Srivastava*, 1989). However, in this study a single station was chosen to represent each neighbouring CU.

Potential evapotranspiration rate: The model requires average ET_p values on a 10-day period basis. Daily weather data from the meteorological station at Haryana Agricultural University (HAU), Hisar were used to compute ET_p by the Penman-Monteith (P-M) approach (*Allen et al.*, 1998). The ET_p was computed for different crop heights and provided as tabulated input

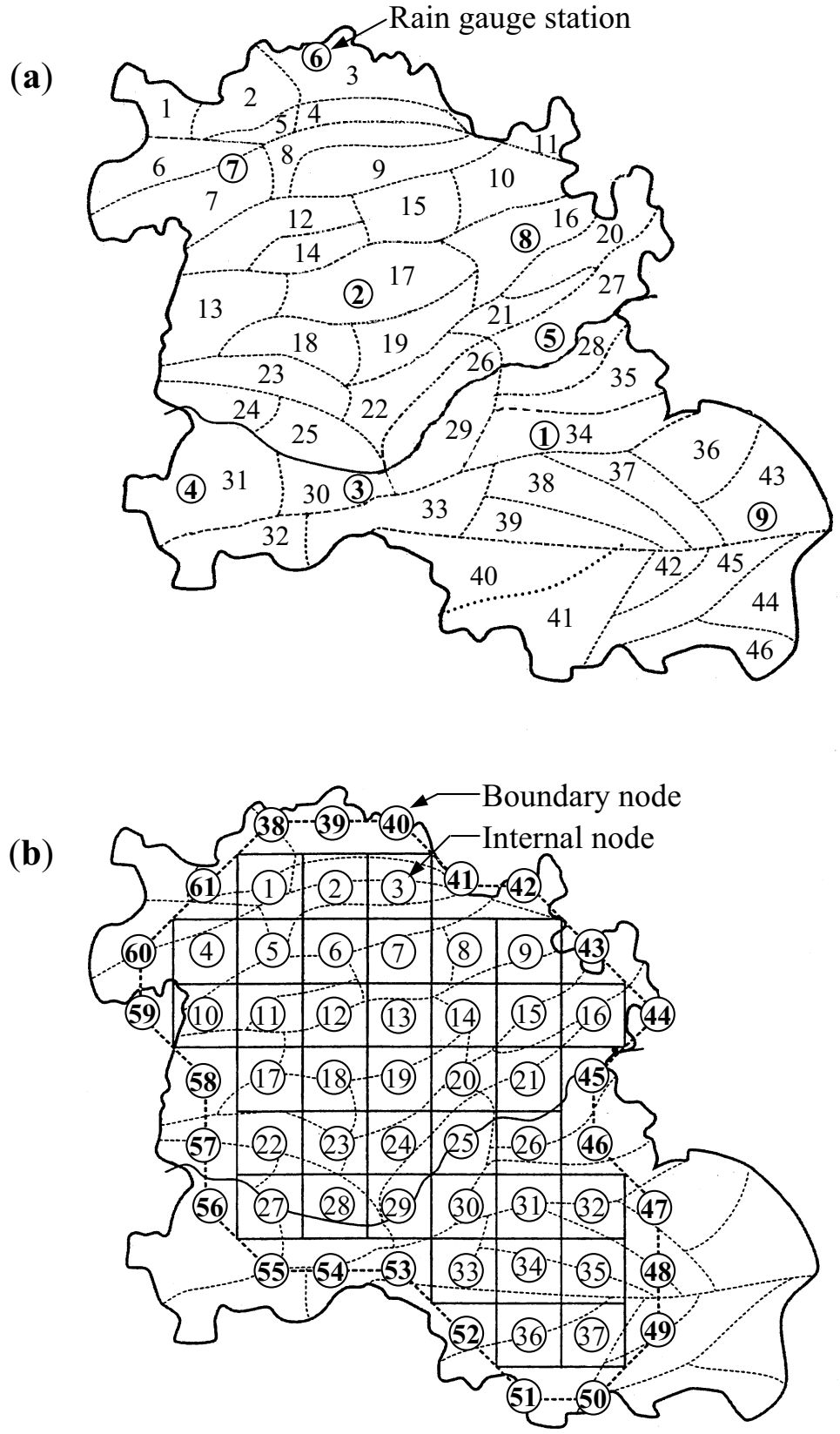

Figure 6.1. Subdivision of the Sirsa Irrigation Circle into (a) Calculation units for the SIWARE model and (b) Nodal areas for the SGMP model. Also shown is the location of 9 rain gauge stations.

to the model. Reduction factors for incomplete soil cover (*Rijtema and Abou Khaled*, 1975) were also provided.

Canal water Supply: The discharges through all the main canals that enter and leave the area (Fig. 2.1) were monitored twice a day (morning and evening) through gauge readings by the Irrigation Department. FRAME requires the total annual canal water supply and fraction of the total supply during different periods. Daily values of discharge measurements were converted to this required input data.

Crop data: This category of data comprises crop growth development, sensitivity to moisture and salt stress, irrigation schedules, crop rotation and area under different crops. Crop growth development is expressed in the evolution of crop height, soil cover and rooting depth. The information on crop growth development was based on experimental observations at the HAU farm (*Kumar and Singh*, 1994). A total of 13 crops were defined in the model: 6 in winter and 7 in summer. To account for the fallow area, two additional hypothetical crops with zero rooting depth, crop height and soil cover were included. Sensitivity to moisture and salinity stress has been provided through critical leaf water potentials for different crops (*Roest et al.*, 1993). The model computes the value of leaf water potential based on simulated available moisture as well as simulated salt content in the root zone. The irrigation schedules for different crops were based on local guidelines (*Agarwal and Khanna*, 1983). In the model a score value is assigned to a certain crop to be grown after another crop. A high score value means that most probably the considered crop will be grown after the crop for which it has such a high preference. The area occupied by different crops in the Sirsa Irrigation Circle were obtained per village and aggregated at the level of CUs (*Kumar and Singh*, 1994). Wheat, gram, oil seeds and cotton were the major crops in the study area.

Properties of the aquifer system: The Sirsa Irrigation Circle is predominantly underlain by the alluvial sediments of the Ghaggar basin. The alluvial sediments mainly consist of fine to medium sand, silt and clay, and nodules of 'kankar'. Exploratory drillings revealed that the basement rocks are encountered at depths varying from 180 to 300 m below soil surface (*Chadha*, 1983). *Gupta* (1983) and *Chadha* (1983) reported transmissvity and aquifer thickness data for the study area, which reveal that the hydraulic conductivity of the underlying aquifer varies from 3 to 20 m d^{-1}. *Boonstra et al.* (1996) analysed existing pumping test data and found the values of specific yield or drainable porosity varying from 1

to 29 %. *Boonstra et al.* (1996) also defined physical properties of the aquifer system i.e. nodal surface elevations and bottom elevations based on topographical and aquifer base maps for the study area.

Groundwater data: Groundwater is abstracted in the area through a number of both shallow and deep tube-wells. Knowing the number of such units and their installed capacity, the maximum possible groundwater withdrawal along with its quality was specified for each CU. The model computes actual groundwater pumpage depending on deficit in canal/rain water supply and maximum installed capacity. The groundwater levels in the study area were monitored through a network of observation wells twice a year (June and October). The period of measurements coincided with the general trend of deepest (June- before rainy season) and shallowest (October-end of monsoon) water levels.

Actual evapotranspiration rate: Remote sensing techniques have been shown to be promising in assessing regional patterns of actual evapotranspiration ET_a (*Moran and Jackson*, 1991). A large number of remote sensing ET_a algorithms have been developed (e.g. *see Bastiaanssen et al.*, 1999). In this study, the SEBAL (Surface Energy Balance Algorithm for Land) algorithm was used to determine ET_{RS} from remote sensing measurements (*Bastiaanssen et al.*, 1998). SEBAL requires spatially distributed visible, near-infrared and thermal infrared data. For this study AVHRR (Advanced Very High Resolution Radiometer) images of the NOAA-11 (National Oceanic and Atmospheric Administration) satellite for 23 cloud free days were used. The images have a spatial resolution of 1.1 km x 1.1 km and can be freely downloaded from http://www.saa.noaa.org (verified on 28-10-2001). The basic procedure as employed in SEBAL is to solve the energy balance during satellite overpass to compute instantaneous evaporative fraction for cloud free days. The evaporative fraction is defined as the latent heat divided by the net available energy. The instantaneous evaporative fraction is considered similar to its 24-h counterpart (*Kustas et al.*, 1994). For cloudy days, known values of evaporative fraction together with routine weather data were used to compute ET_a. This results in a 1.1 km grid of ET_{RS} obtained under all weather conditions.

6.3 Calibration strategy

Identification of parameters to be adjusted: The integrated regional water management model FRAME has a large number of parameters (Table 6.1). In simple cases, it may be possible to estimate all the model parameters. In general, however, this is not possible due to the large computation times and non availability of sufficient accurate observations. One approach is to carry out a sensitivity analysis of the model and to adjust only the most sensitive parameters. Another different approach is to start with an estimation of a few parameters and then add further parameters if they improve the model predictive quality (*Wallach et al.*, 2001). The present study makes use of both approaches. First a sensitivity analysis was carried out to identify the most sensitive parameters, thereafter the parameters which helped indeed improving the model predictive quality were added. The other parameters were fixed to the values determined during the previous calibration study (*Boels et al.*, 1996).

Parameter optimization criteria: A model should be validated for the types of applications for which it is intended. Thus, performance criteria as well as calibration and validation schemes should be tailored to the objective of study (*Refsgaard*, 1997). The ultimate objective of this study is to use the FRAME model to test different water management scenarios at regional scale. Actual evapotranspiration rate ET_a and groundwater levels (head) h_{gw} are of prime importance for this study. Therefore, the model parameters were calibrated to obtain a good fit between ET_{RS} and h_{gw} data. In the integrated model, ET_a is simulated by SIWARE and h_{gw} by SGMP.

Let $ET_a(\boldsymbol{b}, t_i)$ and h_{gw} $(\boldsymbol{b}, t_j)$ be the calculated values of ET_a and h_{gw}, respectively, at time t_i and t_j corresponding to a trial vector of selected parameter values $\{\boldsymbol{b}\}$, where $\{\boldsymbol{b}\}$ is the n-dimensional vector containing the parameters that are optimized simultaneously. The inverse problem is then to find an optimum combination of parameters $\{\boldsymbol{b^0}\}$ that minimizes the following objective functions:

$$\Phi(b) = \sum \left[w_i \left\{ ET_a(t_i) - ET_a(t_i, \mathbf{b}) \right\} \right]^2 \tag{6.1}$$

$$\Phi(b) = \sum \left[v_j \left\{ h_{gw}(t_j) - h_{gw}(t_j, \mathbf{b}) \right\} \right]^2 \tag{6.2}$$

where Φ is the objective function, w_i and v_i are the weighting factors accounting for data points. Eq. 6.1 is used to calibrate model parameters sensitive to ET_a and and Eq. 6.2 is used to calibrate model parameters sensitive to h_{gw}.

Table 6.1. Parameters of the FRAME model and their reference values for the applied sensitivity analysis for calculation unit 17.

Parameter	Description	Units	Reference value
	A) Top system – SIWARE		
Soil characteristics (for each calculation unit)			
θ_s	Moisture content at saturation	$m^3\ m^{-3}$	0.425
θ_{fc}	Moisture content at field capacity	$m^3\ m^{-3}$	0.260
θ_{wp}	Moisture content at wilting point	$m^3\ m^{-3}$	0.110
Z_{cz}	Thickness of capillary zone	m	0.50
I_b	Basic infiltration rate	$m\ d^{-1}$	0.20
Surface irrigation process (for each calculation unit)			
X_{pl}	Plot length	m	60
X_{pw}	Plot width	m	7.5
s	Plot slope	-	0.0020
η	Manning's coefficient	$s\ m^{-1/3}$	0.10-0.15
q_o	On-farm stream discharge capacity	$m^3\ s^{-1}$	0.0150
q_s	On-farm conveyance losses	$m^3\ s^{-1}$	0.0015
Hydrological characteristics (one value for entire region)			
R_{cc}	Resistance against vertical flow	d	275
R_{pud}	Resistance of puddled layer	d	999
	B) Aquifer system – SGMP (for each node)		
K	Hydraulic conductivity	$m\ d^{-1}$	10.0
S_y	Specific yield/drainable porosity	-	0.10

Parameter estimation procedure: The calibration was achieved in two phases. During the first phase, ET_{RS} data were used to calibrate the parameters of FRAME to which ET_a rates are sensitive. As ET_{RS} rates from remote sensing analysis were obtained for the year 1990 only, this year was selected for the first phase of calibration. During the second phase, h_{gw} data were used to calibrate drainable porosity of the aquifer. The years 1977-1981 were selected for the second phase of calibration. Accordingly, during the first phase Eq. 6.1 and during the second phase Eq. 6.2 was used. Initial values of parameters were taken from the previous

study (*Boels et al*., 1996) and during parameter optimization a reasonable parameter range around these values was specified. The inverse problem was solved using the parameters estimation program PEST (*Doherty et al.*, 1995). An overview of the parameter estimation procedure is shown in Fig. 3.6. A brief description of PEST was included in Chapter 3.

Because the study area modelled is divided into 46 CUs (Fig. 6.1a), which are explicitly parameterized, the number of parameter values characterizing the study area would be very high. It is neither possible nor meaningful to optimize all these parameter values simultaneously (*Eckhardt and Arnold*, 2001). Therefore, during the first phase of calibration, parameters were estimated independently for each of the 46 CUs. During the first phase, the SGMP model was prevented from simulating groundwater levels. Observed groundwater levels were specified to avoid any effect of simulated groundwater depth on ET_a. In the FRAME model a maximum of 8 different soil types may be specified. Therefore, before the second phase of calibration, all the CUs were categorized into different sub-groups depending on the optimized/assigned parameter values in phase one. To each sub-group, a particular soil code was assigned in the input file containing the optimized parameters. During the second phase of calibration, the parameters optimized during the first phase were kept constant and values of aquifer drainable porosity were optimized for the internal nodes (Fig. 6.1b).

6.4 Sensitivity of model parameters to ET_a

The sensitivity analysis was restricted to CU number 17 (Fig. 6.1a) which is located in the central part of the study area. The sensitivity analysis presented here focuses on the parameters of the top system only. In a previous study (*Boonstra et al.*, 1996), the *sensitivity analysis of the aquifer parameters showed that model results were not sensitive to aquifer hydraulic conductivity in the reported range of values but quite sensitive to aquifer drainable porosity*.

The sensitivity of simulated annual actual evapotranspiration $\boldsymbol{ET_a}$ to changes in different model parameters (Table 6.1) is shown in Fig. 6.2. The parameters sensitivity is reported as the change in model output for a fixed per cent change in each parameter's value. For the sake of clarity, model parameters which showed insignificant or no sensitivity are not plotted

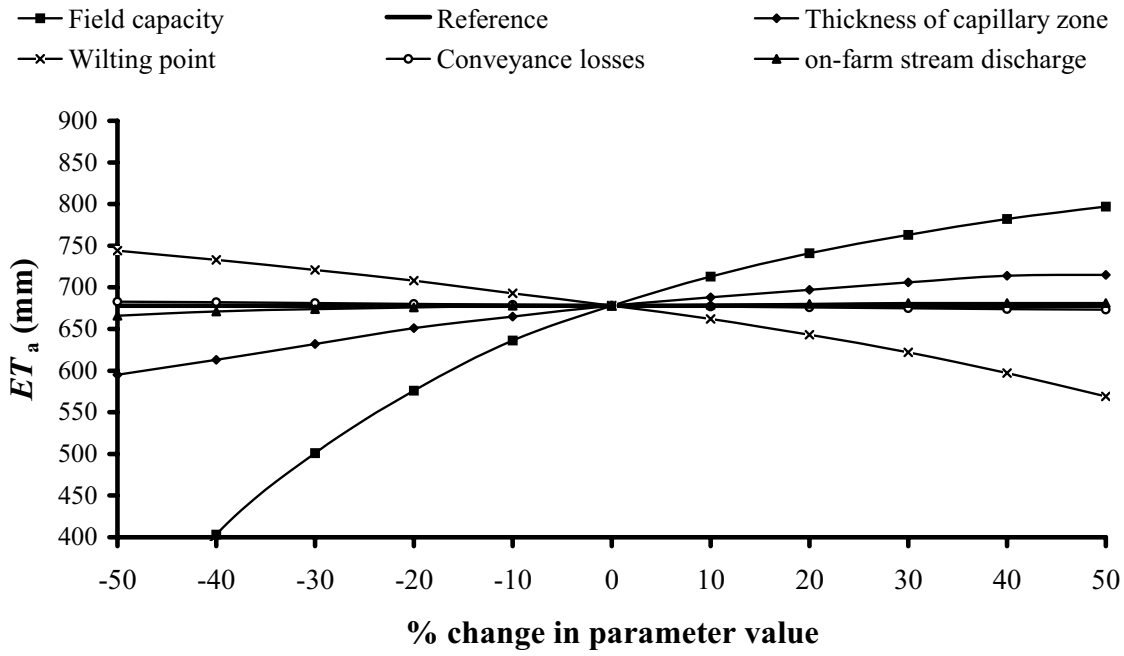

Figure 6.2. Sensitivity of different parameters of the FRAME model to simulated annual actual evapotranspiration $\boldsymbol{ET_a}$.

e.g. soil saturation percentage showed no effect on $\boldsymbol{ET_a}$ and hence, was excluded from Fig. 6.2. Parameters that have relatively little influence on simulated $\boldsymbol{ET_a}$ show more or less horizontal lines. By contrast, parameters that have a major influence on $\boldsymbol{ET_a}$, show steeply sloping lines.

It can be observed from Fig. 6.2 that *moisture content at field capacity* θ_{fc} *is the most sensitive investigated parameter for simulated* $\boldsymbol{ET_a}$ *followed* by the *moisture content at wilting point* θ_{wp}. In fact ET_a is sensitive to the Total Available soil Moisture θ_{TAM} ($=\theta_{fc}$ - θ_{wp}). The fact that θ_{fc} appears to be more sensitive than θ_{wp} is due the choice of the scale of the x-axis and due to the reference values of θ_{fc} (0.26, Table 6.1) and θ_{wp} (0.11, Table 6.1). A fixed % change in θ_{fc} causes a larger change in θ_{TAM} than a corresponding % change in θ_{wp}. The opposite influence of θ_{fc} and θ_{wp} on $\boldsymbol{ET_a}$ is due to the fact that an increase in θ_{fc} causes an increase in θ_{TAM} while an increase in θ_{wp} decreases θ_{TAM}. Furthermore *a certain % increase in* θ_{fc} (or decrease in θ_{wp}) *is shown to be less sensitive than a corresponding % decrease in* θ_{fc} (or increase in θ_{wp}) *due to the limiting influence of specified* ET_p *and water*

supply on $\boldsymbol{ET_a}$. The next most sensitive parameter for $\boldsymbol{ET_a}$ is *the thickness of the capillary zone* Z_{cz} and the on-farm conveyance losses. Stream size showed sensitivity only for a decrease in size. Stream size represents the discharge rate of inlet stream during field irrigation.

The sensitivity analysis presented in Fig. 6.2 can also be used to predict the likely influence of errors (particularly systematic errors) in the observations. Relatively small errors in $\boldsymbol{ET_a}$ could lead to less sensitive parameters (e.g. conveyance losses and stream discharge) being fitted far away from their actual value. Moreover, the difference in magnitude of sensitivity (indicated by the vertical difference in reference line and parameter line in Fig. 6.2) for equal increase and decrease in parameter values means that an equivalent amount of under-prediction and over-prediction in ET_a could be differently critical for the inversely fitted parameters values. For example, an over-prediction in ET_a could cause the fitted value of θ_{fc} being more away from the true value than that caused by an equivalent amount of under prediction in ET_a.

6.5 Prior analysis of calibration strategy

Based on the sensitivity of simulated $\boldsymbol{ET_a}$ to different parameters, the obvious choice would be to include the relatively more sensitive parameters (θ_{fc}, θ_{wp} and Z_{cz}) in the optimisation process. However, the choice is not straightforward in case correlation exists between different parameters. Therefore, a prior analysis of the optimization process was carried out to decide how many parameters can be adjusted. During this analysis the ET_a data used were generated with forward FRAME simulations and corrupted with random error (Eq. 4.4). The ET_a data with added error were then used in the objective function (Eq. 6.1) to optimize different combinations of the sensitive parameters (θ_{fc}, θ_{wp} and Z_{cz}). The results of the prior analysis are presented in Table 6.2.

To evaluate the impact of inclusion of additional parameters in the optimization process, run number 1 (Table 6.2), wherein only the most sensitive parameter i.e. θ_{fc} is optimized, was treated as reference. The 95 % confidence interval *CI* (Table 6.2) provides a useful means of comparing the certainty with which different parameter values are estimated by PEST (*Doherty et al.*, 1995).

Table 6.2. Results of prior optimization runs to decide the number of parameters to be adjusted

Number run	Optimized parameter(s)	Optimized value [1] ± 95 % *CI*	Correlation coefficient	Objective function[2]
1	θ_{fc}	0.23 ± 0.03	-	4476
2	θ_{fc} θ_{wp}	0.25 ± 0.41 0.13 ± 0.38	$\{\theta_{fc}, \theta_{wp}\}$ = 0.997	4474
3	θ_{fc} Z_{cz}	0.24 ± 0.04 0.45 ± 0.18	$\{\theta_{fc}, Z_{cz}\}$ = 0.591	4007
4	θ_{fc} θ_{wp} Z_{cz}	0.19 ± 0.59 0.07 ± 0.52 0.52 ± 0.27	$\{\theta_{fc}, \theta_{wp}\}$ = 0.998 $\{\theta_{fc}, Z_{cz}\}$ = 0.684 $\{\theta_{wp}, Z_{cz}\}$ = 0.654	4470

[1] Reference value θ_{fc} =0.26 (cm^3 cm^{-3}), θ_{wp} = 0.11 (cm^3 cm^{-3}) and Z_{CZ} = 0.50 m; *CI* = Confidence Interval
[2] Starting value of objective function (Eq. 6.1) = 5837

It is clear that simultaneous inclusion of both θ_{fc} and θ_{wp} (run number 2) in the optimization process results into unreliable estimates of parameters values as indicated by the unacceptably high *CI* as compared to the parameter estimate. Moreover, there is no significant impact on the minimization of objective function. This is due to the high correlation between θ_{fc} and θ_{wp} (Table 6.2).

Inclusion of Z_{cz} into the optimization process (run number 3) on the other hand, improves the objective function with the optimized values being identified with acceptable *CI* values. Also the correlation between θ_{fc} and Z_{cz} is not too high. The general notion (*Wallach et al.*, 2001) that adjusting additional parameters always reduces the adjustment error (objective function) is not supported by the results presented in Table 6.2. When θ_{wp} was added for adjustment along with θ_{fc} and Z_{cz} (run number 4) the minimum value of the objective function was more than that obtained when only θ_{fc} and Z_{cz} were optimized (run number 3). This indicates that *inclusion of highly correlated parameters in the optimization process could further prevent global minima being found. A high correlation between* θ_{fc} *and* θ_{wp} *requires that one of these parameters should be assigned a fixed value.* Therefore, during parameter optimization, θ_{wp} was independently assigned a fixed value depending on the available soil textural information for the study area. Based on the prior analysis of the

optimization process, *during the first phase of calibration only* θ_{fc} *and* Z_{cz} *were optimized using* ET_{RS} *rates*.

6.6 Calibration of selected model parameters using ET_{RS} rates

The ET_a data as obtained from Remote Sensing ET_{RS} were summarised into 16 model time steps (Table 6.3) to have a one to one correspondence with the FRAME simulated ET_a i.e. ET_{SIWARE}. The rainfall as observed at 9 rain gauge stations during 1990 is presented in Fig. 6.3. Also shown in Fig. 6.3 are the days for which satellite images were used for ET_{RS} analysis. This information on rainfall and satellite image dates will be used to explain some differences between ET_{RS} and ET_{SIWARE}, for the periods when no satellite images were available or when rainfall occurred between two image dates. Initial optimization runs indicated that ET_{RS} for time steps 6, 7 and 8 (Table 6.3) was usually much higher than that ET_{SIWARE}. It may be noted that time step 6 coincides with the specified date of harvest of most of winter crops and sowing of summer crops. A further analysis of the remotely sensed bio-mass (not presented here) during different time steps also indicated a sudden drop in bio-mass production for the period 4 to 6 showing that most of the fields became fallow due to harvest of winter crops. Since during time steps 5-8 there was not much rainfall (Fig. 6.3), a higher evaporation from these fallow lands is unlikely to occur. This suggests that ET_{RS} for time step 6-8 is an overestimate of ET_a. Contrary to time steps 6-8, ET_{SIWARE} during time step 9 was higher than ET_{RS}. Referring to Fig. 6.3, during time step 9, it is clear that a considerable amount of rainfall occurred. Moreover, because of cloud cover there was no satellite image available during this period. ET_{RS} under this condition was estimated based on images available during the beginning of time step 8 and end of time step 11. Therefore, it is likely that during time step 9, ET_{RS} could not capture the effect of excess rainfall. Keeping in view the above known discrepancies between ET_a and ET_{RS}, during the parameter optimization runs the ET_{RS} data for time step 6, 7, 8 and 9 were not used.

Table 6.3. Time steps used for linkage between SIWARE and SGMP. All the time steps, except 5, are of 24 days duration. Time step 5 is of 5 days duration.

Time step	1	2	3	4	5	6	7	8	9	10	11	12	13	14	15	16
Days of the year	1-24	25-48	49-72	73-96	97-101	102-125	126-149	150-173	174-197	198-221	222-245	246-269	270-293	294-317	318-341	342-365

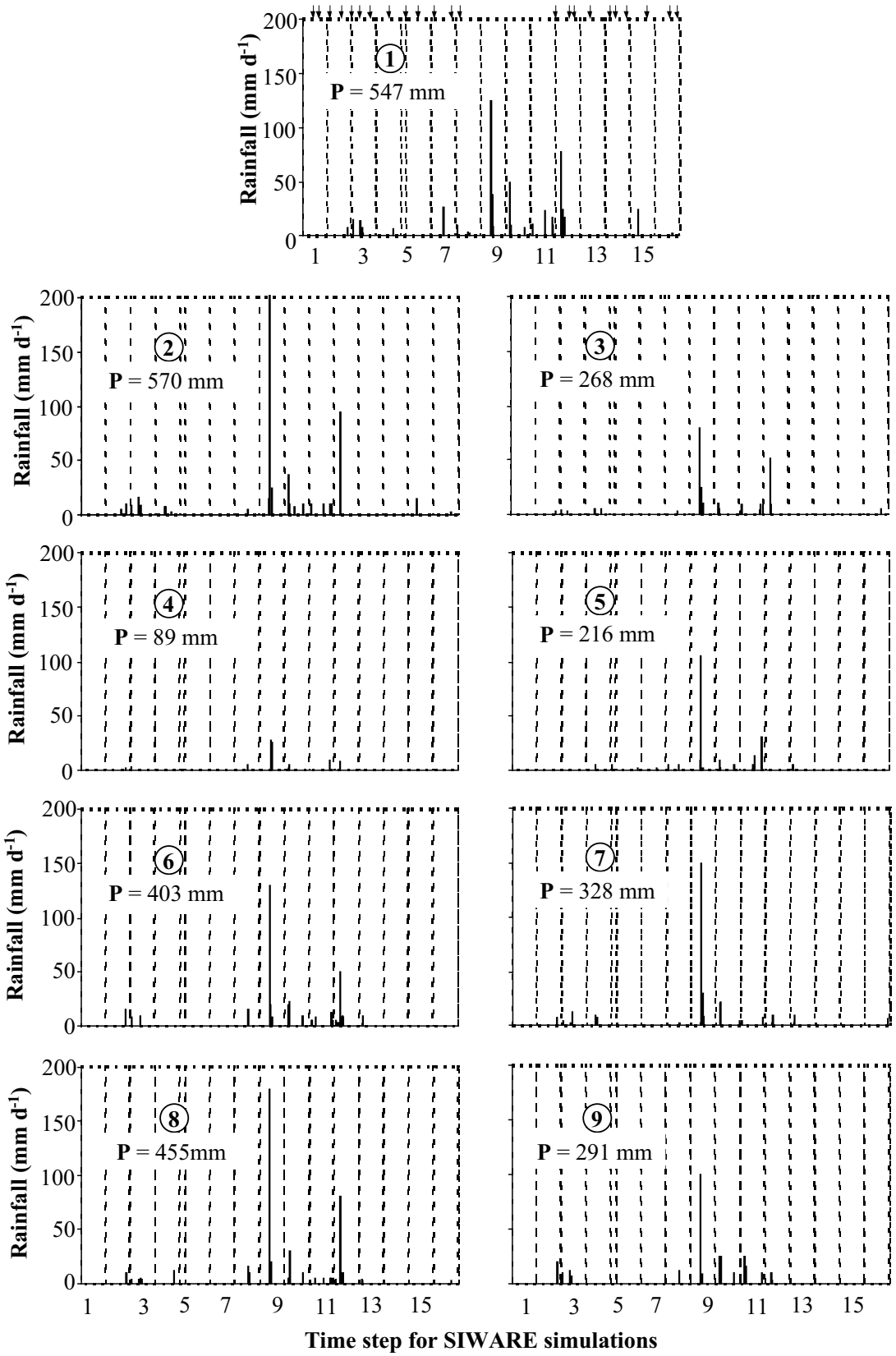

Figure 6.3. Daily rainfall during 1990 at different rain-gauge stations located in the Sirsa Irrigation Circle. Rain-gauge station number is indicated in circles. Arrows shows the days for which satellite images were used. **P** is total annual rainfall.

First, the parameter optimization process was carried out using temporal ET_{RS} rates for 12 time steps. Thereafter, cumulative $\boldsymbol{ET}_{RS}$ for the 12 time steps were used. The reason for this choice will be explained later. The optimized values of (θ_{fc} -θ_{wp}) are presented in Table 6.4. Table 6.5 presents the reported values of (θ_{fc} -θ_{wp}) for the different soil textural classes encountered in the study area (see column 6, Table 6.4). First, the results of parameter optimization using temporal ET_{RS} are discussed.

Parameter estimation using temporal $\boldsymbol{ET}_{RS}$ data: As can be observed from Table 6.4 (column 2 and 3), for some of the CUs the optimized parameter values are at the upper bound of the specified range. *This indicates that there is some temporal discrepancy between ET_{RS} and ET_{SIWARE} under the specified conditions of crop and water supply.* There could be many reasons for this discrepancy.

In model FRAME, similar crop growth parameters are specified for all the CUs implying plant growth being similar in all CUs, while in reality this is different. However, care is taken for the fractional area of different crops that may be different in different CUs. During simulations, the specified irrigation dates for a particular crop was same for all the CUs and it was assumed that total area under that particular crop is irrigated on the specified date. In reality, the irrigation to a particular crop is completed over a period of time depending on farmer's rotation for canal water supply. Also in the FRAME simulation study, the ET_p values specified were the same for all the CUs while in reality micro climatic conditions could make spatial differences in ET_p. Another major source for the temporal discrepancy between ET_{RS} and ET_{SIWARE} could be that during the simulation study, canal water allocation to different CUs was based on strict official rules (based on culturable command area). A recent study from Pakistan (*Wahaj*, 2001), where similar irrigation system and canal water allocation rules are followed, showed that the actual allocation may deviate from designed rules. All the above factors could cause temporal variations in ET_a, which may not be captured in simulations. Therefore, as a next step *total annual* $\boldsymbol{ET}_{RS}$ (excluding time steps 6 to 9, as explained earlier) was used to optimize the different parameters.

Table 6.4 Optimised values of total available soil moisture (θ_{fc} - θ_{wp}) and thickness of capillary zone (Z_{cz}) along with available soil textural information for different Calculation Units (CU). Simulated annual groundwater use and annual rainfall (**P**) are also included to explain their role in the fitted parameter values. Soil texture information is based on the soil map of the study area reported by *Ahuja et al.* (2001). For soil texture symbols see Table 6.5

CU	Based on temp. ET_{RS}		Based on cum. $\boldsymbol{ET}_{RS}$		Soil texture	***P***	Simulated Groundwater use
	θ_{fc} - θ_{wp} (-)	Z_{cz} (m)	θ_{fc} - θ_{wp} (-)	Z_{cz} (m)		(mm)	(mm)
1	**0.360**	0.90	0.223	0.20	LS/SiL	328	4
2	0.164	0.31	0.140	0.20	LS/ SiL	403	40
3	**0.360**	**1.20**	0.157	0.20	LS	403	35
4	0.173	0.20	0.148	0.20	LS	403	75
5	**0.360**	0.68	0.150	0.20	LS	328	15
6	**0.360**	0.78	0.227	0.30	SiL	328	10
7	**0.360**	1.00	0.209	0.30	S/LS/SL/SiL	328	13
8	**0.360**	**1.20**	0.174	0.20	LS	403	30
9	**0.360**	**1.20**	0.156	0.20	LS	403	25
10	0.154	0.18	0.137	0.20	LS	455	162
11	0.209	0.29	0.204	0.30	LS , SiL	455	21
12	0.121	0.10	0.112	0.20	S/ LS/ SL	570	5
13	0.108	0.12	0.097	0.10	S/SL	570	25
14	0.137	0.10	0.133	0.20	S/LS/ SL	570	41
15	0.137	0.10	0.122	0.20	LS/ SiL	570	23
16	0.133	0.54	0.125	0.30	S/ LS/ SL/ SiL	455	66
17	0.140	0.10	0.121	0.20	S/LS /SL	570	18
18	0.070	**1.20**	0.087	0.10	S/LS	570	47
19	0.115	0.12	0.107	0.20	S/ SL/ LS	570	74
20	0.146	0.19	0.132	0.30	LS/SiL	455	116
21	0.261	**1.20**	0.203	0.30	LS/ SiL	216	231
22	0.114	0.10	0.111	0.30	S/ LS/ SiL	547	322
23	**0.320**	0.18	0.108	0.20	S/ SL/ SiL	570	164
24	0.199	0.68	**0.320**	0.30	SiL	89	118
25	0.183	0.99	**0.320**	0.30	LS/ SiL/ SiCL	268	180
26	0.115	**1.20**	0.131	0.30	LS/SiL	547	562
27	0.215	0.29	0.207	0.30	LS/ SiL	216	225
28	**0.320**	0.93	0.210	0.30	SL/SiL	216	121
29	0.129	**1.20**	0.153	0.30	SiL/ SiCL	547	208
30	**0.320**	0.50	**0.320**	0.20	S/LS/SL/SiCL	268	140
31	**0.320**	0.16	**0.320**	0.20	S/LS/SL/SiCL	89	88
32	0.164	0.56	0.111	0.10	S/ SL	268	124
33	**0.400**	0.43	**0.400**	0.10	S/ LS/ SL/ SiL	268	67
34	**0.320**	0.62	0.225	0.30	SiCL	547	113
35	**0.320**	0.89	0.224	0.30	SiL/ SiCL	216	64
36	**0.320**	0.54	**0.320**	0.30	LS/ SiCL	291	68
37	**0.360**	0.93	**0.360**	0.46	LS	291	42
38	0.156	0.10	0.156	0.20	LS/ SL	547	39
39	0.147	0.10	0.150	0.20	LS/ SL	547	45
40	0.129	0.10	0.121	0.10	S/LS/ SL	547	59
41	0.113	0.15	0.104	0.10	S/LS/ SL	547	89
42	**0.360**	0.36	**0.360**	0.20	-	291	30
43	**0.360**	0.40	**0.360**	0.20	-	291	50
44	**0.360**	0.71	**0.360**	0.20	-	291	51
45	**0.360**	0.51	**0.360**	0.20	-	291	28
46	**0.360**	0.65	**0.360**	0.20	-	291	56

Note: The numbers in boldface indicate the values which were fitted to the upper bound as specified during optimization.

Table 6.5. Reported values of plant available water capacity (θ_{fc} -θ_{wp}) for different soil textural groups encountered in the Sirsa Irrigation Circle.

Soil texture	Bulk density (g cm^{-3})	θ_{fc} -θ_{wp}[1] (-)		
		USDA (1955)[2]	*Agarwal and Khanna* (1983)[3]	*Bastiaanssen et al.* (1996)
Sand (S)	1.6	0.08	0.12	0.04
Loamy sand (LS)	1.6	-	0.13	0.18
Sandy loam (SL)	1.5	0.12	0.14	0.15
Silt Loam (SiL)	1.4	0.17	0.25	-
Silty Clay Loam (SiCL)	1.3	-	0.23	0.19

[1]Reported values by *USDA* and *Agarwal and Khanna* are on mass basis. [2]Quoted by *Miller and Donahue* (1990). [3]*Agarwal and Khanna* (1983) reported empirical relationship for available water capacity as a function of sand, silt and clay percentage. The sand, silt and clay percentage of typical soil profiles (aggregated for 1 m depth) as reported by *Ahuja et al.* (2001) was used to compute (θ_{fc} -θ_{wp}).

Parameter estimation using cumulative ET_{RS} data: The results of the optimized values of (θ_{fc} -θ_{wp}) using cumulative $\boldsymbol{ET}_{RS}$ data are again presented in Table 6.4. In the northern part of the study area, the fitted values of (θ_{fc} -θ_{wp}) follow the soil textural information and are in good agreement with the reported values (Table 6.5). For example, CUs 1, 6 and 7 have heavy texture soils (Table 6.4) as compared to the CUs 2 –5 and 8-10. The same is reflected in the fitted values of (θ_{fc} -θ_{wp}). On the other hand, for some CUs along river Ghaggar (see for example CUs 26 and 29, column 4: Table 6.4), the fitted values of (θ_{fc} -θ_{wp}) are lower than expected values (Table 6.5) as per soil textural information (column 6: Table 6.4). It is important to note that in these CUs rice is a major crop during summer season. During year 1990, CUs 22, 24, 25, 26, 29 and 30 had more than 40 % area under rice. For rice crops, fields are kept flooded and ET_a does not depend on soil hydraulic parameters i.e. (θ_{fc} -θ_{wp}) in this study. Therefore, *in principle, for areas where rice is a major crop,* $\boldsymbol{ET}_{RS}$ *cannot be used inversely to identify soil hydraulic parameters*. Under such situations, $\boldsymbol{ET}_{RS}$ for the non rice growing period may be used. However, as pointed out earlier this option was not implemented in this study considering temporal discrepancy between ET_{RS} and ET_{SIWARE}. Moreover, during the winter season, one may expect less moisture stress and as observed in

Chapter 4, the moisture stress period is more appropriate to identify soil hydraulic parameters using ET_a rates.

Contrary to the above situation, the fitted values of (θ_{fc} -θ_{wp}) for some of the CUs are still at the upper bound. The problem of parameters being fitted to the upper bound is now concentrated in the CUs in the south western and south eastern part of the study area (Fig. 6.1a and Table 6.4). In order to further examine this discrepancy in those particular regions, cumulative values of $\boldsymbol{ET}_{SIWARE}$ and $\boldsymbol{ET}_{RS}$ (excluding time step 6-9) for all the CUs were compared. Fig. 6.4. presents the 1:1 comparison of $\boldsymbol{ET}_{SIWARE}$ and $\boldsymbol{ET}_{RS}$.

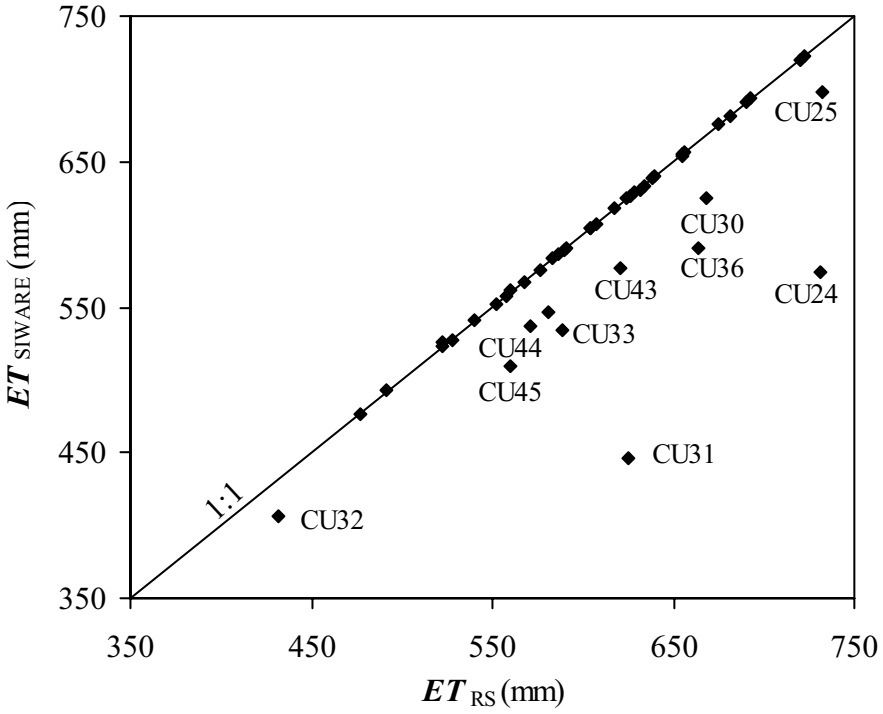

Figure 6.4. Comparison of cumulative (excluding time step 6-9) evapotranspiration for different calculation units as estimated from remote sensing $\boldsymbol{ET}_{RS}$ and simulated $\boldsymbol{ET}_{SIWARE}$ after parameter optimization

The $\boldsymbol{ET}_{\text{SIWARE}}$ is based on the fitted values of parameters reported in column 4 and 5 of Table 6.4. This comparison between $\boldsymbol{ET}_{\text{SIWARE}}$ and $\boldsymbol{ET}_{\text{RS}}$ should neither be taken as a proof of good or poor calibration nor should it be used to draw conclusions that ET_{RS} was a good or poor estimate of ET_{a}. This is because *both* $\boldsymbol{ET}_{\text{RS}}$ *and* $\boldsymbol{ET}_{\text{SIWARE}}$ *were used in the objective function* (Eq. 6.1) and close match between them only shows the capability of the PEST to force model parameters to have as good a match as possible. *Therefore, based on Fig. 6.4, no conclusions should be drawn on the accuracy of either* ET_{RS} *estimates or* ET_{SIWARE} *simulations.*

In general $\boldsymbol{ET}_{\text{SIWARE}}$ is within 10% of the $\boldsymbol{ET}_{\text{RS}}$ (Fig. 6.4). However, serious under-predictions can be observed for some of the CUs. The CUs for which notable deviation is observed from 1:1 line are among those for which the optimized values of (θ_{fc} -θ_{wp}) were fitted at the upper bound (Table 6.4, column 4). A possible reason could be a shortage in the specified water supply conditions for these CUs. Neglecting any likely deviations in the actual allocation of water among different CUs than that allocated according to designed rules in the model, groundwater use could be a major source of discrepancy in the supply conditions. This is particularly true for areas where considerable groundwater use takes place as the amount of groundwater use is decided by the farmers and no actual measurements were available.

In order to further investigate this possibility, the model FRAME was used to simulate groundwater depth for the period 1977-90 without previous calibration against groundwater heads. The CUs 24 and 31 (Fig. 6.1a) which showed maximum deviation in $\boldsymbol{ET}_{\text{RS}}$ and $\boldsymbol{ET}_{\text{SIWARE}}$ (Fig. 6.4) are underlain by groundwater nodes 22 and 27 (see Fig. 6.1b). The simulated groundwater depth along with observed groundwater depth is shown in Fig. 6.5. *The simulated groundwater depth for node 22 and 27 is consistently shallower than observed. A possible reason could be that more groundwater was being used in the overlying calculations units than specified in the simulation study*.

No such check on uncertainty of groundwater use could be investigated for the CUs located in the south eastern part as the underlying groundwater nodes were defined as boundary nodes. Next possible source of discrepancy in available water supply could come from uncertainty in the specified rainfall. For example, observed rainfall for year 1990 (Fig. 6.3) shows large spatial variation in the study area. The observed annual rainfall at different rain-

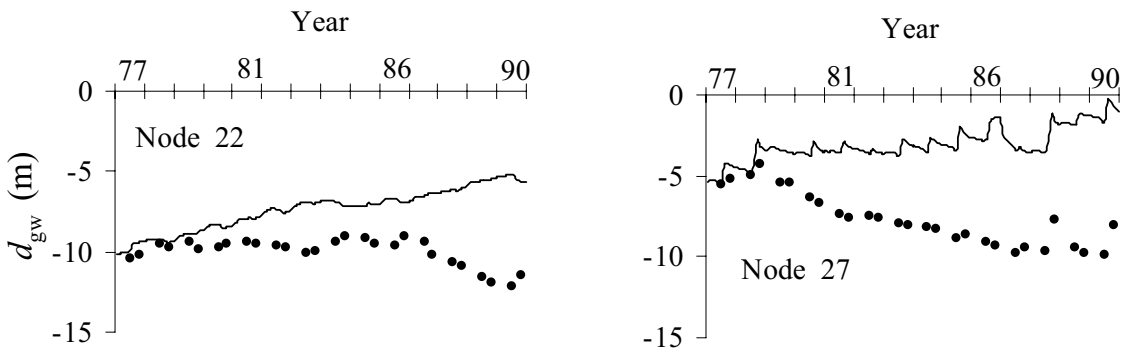

Figure 6.5. Simulated (line) and observed (points) groundwater depth d_{gw} for the period 1977 to 1990. The simulation results are based on 'without previous calibration against groundwater levels' to show the uncertainty in specified amounts of groundwater use

gauge station during 1990 varied from 89 – 570 mm (Fig. 6.3). As pointed out earlier, different CUs were assigned to the nearby rain-gauge station. Accordingly, all the CUs in the south-eastern part which show parameter estimation problems were assigned to rain-gauge station 9 (Fig. 6.1a). An examination of the rainfall data for CUs 42-46 (Table 6.3) indicate that these CUs, (during the simulation study) received less rainfall than the nearby CUs 38-41 which receive water from the same canal. Historical observation on rainfall (1977-1990) showed that for some of the years the rainfall data for rain-gauge station 9 were missing. It is more likely that the rainfall for station 9 was not being monitored regularly. Therefore, assignment of inaccurate rainfall may also be responsible for the low ET_{SIWARE} for these CUs. One option was to assign these CUs to rain-gauge station number 1, as was done for groundwater simulation study during the years when no data from rain-gauge station number 9 were available. However, instead of repeating the exercise with this option, the fitted values of (θ_{fc} -θ_{wp}) for CUs with similar soil texture were assigned to CUs 42-48. Likewise, the CUs having rice as major crops were assigned parameter values optimized for other CUs with similar soil texture. For CUs in the south western part which indicated uncertainty in specified groundwater use, the maximum limit on groundwater use, as specified in the model input, was adjusted before the second phase of calibration i.e. calibration against groundwater levels.

Categorization of calculation units into sub-groups: Because of the limited number of total soil types that can be defined in model FRAME input, all the CUs were categorized into different sub-groups (Table 6.6) depending on optimized parameters values. The CUs which showed parameters estimation problems during their individual parameter optimization process, were assigned to different sub-groups based on soil textural information. The assigned parameters for different sub-groups of CUs are also given in Table 6.6.

Table 6.6. Categorization of CUs into different sub-groups and assigned values of total available soil moisture (θ_{fc} -θ_{wp}) and thickness of capillary zone (Z_{cz})

Number Sub-group	Calculation units[1]	(θ_{fc} -θ_{wp}) (-)	Z_{cz} (m)
1	1, 6, **24**, **25**, **26**,28, **29**, **30, 31**, 34, 35	0.225	0.30
2	7, 11, 21, **22, 23**, 27, **33**, **36**	0.207	0.30
3	13, 18, **32**	0.092	0.10
4	2, 3, 4, 5, 8, 9, 10, **37**, 38, 39, **42, 43. 44, 45, 46**	0.152	0.20
5	12, 14, 15, 17, 19, 40, 41	0.117	0.20
6	16, 20	0.129	0.30

[1] Because of the uncertainty in the optimized parameters calculation units with number in bold face were included in a particular sub-group based on soil textural information.

$\boldsymbol{ET}_{SIWARE}$ as simulated with grouped parameters (Table 6.6) and $\boldsymbol{ET}_{RS}$ was compared to check any discrepancy resulting due to categorization of CUs into different sub-groups. It may be noted from Fig. 6.4 that $\boldsymbol{ET}_{SIWARE}$ as simulated with differentiated parameters (Table 6.4) and $\boldsymbol{ET}_{RS}$ was almost equal except for some outliner CUs as discussed before. In general, the discrepancy between $\boldsymbol{ET}_{SIWARE}$ as simulated with grouped parameters and $\boldsymbol{ET}_{RS}$ is less than 10 % (see Fig. 6.6). The maximum discrepancy between $\boldsymbol{ET}_{SIWARE}$ and $\boldsymbol{ET}_{RS}$ was observed for the same CUs where the specified rainfall and groundwater use amounts are questionable. Therefore, the categorization of CUs in different sub-groups (Table 6.6) was considered acceptable.

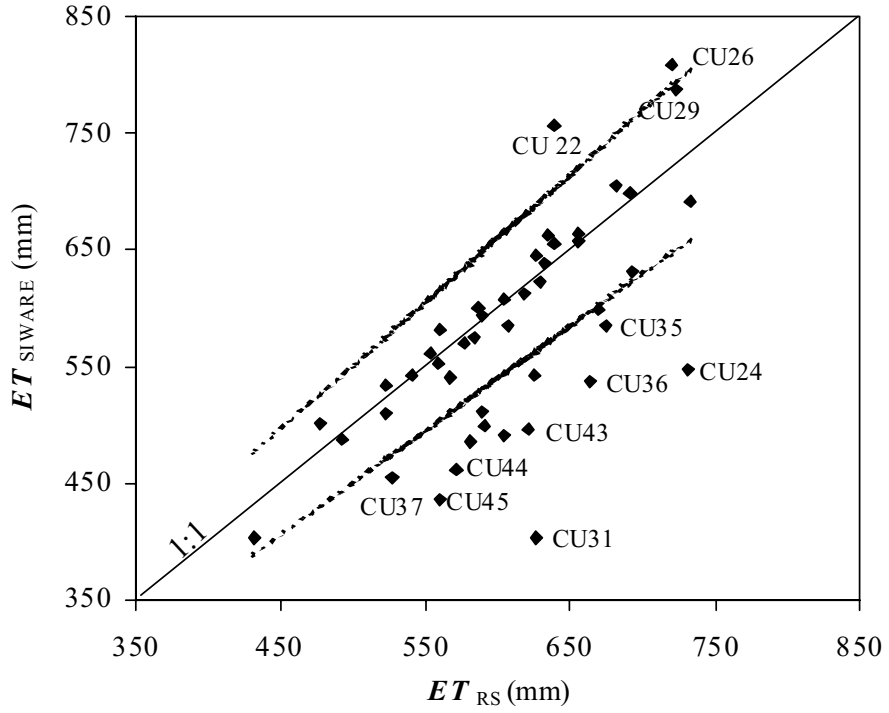

Figure 6.6. Comparison of ET_{SIWARE} simulated by using grouped soil parameters (Table 6.6) with ET_{RS}.

6.7 Calibration of selected model parameters using groundwater heads

Before calibrating drainable porosity of the aquifer, an attempt was made to correct the uncertainty in groundwater use. Two factors i.e. ET_a and groundwater levels, governed the adjustment of the specified groundwater extraction limit. The maximum limit on groundwater extraction was increased if ET_{SIWARE} was less than ET_{RS} and also the simulated groundwater depth was shallower than the observed groundwater depth. The maximum limit on groundwater extraction was also increased for CUs where simulated groundwater levels in the underlying nodes showed a rising trend, while observed groundwater levels showed a declining trend. This resulted into an increase in specified maximum limit of groundwater extraction upto 3.0 times for some of the CUs along the river Ghaggar. Before the adjustment of maximum limit on groundwater extraction, the specified limit was based on fixed norms (e.g. groundwater abstraction from a shallow tubewell was taken as 0.0145 million m^3 yr^{-1}). These standard norms may not be applicable for the CUs along river Ghaggar where rice was a major crop and good quality groundwater was available at relatively shallower depth.

Accurate assessment of leakage losses from Ghaggar river was also essential to properly simulate groundwater levels in the nodes underlying the river. Unfortunately no field data with respect to the leakage losses from the river were available. The leakage losses from the river is a function of volume of flow, permeability of the river bed and width of the flow section. Volume of water flow in the river as measured at the Ottu weir (Fig. 2.1) was used to estimate the river leakage losses as:

$$\boldsymbol{L}_{\text{river}} = a\, \boldsymbol{Q}^{b}_{\text{river}} \tag{6.3}$$

where $\boldsymbol{L}_{\text{river}}$ is the leakage loss [L^3 L^{-1}] from the river section, a and b are empirical coefficients and $\boldsymbol{Q}_{\text{river}}$ is the volume [L^3] of flow in the river section. The empirical coefficients a and b were also optimized during the second phase of calibration. The fitted values of coefficient a ranged from 0.19 to 0.29 and that of b ranged from 0.67 to 0.77 for different sections of the river.

The optimized values of drainable porosity are presented in Table 6.7. These values lie within the range of values as reported by *Boonstra et al.* (1996). The coefficient of correlation between simulated and observed groundwater depth and RMSE were computed for the calibration and validation period and are presented in Table 6.7.

The model FRAME reproduced the observed tendencies in groundwater level behaviour quite satisfactory in the calibration period (1977-1981). Calibration was very successful in about 70 % of the study area with a correlation coefficient between simulated and observed groundwater levels of more than 0.80. In about 28 % of the study area the calibration was considered sufficient with correlation coefficient between 0.50 and 0.80.

Fig. 6.7 shows the comparison between simulated and observed groundwater levels for six selected nodes for the validation period (1982 to 1990). In the northern part of the study area where the groundwater levels were rising monotonously, the validation results were very successful (see node 4 and 9, Fig. 6.7).

Table 6.7. Optimized values of drainable porosity for different nodes in the Sirsa Irrigation Circle along with the coefficient of correlation between simulated and observed groundwater depth and root mean square error (RMSE) for the calibration (1977-81) and validation (1982-90) period.

Number node	Drainable porosity (-)	Coefficient of correlation		RMSE (m)	
		Calibration	Validation	Calibration	Validation
1	0.11	0.97	0.83	1.04	2.30
2	0.14	0.98	0.95	0.83	1.32
3	0.11	0.98	0.28	0.86	3.16
4	0.04	0.99	0.98	0.69	1.45
5	0.06	0.99	0.99	0.64	2.11
6	0.15	0.99	0.97	0.39	0.98
7	0.18	0.97	0.93	0.39	1.36
8	0.23	0.91	0.98	0.71	0.89
9	0.21	0.98	0.97	0.67	0.51
10	0.09	0.98	0.94	0.56	0.92
11	0.06	0.99	0.98	1.41	1.67
12	0.05	0.98	0.96	0.94	1.86
13	0.07	0.98	0.96	0.41	1.34
14	0.12	0.95	0.96	0.97	1.27
15	0.25	0.97	0.88	0.73	0.54
16	0.15	0.62	0.13	0.78	1.22
17	0.13	0.98	0.88	0.48	1.41
18	0.07	0.97	0.94	1.00	1.44
19	0.06	0.97	0.72	0.86	1.73
20	0.17	0.84	0.30	1.20	1.10
21	0.25	0.54	0.12	0.82	0.65
22	0.06	0.68	0.40	0.61	0.96
23	0.04	0.75	-0.12	1.50	0.84
24	0.02	0.33	0.07	1.62	1.67
25	0.02	0.68	0.61	1.14	1.06
26	0.14	0.73	-0.22	0.64	1.63
27	0.04	0.90	0.27	0.56	1.08
28	0.04	0.93	0.09	0.38	2.06
29	0.08	0.44	0.31	0.82	2.37
30	0.04	0.74	0.43	1.35	1.69
31	0.25	-0.53	0.93	1.63	0.53
32	0.25	0.80	0.96	0.80	2.59
33	0.25	0.71	0.83	0.57	0.57
34	0.25	0.97	0.87	0.40	0.94
35	0.18	0.97	0.98	0.29	0.49
36	0.06	0.96	0.80	0.58	1.97
37	0.05	0.91	0.99	0.74	0.63

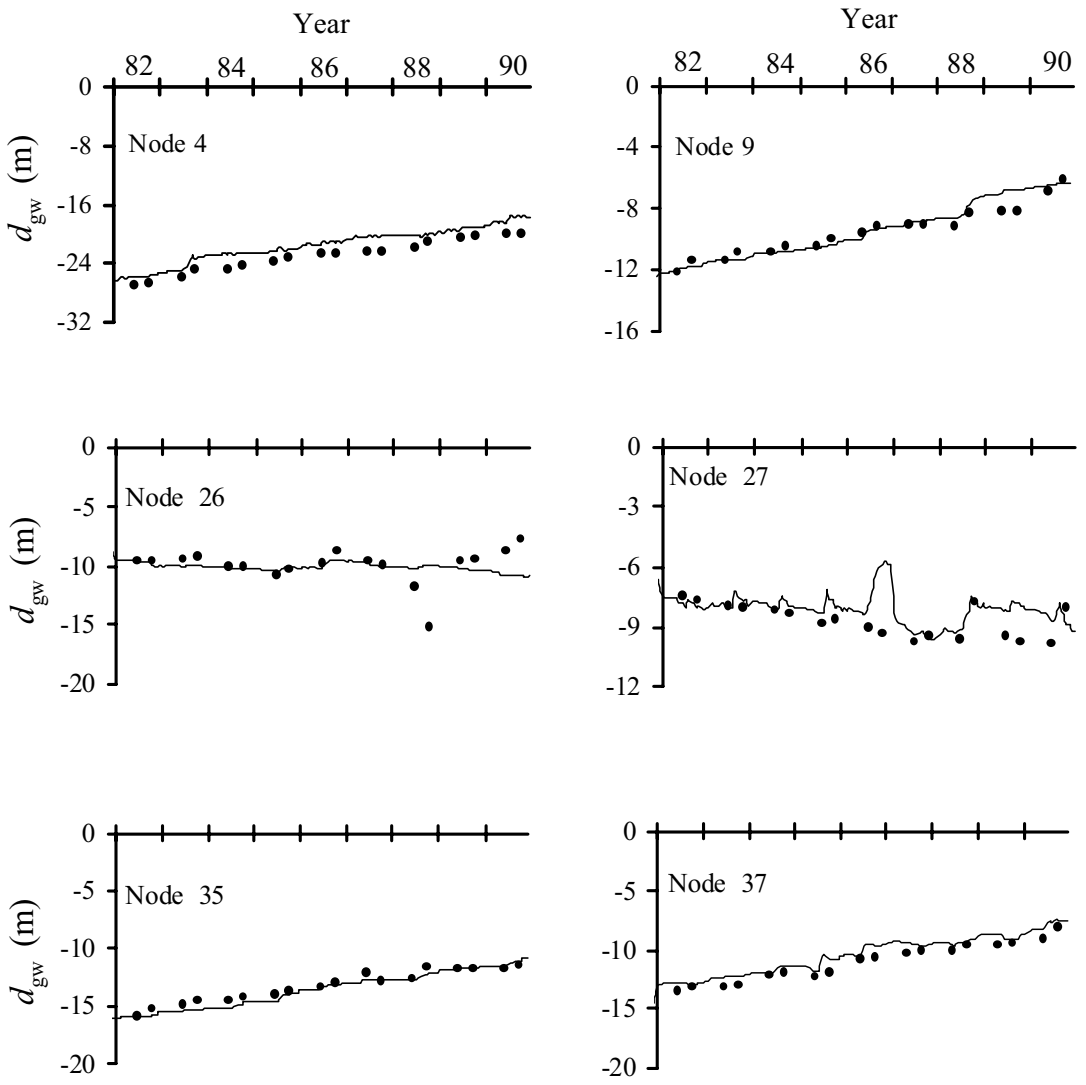

Figure 6.7. Simulated (lines) and observed (points) groundwater depth d_{gw} below soil surface for the validation period (1982-1990) in selected nodes of the Sirsa Irrigation Circle.

In the central part of the study area along the river Ghaggar, the validation results were relatively less successful (see node 26 and 27, Fig. 6.7). There are different reasons for the relatively less successful validation in the central part. As already mentioned, because of rice crop, the soil hydraulic parameters for this region could not be estimated using $\boldsymbol{ET}_{\mathbf{RS}}$ data. Another reason is the uncertainty with respect to river losses and groundwater pumping. Finally, in the south-eastern part of the study area, where the groundwater levels were also rising monotonously, the validation results were again successful (see node 35 and 37, Fig. 6.7).

Overall good agreement was obtained between the simulated and observed tendencies of groundwater fluctuations in the study area. *It may thus be concluded that the calibrated model FRAME could be used to evaluate alternative water management scenarios by studying their effects on ET_a and regional groundwater levels.*

6.8 General discussion

Parameter estimation by inverse methods always faces the problem of parameter uncertainty. Therefore, it is difficult to say whether the identified model parameters are right or wrong and no proof of their validity is possible at the spatial scale of model application. However, they can be judged as appropriate or inappropriate. Such a judgement should take into account the goals of the study and may benefit considerably from the qualitative information about the data set. The optimized values of (θ_{fc} -θ_{wp}) appears to be acceptable when compared with reported values for similar soil textural classes. However, under actual conditions there could be considerable variations within a soil textural class.

Assuming no error in the model structure in representing reality, other major factors responsible for likely parameters uncertainty in this study could be: crop parameters used, spatial variability in crop development, differences in canal water allocation and groundwater use and unaccounted spatial variations in rainfall. Spatial variability in crop development at different crop stages can be assessed from multi-spectral satellite data (*Menenti et al.*, 1996). Uncertainty in groundwater use may be checked with the help of observed groundwater levels, as was done in this study. In case actual canal water allocation differs considerably from design rules, actual measurements for different sub-area must be used, at least during the calibration phase. The way rainfall from a particular rain-gauge station was assigned to nearby CUs, could also be a major factor for parameter uncertainty. For example CU23 (Fig. 6.1a) lies between rain-gauge station 2 and 4. Observed annual rainfall for year 1990 at rain-gauge station 2 was 570 mm and that at rain-gauge station 4 was 89 mm (Fig. 6.3). Additional optimization runs indicated that when CU23, was assigned to station 2, the fitted value of (θ_{fc} -θ_{wp}) was 0.108 and when assigned to station 4, the fitted value of (θ_{fc} -θ_{wp}) was at the specified upper bound of 0.32. Considering available soil texture information for CU23, none of the above fitted values appears to be realistic. It is most likely that CU23 may

have neither received as low rainfall as observed at station 4 nor as high rainfall as observed at station 2. Considering the spatial variability in the observed rainfall, a denser network of rain-gauge stations would be highly desirable for this kind of study. Moreover, a more appropriate approach would be to further verify the optimised parameters values using multi year data on ET_{RS}.

Use of cumulative $\boldsymbol{ET}_{RS}$ data in the objective function resulted into only one observation being available for the parameters estimation process. Fundamental to the adopted inverse procedure is that soil hydraulic parameters are fitted in such a way that the ability of the model to reproduce $\boldsymbol{ET}_{RS}$ is optimized. This resulted into $\boldsymbol{ET}_{SIWARE}$ being very close to $\boldsymbol{ET}_{RS}$ (Fig. 6.4). In reality, such a good match can only, if at all, be achieved under the condition that both data and model are error free. The fitted parameters in this study could reliably reproduce long term groundwater fluctuations. The use of only one observation however, may not always reproduce hydrologically realistic parameters. Moreover, as observed in Chapter 4, the number of observations clearly have a positive impact on the parameter identifiability.

6.9 Conclusions

- The optimized values of (θ_{fc} -θ_{wp}) were more reliable when cumulative evapotranspiration rather than temporal evapotranspiration was used in the objective function. This means that when input data are of questionable quality, the selection of the temporal scale for observations in the objective function is a critical consideration.

- For areas where rice is a major crop, evapotranspiration rates for only the non-rice growing periods should be used to inversely identify soil hydraulic parameters using evapotranspiration rates.

- Despite some inconsistencies in the temporal evapotranspiration estimates by simulation model and remote sensing, using the fitted values of (θ_{fc} -θ_{wp}) to predict groundwater behaviour, good agreement was achieved between predicted and observed groundwater levels. Therefore, *it can be concluded that use of remotely sensed evapotranspiration*

rates would be an important input for the calibration of water management simulation models.

- The validation results show that the FRAME model can be used to evaluate alternative water management scenarios at the regional scale by studying their impacts on evapotranspiration and groundwater levels.

Chapter 7

Scenario analysis of irrigation water management at regional scale

7.1 Introduction

In arid and semi-arid areas, provision of irrigation is vital to enhance crop production. For instance, total food grain production in Haryana (India) increased from 2.6 million tonnes in 1967 to 12.1 million tonnes in 1999 as the corresponding area under irrigation increased from 1.7 million ha to 4.8 million ha. Irrigated agriculture will be expected to provide much more food in the future, while using less water than it uses today (*Appelgren*, 1996). However, without appropriate management, irrigated agriculture can be detrimental to the environment and may endanger its sustainability. Over the past decades, part of the canal irrigated areas of Haryana are facing rising groundwater levels, and problems such as water logging and soil salinization are emerging (*Agarwal and Roest*, 1996). It is, therefore, important to conceptualise and develop appropriate water management policy before these problems become a serious issue at larger scale.

Groundwater pumping to lower the groundwater levels and use it conjunctively has been successful in irrigated areas of the alluvial soil region underlain with better quality waters (*Tyagi and Rao*, 1998). In case of poor quality groundwater, however, its applicability in lowering the groundwater level, without negatively affecting crop yields, needs investigation. Research experience in India (*Minhas and Gupta*, 1992, *Kumar et al.*, 1996, *Manchanda*, 1998) and world wide (*Rhoades et al.*, 1992) demonstrated that waters of much higher salinity than usually being considered unsuitable for irrigation can be used effectively under the right conditions.

It has been observed that it is during the rainy season that more than 50% of the total rise in groundwater levels occurs (*Chowdhury*, 1998). Reduction in canal water supply by about 25 % during the rainy season in the areas facing rising groundwater levels is often suggested (*Agarwal and Jhorar*, 1997; *Chowdhury*, 1998) as a preventive measure to combat

waterlogging and salinity problems. This may also encourage farmers to use groundwater in these areas. The canal water thus saved may be diverted to the areas facing groundwater decline to increase groundwater recharge. However, the impacts of such policy have not been quantified systematically.

In order to solve the problem of rising groundwater levels, a number of integrated actions are required. For example, enhanced groundwater use may stop the groundwater level rise, but excessive use of poor quality groundwater may cause soil salinization, thereby affecting crop yields. Likewise, diversion of part of canal water from areas facing rising groundwater levels to the areas facing falling groundwater levels may help to increase recharge in the latter case but may also cause a water deficit in the rising groundwater areas as well.

Many problems and prospects associated with a particular water management option are often not recognised until they are well advanced. Simulation models, by way of their predictive capability, can help to forecast the likely impacts of a particular water management strategy. The results of simulation studies of existing and proposed water management policy, therefore, may form the basis for the identification of appropriate water management plans for the future.

7.2 Reference situation and alternative scenarios

The Sirsa Irrigation Circle faces both rising and declining groundwater levels. During the period 1977 to 1990, the area covered under CUs 1-21 and 36-46 (Fig. 6.1a) faced rising groundwater levels. The area covered under the other CUs either had more of less stabilised groundwater levels or a decline in groundwater levels. The maximum rise in groundwater levels (12 to 14 m for the period 1977-1990) was observed in the north-western and southern most part of the study area. The observed rate of rise in groundwater levels decreased towards the central part of the study area. In fact, in the area along the river Ghaggar, a 2 to 6 m decline in groundwater levels was observed. *The scenario analysis described in this chapter focussed only on the areas facing rise in groundwater levels*.

The annual canal water supply to the study area during 1977 to 1990, including that flowing out of tail ends, varied from about 1720- 2623 million m^3. In general the annual canal water supply was more than 2200 million m^3, however, during 1984 the area received an annual canal water supply of about 1720 million m^3.

Considering the rising groundwater levels in the Sirsa Irrigation Circle, four water management scenarios (Table 7.1) were considered. The likely consequences of alternative water management policies are examined using the calibrated FRAME model.

Table 7.1. Alternative water management scenarios studied using FRAME simulations.

Scenario	Description
1	Reference situation- same as for calibration and validation period.
2	Increase in capacity of groundwater extraction by 60 mm yr^{-1} in areas facing rising groundwater levels.
3	Reduction in canal water supply by 25 % during the rainy season.
4	Increased groundwater extraction capacity as in Scenario 2 and reduction in canal water supply as in Scenario 3

The main objective is to study impacts of alternative water management policies on ET_a, which is directly related to crop production, and depth of groundwater levels, which is related to waterlogging risks. The period 1977-1990 was used for the scenario simulations.

For Scenario 1, all the input information was the same as used during the calibration and validation of the model FRAME (Chapter 6). For Scenario 2, the specified capacity of tubewells for groundwater extraction for CUs facing rising groundwater levels was increased to simulate enhanced groundwater use. This maximum capacity was uniformly increased by an amount of 60 mm yr^{-1} (i.e. the generally recommended irrigation depth per event: *Agarwal and Khanna*, 1983). In the FRAME model, groundwater extracted in a CU is mixed with canal water and made available to different crops according to fixed irrigation schedules. This means that the simulated groundwater use reflected a policy where groundwater is mixed

with canal water at the CU level e.g. through so called augmentation tubewells. In the Sirsa Irrigation Circle, CUs where extensive groundwater use takes place, groundwater extraction is at farm level and not subject to rigid schedules of canal water supply. However, this option, where groundwater extraction creates a flexible water supply, could not be implemented in the present version of the FRAME model. For Scenario 3, the canal water supply during the rainy season (time step 9 to 12: for time steps see Table 6.3) was reduced by 25 % and new time distribution fractions for the revised total canal water supply for the 16 model time steps were computed and provided as input to the model. This option caused a proportional reduction in canal water supply to all the CUs. However, in practice one would not like to reduce canal water supply for CUs facing declining groundwater levels. Such an option, where canal water is reduced only in a part of the study area for the selected period, was not available in the present version of the model. For Scenario 4, both canal water supply and capacity of groundwater extraction were changed as described for the Scenarios 2 and 3.

During the calibration and validation phases, h_{gw} as obtained from the historical observations was specified at the boundary nodes of the groundwater model. However, when simulating alternative scenarios, the h_{gw} in different nodes including boundary nodes was expected to be different from the historical observations. Therefore it was decided to predict the h_{gw} in the boundary nodes based on simulated h_{gw} in the nearby internal nodes. Using historical observations on h_{gw}, linear regression equations were developed taking h_{gw} in the boundary nodes as dependent variable and h_{gw} in the nearby internal nodes as independent variable. The ratio of variance (F- value) for testing coefficient of correlation were statistically significant at 1 % level of significance in all cases. Therefore the developed regression equations were considered acceptable to predict h_{gw} for the boundary nodes.

7.3 Effect of alternative strategies on crop evapotranspiration

The simulated annual $\boldsymbol{ET}_a$ for different scenarios (Table 7.1) along with the annual rainfall $\boldsymbol{P}$ for some selected CUs is presented in Fig. 7.1. To show the role of rainfall on the impact of alternative scenarios on $\boldsymbol{ET}_a$ the selection of CUs was based on the difference in $\boldsymbol{P}$.

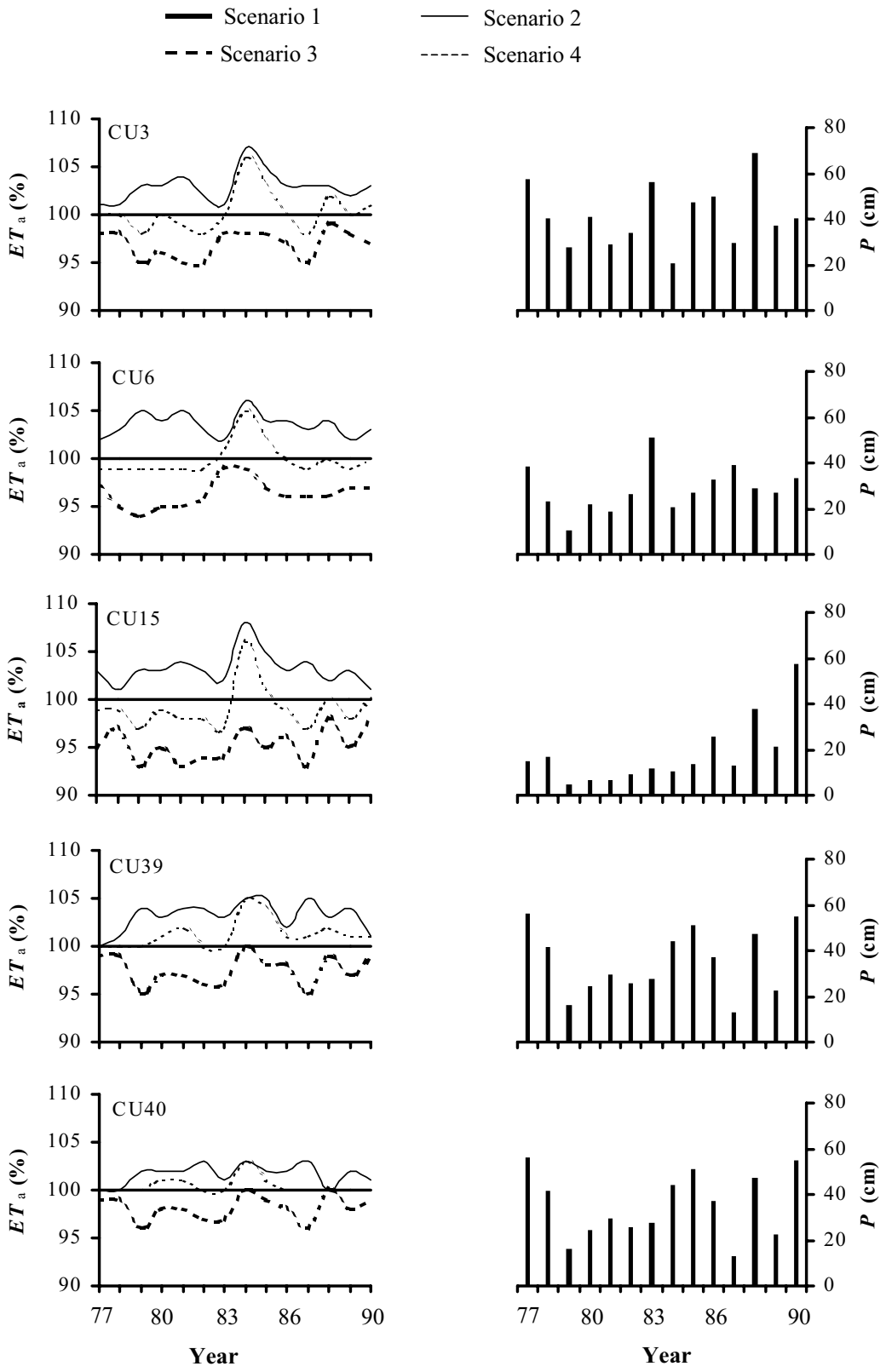

Figure 7.1. Simulated annual ET_a for selected Calculation Units (CU) under 4 different scenarios expressed as % of Scenario 1, which is the Reference Scenario. Also shown is annual rainfall ***P***. Note from Fig 6.3 relatively heavy daily rainfall that may occur due to monsoon rains.

As expected, enhanced use of groundwater (Scenario 2) increased ET_a and reduced canal water supply (Scenario 3) decreased ET_a. However, the effect of a particular scenario is also influenced by the amount of P. For instance, CU3 received relatively higher P during the years 1977, 1983 and 1988 and the influence on ET_a for these years, in general, is less pronounced for both Scenario 2 and 3. In general, the lower the amount of P, the more is the difference in ET_a between the Reference situation and the alternative scenarios. However a few exceptions can be observed from Fig. 7.1. During 1984, CU3 received the least rainfall but the difference in ET_a between Reference situation and Scenario 3 is not maximally as expected. This is due to the fact that during 1984, the study area received relatively low amount of canal water as observed before. A 25 % reduction in canal water supply during the rainy season caused relatively less absolute reduction in the water supply as compared to other years. During 1988, CU3 received the maximum P and one would expect, contrary to what has been displayed in Fig. 7.1, a minimum influence of enhanced groundwater use (Scenario 2) on ET_a. However the maximum value of P was due to relatively higher rainfall (-of 200 mm-) on a single day. This means that the performance of alternative scenarios depends on the available canal water supply, the total amount of rainfall and its distribution.

The simulated ET_a for Scenario 4 lies in between that for Scenario 2 and 3. In general, it appears that to save canal water without any serious reduction in ET_a, Scenario 4 is an appropriate option, at least for the short term.

7.4 Effect of alternative strategies on soil salinity

One major concern for enhanced groundwater use or reduction in canal water supply would be the fear of increase in soil salinity on the long term which may originate from both the application of saline groundwater and less leaching due to reduction in canal water supply. In the present study, the results of FRAME with respect to salinity concentrations were not validated due to non-availability of the historical data. The simulated soil salinity for the selected CUs is however presented (Fig. 7.2) to at least partly address the above issue.

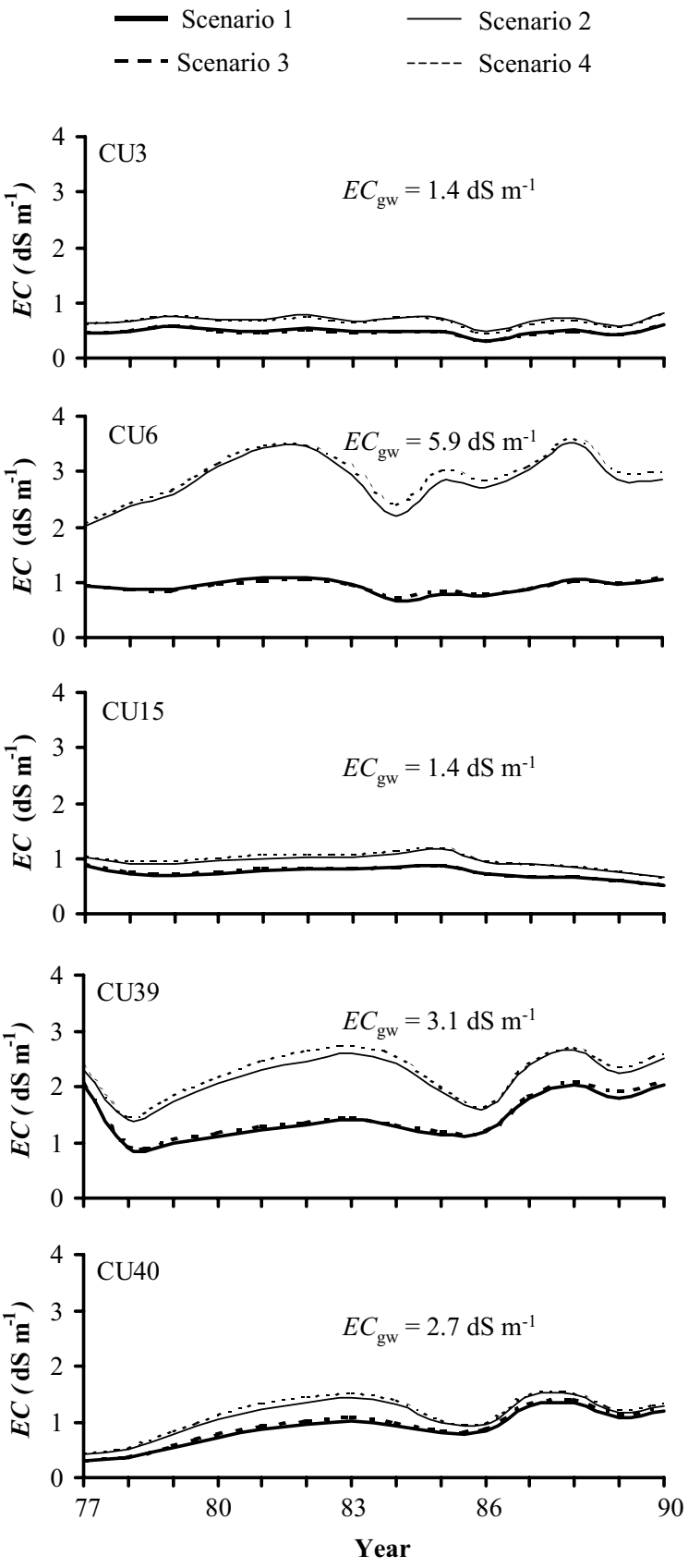

Figure 7.2. Simulated soil salinity (*EC*) in the selected calculation units (CU) under 4 different scenarios. Also indicated is the specified electrical conductivity of groundwater (EC_{gw}).

In general, use of additional groundwater (Scenario 2) results into higher soil salinity (Fig. 7.2). The reduction in canal water supply by 25 % during the rainy season (Scenario 3) alone has however no significant effect on soil salinity. Likewise reduction in canal water supply during the rainy season along with increased groundwater use (Scenario 4) results into almost similar soil salinity development to that under increased groundwater use alone. This shows that during the rainy season, the soils are being leached sufficiently as no specific increase in simulated soil salinity was observed when canal water supply was reduced.

In addition to the amount of groundwater use, the salinity development also depends on the quality of groundwater, soil texture and rate of leaching. CUs having relatively less salts in groundwater (see CU3 and CU15 in Fig. 7.2) show little increase in soil salinity under increased groundwater use. CU6, however, where the groundwater salinity is quite higher, shows a maximum increase in soil salinity for the Scenarios 2 and 4. Compared to the other CUs shown in Fig. 7.2, CU6 not only has a higher groundwater salinity but also a heavier soil texture (see Table 6.4).

Another important feature which can be observed from Fig. 7.2 is that during the simulation period of 14 years there is no consistent increase in the salinity build up under the different scenarios. Intermittent drop in salinity build up is observed due to relatively higher rainfall in different years which causes considerable leaching. For instance, in CU6 simulated soil salinity for Scenarios 2 and 4 reached to about 4 dS m^{-1} by the year 1983. As a result of the received higher rainfall amount in 1983, soil salinity decreased to about 2 dS m^{-1} in the following year. Similar drops in soil salinity may be observed for other CUs as well. *This means that even the groundwater which is of relatively poor quality, may be used for irrigation without excessive long-term build-up of soil salinity because of the seasonal leaching that occurs due to monsoon rains.* This observation is valid only as long as the groundwater remains deep enough so that heavy rainfall does not cause waterlogging problems. Moreover, care should be taken with respect to salinity during certain stages of crop development.

7.5 Effect of alternative strategies on groundwater levels

The simulated groundwater depth d_{gw} in selected nodes as affected by alternative scenarios (Table 7.1) is presented in Fig. 7.3. As can be observed, a reduction in canal water supply alone (Scenarios 3) has a minimum influence on the simulated d_{gw}. On the other hand Scenario 4 where both reduction in canal water supply and increase in groundwater use is simulated, has a maximum impact on the groundwater levels. At the end of 14 years of simulation, Scenario 4 was able to reduce the rise in groundwater level by 3.3 m in node 4 (a rise in groundwater level by 11.7 m against a rise of 15.0 m for Reference Scenario), 1.3 m in node 7 (a rise in groundwater level by 10.0 m against a rise of 11.30 m for Reference Scenario) and 0.7 m in node 34 (a rise in groundwater level by 6.2 m against a rise of 6.9 m for Reference Scenario).

The effectiveness of scenarios to reduce the increase in the groundwater levels varies for the different nodes. The difference in the effectiveness of a particular scenario for nodes 4, 7 and 34 is mainly due to the difference in the optimized value of drainable porosity S_y (Table 6.7) for these nodes. The optimized value of S_y was 0.04 for node 4, 0.18 for node 7 and 0.25 for node 34. For a certain amount of groundwater withdrawal, the node with the lowest value of S_y will show maximum reduction in groundwater level rise. At the end of 14 years of simulation, Scenario 2 where only increased groundwater withdrawal was simulated, brought down the rise in groundwater level by 2.4 m in node 4, 0.6 m in node 7 and 0.3 m in node 34. This means that, the amount of groundwater extraction required to bring the groundwater down at the desired levels is also affected by the drainable porosity of the underlying aquifer.

One of the main objectives of this scenario analysis was to understand how the rising trend of groundwater levels in the study area could be halted. Even Scenario 4, which performs better than the other scenarios in lowering the groundwater levels, was not able to stop the rising trend in groundwater levels as can be observed from the trend of simulated groundwater levels (Fig. 7.3) for the period 1977-90. This does not mean that increased groundwater pumping cannot stop rising trends in groundwater levels. The results of this scenario analysis suggests that the policy of augmentation of canal water supply through groundwater pumping, while still following the rigid water allocation rules, alone cannot stop the rising trends in groundwater levels.

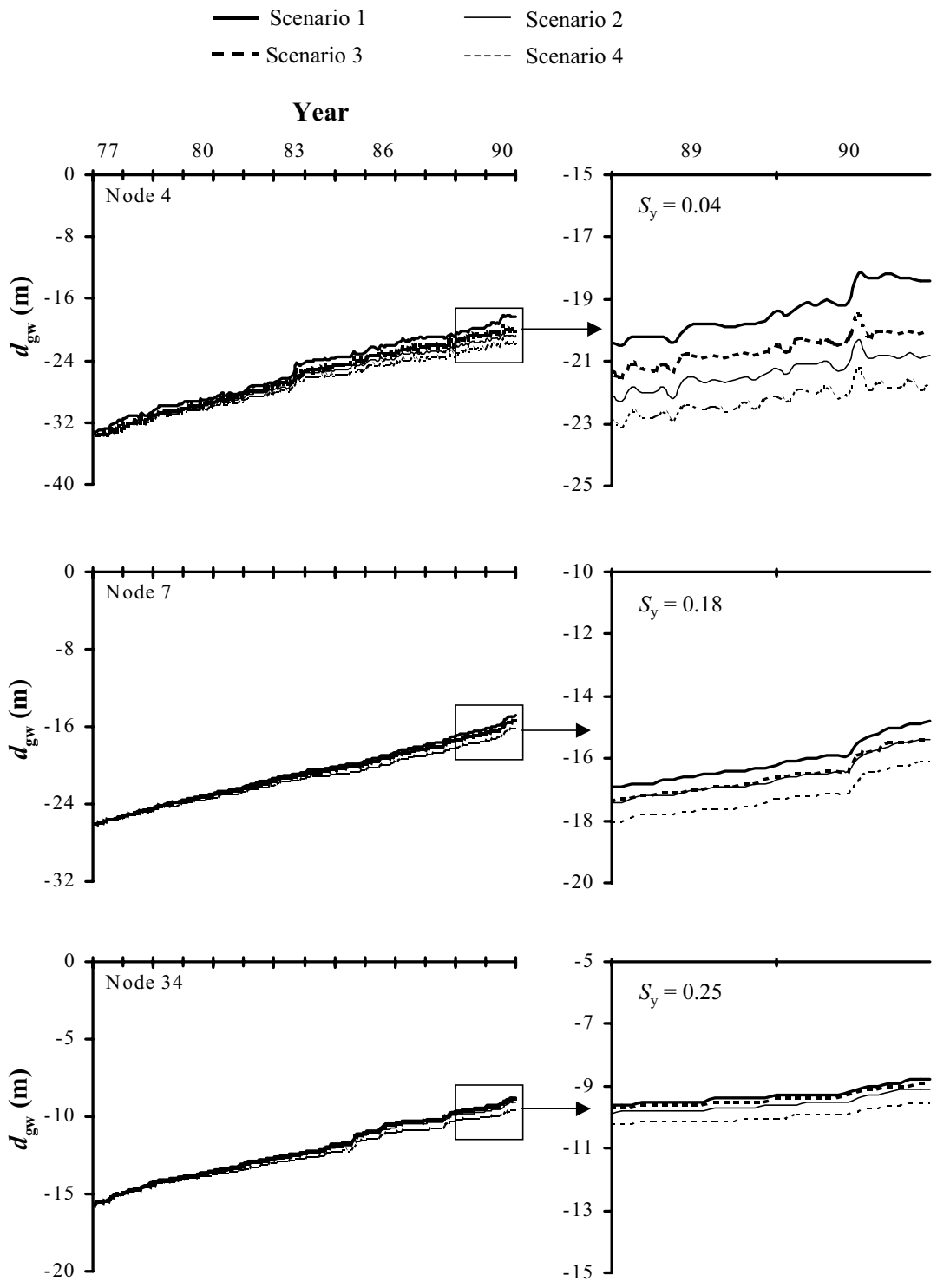

Figure 7.3. Simulated groundwater depth (d_{gw}) in selected nodes under 4 different scenarios for the period 1977-90. Also shown (right hand side) is the exploded view of the d_{gw} development during the last two years of the simulation period. Note the effect of drainable porosity (S_y) on d_{gw}.

It may be argued that a further increase in groundwater use may help to stop the rising trend in groundwater levels. The additional 60 mm yr^{-1} withdrawal of groundwater, if contributing effectively to evapotranspiration, should have caused a decline of about 4.7 m in the node 7 (S_y = 0.18) at the end of the 14 years against 0.6 m simulated for the Scenario 2. However, in the simulated strategy, most of the extra groundwater pumped was re-circulated back to the aquifer. For instance, in CU15 for the year 1990, the Scenario 2 resulted into 59 mm of additional groundwater use but the simulated ET_a increased only by 9 mm. This may be attributed to fact that in the scenario on enhanced groundwater use, the pumped groundwater was subjected to the rigid schedule of canal water supply to the fields. In practice, farmers extract groundwater at the moment that the crop(s) need water. The model simulations do not account for this farmers behaviour. Therefore, it can be expected that the real effects of increased groundwater use on groundwater levels and ET_a will be larger than simulated in the present scenarios.

7.6 General discussion

The alternative scenarios simulated in this study disregard operational, institutional and social aspects, which would be of crucial importance. In the canal irrigation sector, government is incurring the full expenditure. The farmer who is served by canal water for irrigation is able to get the water to his fields without any investment. In the case of usage of groundwater for irrigation, except for the government owned tubewells, the entire capital cost of installation, operation and maintenance of these facilities is borne by the farmer himself. Therefore, owing to the cost of pumping and fears of poor quality water and other technological constraints, a sustained and extensive groundwater utilization in marginal to poor quality groundwater zones is unlikely to emerge on its own and needs support from the organizations concerned.

Water management at regional level is a complex issue and requires a combination of actions to be taken up at field as well as at regional scale. In this study only a limited number of scenarios were studied. Additional actions would be necessary to achieve sustainability of the irrigated agriculture. For instance, in areas having relatively more saline groundwater and heavy soil texture, efforts to stop the rise in groundwater levels must concentrate more on

reducing recharge to the groundwater e.g. through improved on-farm application efficiency and reduced leakage losses from the irrigation system. An improvement in the on-farm application efficiency may be achieved through adoption of more efficient irrigation application methods such as sprinkler systems or through improved design and operation of the present surface irrigation methods. Likewise, while implementing poor quality groundwater use, other actions such as change in cropping pattern and adoption of salt tolerant crops may be of crucial importance. Moreover, for areas where groundwater quality is extremely poor and groundwater becomes relatively shallow, installation of a sub-surface drainage system would be inevitable.

It is also important to take note of the limitations of the present simulation study. For instance, plant growth was pre-defined during the scenario simulations. The effect of soil salinity on ET_a was through increased osmotic potential only. In practice, a relatively higher soil salinity may also affect plant physiology. In the model, if considerable leaching takes place (e.g. by heavy rainfall) and there is no moisture stress in the subsequent period, crops are assumed to transpire as if there was no effect on plant physiology. In practice, however, the soil salinity developed in the pre-leaching period may affect plant growth that seriously that crops are no more able to transpire at the usual rates even if there is no moisture stress. In the model no distinction was made between different crops while allocating groundwater for irrigation. Under actual conditions, salt tolerant crops may be irrigated with poor quality groundwater thereby avoiding the undesirable effects of saline water on salt sensitive crops. Further, in the present simulation study, only the electrical conductivity of the groundwater was considered. In some cases the chemical composition of groundwater is also important, e.g. residual sodium carbonate (RSC). In case of water with a high RSC, application of gypsum may be needed to offset adverse effects on the soil.

Another limitation of this scenario study is that the cropping pattern and irrigation interval defined for the alternative scenarios were the same as for the reference situation. In the reference situation, the cropping pattern (particularly for irrigated crops) was based on the actual available water supply. Creating additional water supply through groundwater extraction while keeping cropping pattern and irrigation frequency identical to that of the reference situation may not be completely logical. In fact, a number of integrated actions are required to take full advantage of the conjunctive use of canal and groundwater. These may

include, adaptations in cropping patterns, planting more salt tolerant crops for instance and changes in on-farm irrigation management practices.

In the past (*Willardson et al.*, 1997), various strategies have been proposed to use saline water for irrigation. These include direct use of saline water without dilution, alternative use of saline and good quality water and mixed use of saline and good quality waters. In this study only the mixed use of groundwater and canal water was simulated. *Kumar et al.* (1996) showed that alternative use of saline water with canal water is a better option than the mixed use of saline and canal water. However, this option could not be implemented in the present formulation of the model FRAME.

7.7 Conclusions

- Crop evapotranspiration and soil salinity development under alternative water management strategies, such as reduction in canal water supply and increase in groundwater use, is largely influenced by the amount and distribution of rainfall.

- Reduction in canal water supply by 25 % during the rainy season is unlikely to have any adverse effect on the development of salinity in the Sirsa Irrigation Circle. Reduction in crop evapotranspiration due to decreased canal water supply can partly be compensated for by the increase in groundwater use.

- Leaching of salts due to the monsoon rains shows that under deep groundwater level conditions, groundwater of even relatively poor quality can be used for irrigation without excessive long term build up of soil salinity.

Chapter 8

Summary and conclusions

India is one of the largest irrigated countries in the world and almost 60 % of its agricultural production comes from irrigated areas. Despite impressive progress in the past, the future of irrigated agriculture is faced with multiple challenges, including deterioration of the environment due to emergence of waterlogging and salinity problems, rising food and water demands, constant water resources, low productivity, poor water management practices and advent of water scarcity. Optimum management of available surface water and groundwater resources is necessary to maintain the sustainability of irrigated agriculture and to meet future demands. Substantial improvement in the performance and water productivity of existing irrigation projects is required. *There is need to identify location specific appropriate water management strategies to meet the challenges faced by the irrigated agriculture.*

Proper water management cannot be accomplished without an understanding of the hydrological processes, their interaction and effects of human interventions. New extrapolation techniques are required to prepare guidelines for regional water management, as large scale field experiments are difficult to implement. Simulation models have the capability to provide detailed insights into the system under different conditions and scales. Successful application of these models requires estimation of the hydraulic parameters describing the various processes within the system. However, there is a general lack of available soil hydraulic data bases for simulation model applications to Indian conditions. Direct measurement of soil hydraulic parameters is often extremely difficult, time consuming and expensive. Alternatively, *inverse modelling is a promising indirect method* to estimate model input parameters. In this technique, the searching program runs the simulation model using the initial guess of the uncertain input parameters and compares the simulation results with corresponding measurements. Next, the input parameters are adjusted using an optimization algorithm and the model is run again. This is repeated until the simulation results and the measurements match as closely as possible.

The study was conducted for the Sirsa Irrigation Circle, Haryana, India. The study area covers about 0.48 million ha, of which about 80% is cropped. The climate is arid with annual evapotranspiration far exceeding the annual rainfall. The Sirsa Irrigation Circle is served by an extensive network of canal irrigation systems which is part of the Bhakra irrigation system. A seasonal river Ghaggar flows through the central part of the study area. The major issues related to water management in the study area are: rising groundwater levels in the poor quality groundwater zones, declining groundwater level in the good quality groundwater zones, occurrence of waterlogging and soil salinity problems in a few pockets and shortage of water to irrigate all agricultural crops.

The ultimate objective of this study was to derive soil hydraulic parameters for selected models to test alternate water management practices in an irrigation context. Both field and regional scale models were used to test the applicability of inverse methodology to derive effective soil hydraulic parameters. In Chapter 3, the main features, relevant to this thesis, of the field scale model SWAP (Soil Water Plant Atmosphere), the distributed irrigation water management model, referred to as FRAME and parameter estimation program PEST have been discussed.

SWAP is a one-dimensional hydrological model, which produces daily water and salt balance components. Options exists for irrigation scheduling, drainage design, salinity management, leaching of nitrogen and pesticides and crop growth simulation. In the present study SWAP was used to simulate soil water flow and actual evapotranspiration ET_a rates under free drainage conditions.

FRAME is a distributed irrigation water management model and simulates canal and on-farm water management as well as regional groundwater flow. FRAME offers a wide range of possibilities to assess different practical scenarios such as improvement of water application efficiency, improvement of hydraulic conditions of the water distribution network, alteration of supplied water quantity to the region, change in water allocation policy, groundwater use, cropping pattern and reuse of drainage water. For this study FRAME was used to investigate the impact of conjunctive use of canal water and groundwater and alteration of supplied water quantity.

PEST is a non-linear parameter estimation program which can easily be linked via template files to any model. The optimization algorithm used by PEST is derived from the Gauss-Marquardt Levenberg method which is very efficient in optimization. *For the present study PEST was linked to both SWAP and FRAME to optimize different model parameters by inverse modelling.*

The inverse optimisation of model parameters at the scale of model application requires that suitable responses of the system are known at the scale of model application. Since ET_a rates can be recovered from remote sensing measurements for a range of spatial scales, a new possibility has been explored to derive soil hydraulic parameters using ET_a rates. In Chapter 4, forward SWAP simulations with a known set of soil hydraulic parameters indicate that different soils act differently in their temporal variable ET_a response under deep groundwater level/free drainage conditions. A number of parameter estimation runs were carried out with different combinations of Van Genuchten (VG) model parameters to identify the soil hydraulic parameters which can be optimized simultaneously. The reliability of estimated parameters was judged by their capability to reproduce different water balance components.

Analysis of the time series of simulated ET_a rates for a cotton crop on three soils (sand, loamy sand and sandy clay loam) showed that ET_a rates during the moisture stress period are most suitable to solve the inverse problem. It was also stressed that the sampling period must coincide with the period when crops are fully developed so that the estimated parameters are representative of the depth of interest (root-zone depth). The adopted parameter estimation methodology was tested using exact (forward simulated) and perturbed (random error added) ET_a observations. Under ideal conditions i.e. no error in ET_a rates, when ET_a data were sufficient (30 observations) it was possible to inversely identify all the VG model parameters. However, when the number of ET_a observations were limited (12 observations across a season), it was necessary to reduce the number of fitting parameters in order to obtain exact parameters. Frequent measurement on ET_a rates is desired not only to precisely estimate the soil hydraulic parameters but also to reduce the undesirable correlation between different fitting parameters.

Next, the effect of random error in the ET_a rates on the fitted parameters was considered to show the accuracy required in the measurement/estimation of ET_a rates. Two levels (10 and 20 %) of random error were added to the exact ET_a rates. At each error level, 10 series of ET_a

rates each consisting of 12 data points were generated. Statistical properties (bias and Confidence Interval *CI*) of the resulting water balance components were computed to evaluate the hydrological performance of the fitted parameters. The estimation of mean water balance components, bias and *CI* indicated that the systematic as well as random error of simulated water balance components increased with increase in the random error incorporated in the ET_a rates. Three VG model parameters (α, n and θ_{sat}) could be optimized simultaneously to reproduce reliable water balance components up to 20 % of random error in the ET_a rates. Assignment of weights to different observations inversely proportional to their magnitude gave better results than equal weights to all the observations.

Although the results described in Chapter 4 are encouraging, they are applicable only for homogeneous soil and crop conditions, free drainage and moisture stress during growing season.

At most sites, *soil hydraulic parameters show a large variability not only in horizontal direction but also in vertical direction*. It is, therefore, *very important to determine representative soil hydraulic parameters at the scale of model application*. The case of soil heterogeneity occurring within a distributary was investigated in Chapter 5. Theoretical field experiments were conducted for seven freely draining heterogeneous soil profiles, cultivated with cotton. These soil profiles have wide variability in their textural layering. The surface layers are mainly sandy while the textural class of sub-surface layers vary from sandy loam to sandy clay loam. To optimize different VG model parameters the ET_a rates and soil moisture observations as generated by SWAP were used inversely. First, the inverse approach was applied to identify effective soil hydraulic parameters for the individual soil profiles. Thereafter, an attempt was made to derive area effective parameters. It was observed that the process of inversely deriving effective soil hydraulic parameters for heterogeneous soil profiles is not as straight forward as for homogeneous soil profiles. When the soil evaporation is simulated purely based on soil hydraulic parameters, inversely identified soil hydraulic parameters for heterogeneous soil profiles reproduce unacceptably high values of evaporation. This was due to relatively higher sand fraction and deviating soil hydraulic properties of the surface layers. On the other hand, the inversely identified soil hydraulic parameters represent effective values for the whole profile and hence the evaporation reduction effect of the sand content in the top layer is not directly present in the inversely

identified parameters. The inverse results improved considerably when soil evaporation was simulated using empirical functions of soil evaporation reduction. *It was also observed that ET_a rates alone are sufficient to inversely identify effective soil hydraulic parameters capable of reproducing different water balance components*.

Application of the inverse method to derive area effective soil hydraulic parameters require information on areal fluxes. The seven soil profiles typically represent an irrigation canal command in the Sirsa Irrigation Circle. Knowing the soil textural variations in the command area, the fraction of area represented by each profile was determined. The forward simulated ET_a rates for the seven profiles were then used to derive areal ET_a rates in a weighted manner. Inversely identified effective soil hydraulic parameters reproduced seasonal water balance components (***ET_a***, deep percolation and change in soil water storage) with a reasonable accuracy i.e. within 10% of the reference values. However, for reliable prediction of the temporal water balance, particularly deep percolation loss, it was necessary to reduce the number of parameters to be optimized. When the VG model parameters '*n*' and 'θ_{res}' were fixed (based on soil textural information), the prediction performance of inversely identified parameters improved considerably with respect to estimated deep percolation losses. The consistency of predicted water balance components was checked by repeating the inverse process with different initial guesses of the optimized parameters. The results showed that ET_a rates are sufficient to derive area effective soil hydraulic parameters. However, general information on the textural layering of the area is an important input to inversely identify soil hydraulic parameters using ET_a rates.

Chapter 6 deals with the calibration of the distributed irrigation water management model FRAME. The model was applied to the Sirsa Irrigation Circle by dividing the study area into 46 calculation units (CUs) for the top system and 61 nodes for the groundwater system. A model should be validated for the types of applications for which it is intended. *The ultimate objective of this study was to use the model FRAME to test different water management scenarios at regional scale*. ET_a rates and groundwater levels (head) h_{gw} are of prime importance to this study. Data on h_{gw} were available from the historical observations on groundwater depth in the study area. The data on ET_a rates were derived from NOAA AVHRR images using the remote sensing ET_a algorithm SEBAL (Surface Energy Balance

Algorithm for Land). Data on both ET_a and h_{gw} were used to calibrate the parameters of model FRAME for the Sirsa Irrigation Circle.

The parameter estimation by inverse method is improved by properly selecting the type and number of parameters to be optimized. A sensitivity analysis was performed to identify the parameters that have significant effect on ET_a. Thereafter, a prior analysis of the optimization process was carried out to know the correlation between sensitive parameters, as this increases the uncertainty of estimated parameters. To reduce the number of parameters that are optimized simultaneously, the calibration of model FRAME was achieved in two phases. During the first phase of calibration, known h_{gw} were specified and soil hydraulic parameters sensitive to ET_a were optimized using PEST. During the second phase of calibration, the parameters optimized during the first phase were kept constant and aquifer drainable porosity and river recharge coefficients were optimized to obtain good correspondence with h_{gw} observations.

For the first phase of calibration the ET_a data obtained from Remote Sensing (ET_{RS}) were summarised into 16 model times steps. First, the parameters optimization process was carried out using temporal ET_{RS} rates, which was not very successful. It was argued that under the specified conditions of crop and water supply this may be due to temporal discrepancy between simulated ET_a and ET_{RS}. Therefore, the first phase of parameter optimization process was repeated again using cumulative $\boldsymbol{ET}_{RS}$ data to minimize the effects of temporal discrepancy in simulated ET_a and ET_{RS} data on the optimized parameter values. *Use of cumulative* $\boldsymbol{ET}_{RS}$ *observations during inverse optimization resulted into better estimates of parameters*. In general, the fitted values of (θ_{fc} -θ_{wp}) for different CUs followed the soil textural information and agreed with the reported values. However, for CUs where rice was a major crop, the parameters optimization process was not successful. The CUs for which the parameters optimization resulted into unreliable estimates, were assigned parameter values being fitted to the other CUs having a similar soil texture.

FRAME simulation runs without calibration against groundwater levels showed that different to the model input more groundwater was being used, particularly along the river Ghaggar. Therefore, the uncertainty in the specified maximum limit on groundwater extraction was corrected before the second phase of calibration. The model FRAME was calibrated against

groundwater heads for a period of five years: 1977-1981. This calibration was very successful in about 70 % of the study area with a correlation coefficient between simulated and observed groundwater levels of more than 80 %. Subsequently the observed groundwater levels for 9 years (1982-1990) were used to validate the model results. The validation results were more successful in the northern and southern part of the study area where groundwater levels were rising monotonously. In the central part of the study area, along the river Ghaggar, the validation results were less successful due to uncertainty in both groundwater use and leakage losses from the river. *Overall, good agreement was obtained between the simulated and observed tendencies of groundwater levels in the study area.*

Chapter 7 deals with the scenario analysis of irrigation water management at regional scale. The calibrated and validated FRAME model was used to simulate alternative water management scenarios for the Sirsa Irrigation Circle. *The scenario analysis was focussed only on the part of the study area where groundwater levels were rising.* Four water management scenarios were simulated for a period of 14 years i.e. 1977 to 1990. Scenario 1 represented the reference situation. In Scenario 2 increased extraction of groundwater was simulated. Scenarios 3 dealt with the reduction of canal water supply during the rainy season. In Scenario 4, both the increased extraction of groundwater and reduction in canal water supply during the rainy season were incorporated. The simulation results of the developed scenarios on crop evapotranspiration, soil salinity and groundwater depths were compared with the reference situation.

As expected, in Scenario 2 ET_a increased because of enhanced groundwater use. For Scenario 3, it decreased because of reduced canal water supply. The results of Scenario 4 showed that a reduction in canal water supply by 25 % during the rainy season with enhanced groundwater use will not cause a serious reduction in ET_a. For different years of the simulation period, *the actual effect of alternative scenarios on ET_a was greatly influenced by the amount and distribution of rainfall*. During high rainfall years enhanced groundwater extraction and reduction in canal water supply had no significant effect on ET_a.

One major concern for enhanced groundwater use or reduction in canal water supply would be the fear of increase in soil salinity. In general use of additional groundwater (Scenario 2) increased soil salinity, however, reduction in canal water supply by 25 % during the rainy season (Scenario 3) had no significant effect on soil salinity. During the simulation period of

14 years, no consistent increase in salinity build up was observed. In fact, intermittent drops in the simulated salinity development were observed due to the relatively higher rainfall in some years. This showed that *in the Sirsa Irrigation Circle, the groundwater which is of relatively poor quality may be used for irrigation without excessive long-term build-up of soil salinity because of the leaching that occurs during the monsoon rains*. However, this observation is valid only as long as the groundwater level remains deep enough.

One of the main objectives of the scenario analysis was to understand how the rising trend in groundwater levels could be halted. As expected, Scenario 4 was most effective in lowering the groundwater levels. However, none of the scenarios was able to reverse the rising trends in groundwater levels. Finally, different limitations of the scenario study are discussed. It was argued that the actual effect of enhanced groundwater use on groundwater levels will be larger than that simulated in this study.

Samenvatting en conclusies

India behoort tot de landen met de grootste geïrrigeerde gebieden. Ongeveer 60% van de landbouwkundige productie komt er van geïrrigeerde velden. Ondanks indrukwekkende vooruitgang in het verleden, moet de geïrrigeerde landbouw in India de komende jaren verschillende nieuwe uitdagingen het hoofd bieden. Dit zijn onder andere afbraak van het milieu door waterverzadiging en verzouting, stijging van voedsel- en waterbehoefte, lage productiviteit, verouderd waterbeheer en ontstaan van waterschaarste. Optimaal beheer van beschikbaar oppervlakte- en grondwater is nodig om de duurzaamheid van geïrrigeerde landbouw te garanderen en om aan de toekomstige vraag te voldoen. Wezenlijke verbetering in waterbeheer en waterproductiviteit van bestaande irrigatieprojecten is vereist. *Om de toekomstige uitdagingen van geïrrigeerde landbouw het hoofd te bieden is het noodzakelijk geschikte locatie-specifieke strategieën voor waterheer te identificeren.*

Goed waterbeheer kan niet worden bereikt zonder begrip van de onderliggende hydrologische processen, hun interactie en effecten van menselijke ingrepen. Nieuwe extrapolatietechnieken zijn nodig om richtlijnen voor regionaal waterbeheer te ontwikkelen, aangezien grootschalige veldexperimenten moeilijk uitvoerbaar zijn. Simulatiemodellen stellen ons in staat het hydrologische systeem te analyseren voor verschillende omstandigheden en op diverse schalen. Succesvolle toepassing van deze modellen vereist de bepaling van de hydraulische parameters die het verloop van de processen in het systeem karakteriseren. Echter, er is een algemeen tekort aan beschikbare bodemfysische gegevensbestanden voor modeltoepassingen in Indiase omstandigheden. Directe meting van bodemfysische parameters is vaak moeilijk, tijdrovend en kostbaar. Daarentegen *is inverse modellering een veelbelovende indirecte methode* om de modelinvoer-parameters te bepalen. In deze techniek runt een zoekprogramma het simulatiemodel met initiële schattingen van de onbekende invoerparameters en vergelijkt de modelresultaten met corresponderende metingen. Vervolgens past het zoekprogramma de invoerparameters aan middels een optimalisatie-algoritme, en runt het simulatiemodel opnieuw. Dit wordt herhaald tot de modelresultaten en metingen zo goed mogelijk overeenstemmen.

De studie is uitgevoerd voor Sirsa Irrigation Circle, een irrigatiegebied in Haryana, India. Het studiegebied beslaat 0,48 miljoen ha, waarvan circa 80% in cultuur is gebracht. Het klimaat is aride, zodat de jaarlijkse evapotranspiratie veel groter is dan de jaarlijkse neerslag. Sirsa Irrigation Circle ontvangt water via een uitgebreid netwerk van irrigatiekanalen, welke onderdeel zijn van het Bhakra irrigatiesysteem. De rivier Ghaggar stroomt door het centrale deel van het studiegebied en voert alleen water in natte perioden. Actuele kwesties met betrekking tot waterbeheer in het studiegebied zijn: stijgende grondwaterstanden in gebieden met slechte grondwaterkwaliteit, dalende grondwaterstanden in gebieden met goede grondwaterkwaliteit, voorkomen van waterverzadiging en bodemverzouting in een aantal gebieden en tekort aan water om alle landbouwgewassen te irrigeren.

Het uiteindelijke doel van deze studie was om bodemfysische parameters vast te stellen voor geselecteerde modellen waarmee verschillende strategieën voor waterbeheer geanalyseerd kunnen worden. Modellen op veld- en regionale schaal werden gebruikt om de toepasbaarheid te testen van de inverse methode voor het afleiden van effectieve bodemfysische parameters. In Hoofdstuk 3 worden de voor dit onderzoek van belang zijnde kenmerken beschreven van het veldschaal model SWAP (Soil Water Atmosphere Plant), het regionale beheersmodel voor irrigatiewater FRAME en het parameter optimalisatie-programma PEST (Parameter ESTimation).

SWAP is een ééndimensionaal agrohydrologisch model die onder andere dagelijkse waarden voor water- en zoutbalanscomponenten produceert. Het model biedt analyse-mogelijkheden voor planning van irrigatiegiften, ontwerp van drainage, beheersing van verzouting, effecten van stress op gewasgroei en uitspoeling van nitraat en pesticiden. In deze studie is SWAP gebruikt om bodemvochtstroming en actuele evapotranspiratiefluxen ET_a te simuleren voor vrij drainerende bodems.

FRAME is een regionaal irrigatiewater-beheersmodel en simuleert waterbeheer van kanalen en veldirrigatie en stroming van grondwater. FRAME biedt een groot aantal mogelijkheden om relevante scenario's te analyseren, zoals verbetering van de efficiëntie van watertoediening, verbetering van de hydraulische condities van het waterverdelingsnetwerk, wijziging van de aangevoerde hoeveelheid water voor een regio, verandering van het waterverdelingsbeleid, grondwatergebruik, gewassenpatroon en hergebruik van irrigatie-

water. In deze studie is FRAME gebruikt om het effect te onderzoeken van gezamenlijk gebruik van kanaal- en grondwater en aanpassing van de hoeveelheid aangevoerd water.

PEST is een programma voor niet-lineaire optimalisatie van parameters, welke relatief eenvoudig kan communiceren met ieder ander model. Het optimalisatie-algoritme van PEST is gebaseerd op de Gauss-Marquardt-Levenberg methode, welke zeer effectief is in zoeken. *In deze studie is PEST gecombineerd met zowel SWAP als FRAME om modelinvoer-parameters te optimaliseren via inverse modellering.*

De optimalisatie van modelparameters voor de schaal van modeltoepassing vereist kennis van het systeemgedrag voor deze schaal. Omdat ET_a fluxen op diverse schalen gemeten kunnen worden via remote sensing met satellieten, is de mogelijkheid onderzocht bodemfysische parameters te bepalen met ET_a fluxen. In Hoofdstuk 4 geven SWAP simulaties aan dat bodems met verschillende bodemfysische parameters bij diepe grondwaterstanden duidelijke verschillen vertonen in het verloop met de tijd van ET_a fluxen. Met verschillende combinaties van Van Genuchten (VG) parameters zijn optimalisaties uitgevoerd om na te gaan welke bodemfysische parameters gelijktijdig geoptimaliseerd kunnen worden. De betrouwbaarheid van de geschatte parameters werd beoordeeld op hun vermogen verschillende waterbalans-componenten te reproduceren.

Analyse van een tijdserie van gesimuleerde ET_a fluxen voor een katoengewas op drie bodems (zand, lemig zand en zavel) liet zien dat ET_a fluxen tijdens een periode met vochtstress het meest geschikt zijn voor inverse modellering. Verder kwam naar voren dat de meetperiode dient samen te vallen met de periode waarin de gewassen volledig ontwikkeld zijn, zodat de geschatte parameters representatief zijn voor de hele wortelzone. De gebruikte methode voor parameter-optimalisatie is getest voor exacte (direct gesimuleerd) en verstoorde (random fout toegevoegd) ET_a fluxmetingen. Onder ideale omstandigheden, dat wil zeggen foutvrije ET_a fluxmetingen, is het mogelijk alle VG modelparameters invers te bepalen als tenminste 30 satellietbeelden gebruikt worden. Bij minder satellietbeelden (12 beelden verdeeld over het groeiseizoen) is het noodzakelijk het aantal te optimaliseren parameters te reduceren. Frequent meten van ET_a fluxen is wenselijk niet alleen om de bodemfysische parameters precies te bepalen, maar ook om correlatie tussen optimalisatie-parameters te verminderen.

Vervolgens is het effect van randomfouten in ET_a fluxmetingen nagegaan om de vereiste nauwkeurigheid van ET_a fluxmetingen vast te stellen. Twee niveau's van random fouten (10 en 20%) werden opgeteld bij exacte ET_a fluxmetingen. Bij ieder niveau werden 10 series van ET_a fluxen gegenereerd, waarbij ieder serie uit 12 beelden bestond. Statistische eigenschappen (bias en betrouwbaarheidsinterval *CI*) van de resulterende waterbalanscomponenten werden berekend om de hydrologische betrouwbaarheid van de gefitte parameters te evalueren. Bij toename van de randomfout in de ET_a fluxen nemen zowel de systematische als de random fout van de gesimuleerde waterbalanscomponenten toe. Drie VG modelparameters (α, n, en θ_{sat}) kunnen gelijktijdig nauwkeurig worden geoptimaliseerd tot maximaal 20% random fout in de ET_a fluxen. Het gebruik van gewichtsfactoren die omgekeerd evenredig zijn met de grootte van de meting levert betere resultaten dan gelijke gewichtsfactoren voor alle metingen.

Ofschoon de resultaten in Hoofdstuk 4 bemoedigend zijn, zijn zij alleen toepasbaar voor homogene bodems, uniforme gewascondities en vrije drainage.

In het algemeen *tonen bodemfysische parameters een grote variatie in zowel de horizontale als verticale richting*. Daarom is het belangrijk om *op het niveau van modeltoepassing representative bodemfysische parameters te bepalen*. De situatie van bodemheterogeniteit langs een 2^e orde kanaal (distributary) is onderzocht in Hoofdstuk 5. Theoretische veldexperimenten werden uitgevoerd voor 7 vrij drainerende heterogene bodemprofielen waarop katoen werd verbouwd. Deze bodempofielen laten een grote variatie in textuuropbouw zien. De bovengronden zijn overwegend zandig, terwijl de textuurklassen van de lagen in de ondergrond variëren van zandig leem tot zandig klei leem. Voor het optimaliseren van de VG parameters werden ET_a fluxen en bodemvochtmetingen gebruikt die door SWAP zelf waren geproduceerd. Eerst werd de inverse methode gebruikt om effectieve bodemfysische parameters te bepalen voor de individuele bodemprofielen. Vervolgens is geprobeerd gebiedseffectieve parameters af te leiden. De methode voor bepaling van effectieve bodemfysische parameters voor heterogene bodemprofielen via inverse modellering bleek minder voor de hand liggend als bij homogen profielen. Indien de bodemverdamping wordt berekend met uitsluitend bodemfysische parameters, resulteerden invers bepaalde bodemfysische parameters voor heterogene bodemprofielen in onacceptabel hoge waarden van bodemverdamping. Dit werd veroorzaakt door het relatief hoge

zandgehalte en afwijkende bodemfysische eigenschappen van de bovenlagen. De invers bepaalde bodemfysische parameters zijn representatief voor het hele bodemprofiel, waardoor de verdampingsreductie door met name het zandgehalte in de bovenlaag niet direct aanwezig is in de invers bepaalde parameters. De optimalisatie-resultaten verbeterden aanzienlijk toen de bodemverdamping werd gesimuleerd met empirische relaties voor verdampingsreductie. Verder bleek dat *ET_a fluxen op zich voldoende zijn om effectieve bodemfysische parameters te bepalen die in staat zijn de waterbalanscomponenten te reproduceren.*

Toepassing van de inverse methode voor het vaststellen van gebiedseffectieve bodemfysische parameters vereist informatie van fluxen op gebiedsschaal. De 7 bodemprofielen vertegenwoordigen een typisch gebied behorend bij een 2^{e} orde irrigatiekanaal in Sirsa Irrigation Circle. Per bodemprofiel werd bepaald welke oppervlakte van het gebied door haar werd vertegenwoordigd. De gesimuleerde ET_a fluxen voor de 7 profielen in combinatie met hun oppervlakten werden vervolgens gebruikt om gebiedsgemiddelde ET_a fluxen af te leiden. Invers bepaalde effectieve bodemfysische parameters reproduceerden seizoensmatige waterbalanscomponenten (***ET_a***, diepe percolatie and verandering van waterberging) binnen 10% van de referentiewaarden. Echter, voor betrouwbare voorspelling van het verloop van de waterbalanscomponenten met de tijd, met name het percolatieverlies, was het noodzakelijk het aantal te optimaliseren parameters te reduceren. Het vastzetten van de VG parameters '*n*' en 'θ_{res}' op grond van textuurinformatie verbeterde aanzienlijk de betrouwbaarheid van de invers bepaalde bodemfysische functies met betrekking tot voorspelling van percolatie-verliezen. De consistentie van de voorspelde waterbalanscomponenten is gecontroleerd door de optimalisatie te herhalen met andere initiële parameters. De resultaten lieten zien dat ET_a fluxen voldoende zijn om gebiedseffectieve bodemfysische parameters af te leiden. Echter, algemene informatie over textuuropbouw in een gebied is noodzakelijk bij het optimaliseren van bodemfysische parameters met ET_a fluxen.

Hoofdstuk 6 beschrijft de calibratie van het regionale beheersmodel voor irrigatiewater FRAME. Het model is toegepast op Sirsa Irrigation Circle. Hiertoe werd het studiegebied verdeeld in 46 rekeneenheden voor de bovenlagen en 61 rekenpunten voor het grondwatersysteem. Een model dient gevalideerd te worden voor het soort toepassing waarvoor het gebruikt gaat worden. *Het uiteindelijke doel van deze studie was om met het model FRAME verschillende scenario's voor waterbeheer te testen op regionale schaal*. ET_a

fluxen en grondwaterstanden h_{gw} (stijghoogten) zijn vooral van belang voor zo'n studie. Gegevens van h_{gw} zijn beschikbaar via historische reeksen van grondwaterstanden in het studiegebied. De gegevens van ET_a fluxen zijn afgeleid van NOAA-AVHRR satellietbeelden met gebruik van het SEBAL algoritme (Surface Energy Balance Algorithm for Land). De gegevens van zowel ET_a fluxen als h_{gw} werden gebruikt om de parameters van het FRAME model te calibreren voor Sirsa Irrigation Circle.

Parameterschattingen met de inverse methode worden nauwkeuriger als de juiste set optimalisatie-parameters wordt gekozen. Een gevoeligheidsanalyse is uitgevoerd om de parameters vast te stellen die een significant effect hebben op ET_a. Vervolgens is een vooranalyse met optimalisatie uitgevoerd om de correlatie tussen gevoelige parameters te bepalen, aangezien correlatie de onnauwkeurigheid van optimalisatieparameters vergroot. Om het aantal parameters dat gelijktijdig geoptimaliseerd wordt te verkleinen, is de calibratie van het model FRAME in twee fasen uitgevoerd. Tijdens de eerste fase van calibratie werden bekende waarden van h_{gw} gebruikt en werden gevoelige bodemfysische parameters geoptimaliseerd met PEST. Tijdens de tweede fase van calibratie werden de optimalisatie-parameters uit fase 1 vastgezet en werden de bergingscoëfficiënten van het watervoerende pakket en de coëfficiënten voor rivierafvoer geoptimaliseerd om goede overeenstemming met de h_{gw} waarden te krijgen.

Voor de eerste fase van calibratie werden de ET_a gegevens van satellietbeelden (ET_{RS}) samengevat in 16 tijdstappen van het model. In eerste instantie werd de optimalisatie uitgevoerd met tijdsafhankelijke ET_{RS} fluxen, wat niet erg succesvol was. Dit werd waarschijnlijk veroorzaakt door tijdsafhankelijke verschillen tussen ET_a en ET_{RS} bij de specificeerde invoer voor gewas en watertoevoer. De eerste fase van de calibratie werd daarom herhaald met cumulatieve $\boldsymbol{ET_{RS}}$ data. *Het gebruik van cumulatieve* $\boldsymbol{ET_{RS}}$ *data bij de optimalisatie resulteerde in betere schattingen van de parameters.* In het algemeen volgden de geoptimaliseerde waarden van beschikbaar vocht (θ_{fc} - θ_{wp}) de textuurinformatie van de rekeneenheden en stemden overeen met gerapporteerde waarden. Echter, bij rekeneenheden waar rijst het belangrijkste gewas is, was de optimalisatie niet succesvol. De rekeneenheden waarvoor de parameteroptimalisatie leidde tot onnauwkeurige schattingen, kregen parameterwaarden toegewezen van rekeneenheden met soortgelijke textuurgegevens.

Simulaties van FRAME voorafgaand aan calibratie met grondwaterstanden lieten zien dat meer grondwater wordt gebruikt, met name langs de Ghaggar rivier, dan gewoonlijk wordt aangehouden voor grondwateronttrekking. Daarom werden de limieten voor grondwater-onttrekking verhoogd in een aantal rekeneenheden vòòr de tweede fase van calibratie. FRAME werd gecalibreerd met grondwaterstanden voor de 5-jarige periode 1977-1981. Deze calibratie was zeer succesvol in 70% van het studiegebied met een correlatiecoëfficiënt tussen gemeten en gesimuleerde grondwaterstanden hoger dan 80%. Vervolgens werden gemeten grondwaterstanden van een 9-jarige periode (1982-1990) gebruikt om het model te valideren. De validatie was het meest succesvol in het noordelijk en zuidelijk deel van het studiegebied waar de grondwaterstanden continue stijgen. In het centrale deel van het studiegebied, langs de Ghaggar rivier, de validatie was minder succesvol door onzekerheden in grondwatergebruik en wegzijging van de rivier. *In het algemeen werd goede overeenstemming verkregen tussen gesimuleerde en geobserveerde trends van grondwater-standen in het studiegebied.*

Hoofdstuk 7 beschrijft scenario-analyses van irrigatiewaterbeheer op regionale schaal. Het gecalibreerde en gevalideerde model FRAME is gebruikt om alternatieve scenario's voor waterbeheer te simuleren voor Sirsa Irrigation Circle. *De scenario-analyse richtte zich op het deel van het studiegebied waar de grondwaterstanden stijgen.* Vier scenario's werden gesimuleerd voor de 14-jarige periode 1977-1990. Scenario 1 vertegenwoordigde de referentiesituatie. In Scenario 2 werd een toename van grondwateronttrekking gesimuleerd. Scenario 3 richtte zich op verminderde wateraanvoer tijdens het regenseizoen. In Scenario 4 werden zowel de toename van grondwateronttrekking als de verminderde wateraanvoer tijdens het regenseizoen opgenomen. De simulatieresultaten van de scenario's met betrekking tot gewasverdamping, bodemverzouting en grondwaterstanden werden vergeleken met de referentiesituatie.

Zoals verwacht nemen in Scenario 2 de ET_a fluxen toe door meer grondwatergebruik. In Scenario 3 nemen de ET_a fluxen af door verminderde aanvoer van kanaalwater. De resultaten van Scenario 4 laten zien dat een reductie van kanaalwater met 25% tijdens het regenseizoen slechts tot een geringe afname van ET_a leidt. Voor verschillende jaren van de simulatieperiode werd het uiteindelijke effect van de scenario's op ET_a vooral bepaald door de hoeveelheid en verdeling van de neerslag. Tijdens jaren met hoge neerslag hadden

toegenomen grondwatergebruik en gereduceerde aanvoer van kanaalwater geen significant effect op ET_a.

Een belangrijke zorg bij toegenomen grondwatergebruik en gereduceerde aanvoer van kanaalwater is de kans op bodemverzouting. In het algemeen leidde het gebruik van meer grondwater tot hogere zoutconcentraties in de bodem (Scenario 2), terwijl reductie van kanaalwater met 25% tijdens het regenseizoen geen significant effect had op de zoutconcentraties in de bodem (Scenario 3). Tijdens de simulatieperiode van 14 jaar viel geen consistente toename van de verzouting waar te nemen. In jaren met relatief meer neerslag zijn duidelijke afnamen in verzouting waarneembaar. Dit toont aan dat *in Sirsa Irrigation Circle ook grondwater van minder goede kwaliteit gebruikt kan worden voor irrigatie zonder drastische zouttoename in de bodem op lange termijn*. Echter, dit geldt zolang de grondwaterstanden diep genoeg zijn.

Een van de belangrijkste doelen van de scenario-analyse was om te begrijpen hoe de stijgende trend van grondwaterstanden kan worden gestopt. Scenario 4 was het meest effectief in het verlagen van de grondwaterstanden. Echter, geen van de scenario's bleek in staat de stijgende trend van grondwaterstanden om te buigen. Verschillende beperkingen van de scenario-analyse zijn aangegeven. Beargumenteerd werd dat het werkelijke effect van toegenomen grondwatergebruik op de grondwaterstanden groter zal zijn dan gesimuleerd door het model.

References

Abdel Gawad, S.T., M.A. Abdel Khalek, D. Boels, D.E. El Quosy, C.W.J. Roest, P.E. Rijtema and M.F.R. Smit. 1990. Analysis of water management in the Eastern Nile Delta. Final report Reuse Model, Reuse of Drainage Water Project, Report 30, Drainage Research Institute, Cairo, Egypt and The Winand Staring Centre for Integrated Land, Soil and Water Research, now Alterra, Wageningen, The Netherlands, 245 p.

Agarwal, M.C. and C.W.J. Roest. 1996. Towards improved water management in Haryana state. Final report of the Indo-Dutch Operational Research Project on Hydrological Studies. Chaudhary Charan Singh Haryana Agricultural University, Hisar, International Institute for Land Reclamation and Improvement, Wageningen, DLO Winand Staring Centre for Integrated Land, Soil and Water Research, now Alterra, Wageningen, The Netherlands, 80 p.

Agarwal, M.C. and R.K. Jhorar. 1997. Natural resource degradation by waterlogging and soil salinisation and remedial measures. Mohenjodaro, 1: 53-57.

Agarwal, M.C. and S.S. Khanna. 1983. Efficient soil and water management in Haryana. Haryana Agricultural University, Hisar, India, 118 p.

Ahuja, L.R., J.W. Naney and D.R. Nielsen. 1984. Scaling soil water properties and infiltration modeling. Soil Sci. Soc. Am. J., 48: 970-973.

Ahuja, R.L., D. Ram, B.S. Panwar, M.S. Kuhad and Jagan Nath. 2001. Soils of Sirsa district (Haryana) and their management. CCS Haryana Agricultural University, Hisar, 81 p.

Allen, R.G., L.S. Pereira, D. Rates and M. Smith. 1998. Crop evapotranspiration. Guidelines for computing crop water requirements. Irrigation and Drainage Paper 56, FAO, Rome, 300 p.

Appelgren, B.G. 1996. A management approach to national water scarcity. In: P. Howsan and R.C. Carter (Eds.), Water Policy: Allocation and Management in Practice. Proc. International Conference on Water Policy, Cranfield University, September 23-24, 1996, pp. 61-67.

Bard, Y. 1974. Nonlinear parameter estimation. Academic Press, Orlando, Florida, 340 p.

Bastiaanssen, W.G.M., C.W.J. Roest, M.A. Abdel Khalek and H. Pelgrum. 1992. Monitoring crop growth in large irrigation schemes on the basis of actual evapotranspiration: comparison of remote sensing algorithm and simulation model results. In: J. Feyen, E. Mwendera and M. Badji (Eds.), Advances in Planning, Design and Management of Irrigation Systems as related to Sustainable Land Use. Proc. Katholieke Universiteit Leuven, Center for Irrigation Engineering, September 14-17, 1992, Volume 2: 473-483

Bastiaanssen, W.G.M., R. Singh, S. Kumar, J.K. Schakel and R.K. Jhorar. 1996. Analysis and recommendations for integrated on-farm water management in Haryana, India: a model approach. Report 118, DLO Winand Staring Centre for Integrated Land, Soil and Water Research, now Alterra, Wageningen, The Netherlands, 152 p.

Bastiaanssen, W.G.M., M. Menenti, R.A. Feddes and A.A.M. Holtslag. 1998. A remote sensing surface energy balance algorithm for land (SEBAL) 1. Formulation. J. Hydrol., 212-213: 198-212

Bastiaanssen, W.G.M., R. Sakthivadivel and A. van Dellen. 1999. Spatially delineating actual and relative evapotranspiration from remote sensing to assist spatial modelling of non-point source pollutants. In: D.L. Corwin, K. Loague and T.R. Ellsworth (Eds.), Assessment of Non-Point Source Pollution in the Vadoze Zone. Geophysical Monograph 108, American Geophysical Union, Washington DC., pp. 179-196.

Batjes, N.H. 1996. Development of a world data set of soil water retention properties using pedotransfer rules. Geoderma, 71: 31-52.

Belmans, C., J.G. Wessling and R.A. Feddes. 1983. Simulation of the water balance of a cropped soil: SWATRE. J. Hydrol., 63: 271-286.

Binley, A., J. Elgy and K. Beven. 1989. A physically based model of heterogeneous hillslopes 1. Runoff production. Water Resour. Res., 25: 1219-1226.

Black, T.A., W.R. Gardner and G.W. Thurtell. 1969. The prediction of evaporation, drainage and soil water storage for a bare soil. Soil Sci. Soc. Am. J., 33: 655-660.

Boels, D., M. Abdel Khalek, C.W.J. Roest and M.F.R. Smit. 1989. Simulation of water management in Arab Republic of Egypt: Reuse of drainage water model, Reuse report 25. Drainage Research Institute, Cairo, Egypt and DLO Winand Staring Centre for Integrated Land, Soil and Water Research, now Alterra, Wageningen, The Netherlands, 52 p.

Boels, D., A.A.M.F.R. Smit, R.K. Jhorar, R. Kumar and J. Singh. 1996. Analysis of water management in Sirsa District in Haryana: model testing and application. Report 115. DLO Winand Staring Centre for Integrated Land, Soil and Water Research, now Alterra, Wageningen, The Netherlands, 50 p.

Boesten, J.J.T.I. and L. Stroosnijder. 1986. Simple model for daily evaporation from fallow tilled soil under spring conditions in a temperate climate. Neth. J. Agric. Sci., 34: 75-90.

Boonstra, J. and N.A. De Ridder. 1990. Numerical modelling of groundwater basins (2nd Ed.). Publication 29, International Institute for Land Reclamation and Improvement, Wageningen, The Netherlands, 226 p.

Boonstra, J., J. Singh and R. Kumar. 1996. Groundwater model study for Sirsa district, Haryana. International Institute for Land Reclamation and Improvement, Wageningen, The Netherlands, 87 p.

Boyle, D.P., H.V. Gupta and S. Sosooshian. 2000. Towards improved calibration of hydrologic models: combining the strengths of manual and automatic methods. Water Resour. Res., 36: 3663-3674.

Braun, H.M.H. and R. Kruijne. 1994. Soil conditions. In: Ritzema, H.P. (Ed.), Drainage Principles and Applications. ILRI Publication 16, International Institute for Land Reclamation and Improvement, Wageningen, The Netherlands, pp. 77-110.

Burke, E.J., R.J. Gurney, L.P. Simmonds and T.J. Jackson. 1997. Calibrating a soil water and energy budget model with remotely sensed data to obtain quantitative information about the soil. Water Resour. Res., 33: 1689-1697.

Burke, E.J., R.J. Gurney, L.P. Simmonds and P.E. O'Neill. 1998. Using a modeling approach to predict soil hydraulic properties from passive microwave measurements. IEEE Trans. Geosci. Remote Sens., 36: 454-462.

Carsel, R.F. and R.S. Parrish. 1988. Developing joint probability distributions of soil water characteristics. Water Resour. Res., 24: 755-769.

Chadha, D.K. 1983. Geology. Studies for the use of saline water in command areas of irrigation projects. Haryana State Minor Irrigation and Tubewells Corporation, Chandigarh, India, 39 p.

Chaudhary, T.N. 1997. Vision- 2020, DWMR Perspective Plan. Directorate of Water Management Research, Patna, India, 73 p.

Chowdhury, J.B. 1998. Management of waterlogging and salinity problems in Haryana, Master Plan, Government of Haryana, India, 106 p.

Clapp, R.B. and G.M. Hornberger. 1978. Empirical equations for some soil hydraulic properties. Water Resour. Res., 14: 601-604.

Clausnitzer, V. and J.W. Hopmans. 1995. LM-OPT: General purpose optimization code based on the Levenberg-Marquardt algorithm. LAW Resources Paper 100032, Hydrol. Science, Dept. LAW, US Davis, California, 16 p.

Clausnitzer, V., J.W. Hopmans and D.R. Nielsen. 1992. Simultaneous scaling of soil water retention and hydraulic conductivity curves. Water Resour. Res., 28: 19-31.

Cosby, B.J., G.M. Hornberger, R.B. Clapp and T.R. Ginn. 1984. A statistical exploration of the relationships of soil moisture characteristics to the physical properties of soil. Water Resour. Res., 20: 682-690.

Cooley, R.L. 1985. A comparison of several methods of solving nonlinear regression groundwater flow problems. Water Resour. Res., 21: 1525-1538.

Dhindwal, A.S. and V. Kumar, 2000. Water resources in Haryana. In: V. Kumar, A.S. Dhindwal, M.S. Kuhad and B.C. Sethi (Eds.), Efficient Management of Irrigation Water in Haryana. CCS Haryana Agricultural University, Hisar, India, pp. 7-15.

Dirksen, C. 1991. Unsaturated hydraulic conductivity. In: K.A. Smith and C.E. Mullins (Eds.), Soil Analysis: Physical Methods. Marcel Dekker, New York, pp. 209-269.

Doherty, J., Brebber, L. and P. Whyte. 1995. PEST. Model independent parameter estimation. Australian Centre for Tropical Freshwater Res., James Cooke University, Townsville, Australia, 140 p.

Doorenbos, J. and A.H. Kassam. 1979. Yield response to water. Irrigation and Drainage Paper 33, FAO, Rome, Italy, 193 p.

Doorenbos, J. and W.O. Pruitt. 1977. Guidelines for predicting crop water requirements. Irrigation and Drainage Paper 24, FAO, Rome, Italy, 144 p.

Droogers, P. and G. Kite. 1999. Water productivity from integrated basin modeling. Irrigation and Drainage Systems, 13: 275-290.

Droogers, P., W.G.M. Bastiaanssen, M. Beyazgul, Y. Kayam, G.W. Kite and H. Murray-Rust. 2000. Distributed agro-hydrological modeling of an irrigation system in western Turkey. Agric. Water Manage., 43: 183-202.

D'Urso, G., M. Menenti and A. Santini. 1999. Regional application of one-dimensional water flow models for irrigation management. Agric. Water Manage., 40: 291-302.

Eckhardt, K. and J.G. Arnold. 2001. Automatic calibration of a distributed catchment model. J. Hydrol., 251: 103-109.

Feddes, R.A., P.J. Kowalik and H. Zarandy. 1978. Simulation of field water use and crop yield. Simulation Monographs, Pudoc, Wageningen, 189 p.

Feddes, R.A., M. Menenti, P. Kabat and W.G.M. Bastiaanssen. 1993a. Is large-scale inverse modelling of unsaturated flow with areal evaporation and surface soil moisture as estimated from remote sensing feasible? J. Hydrol., 143: 125-152.

Feddes, R.A., G.H. de Rooij, J.C. van Dam, P. Kabat, P. Droogers and J.N.M. Stricker. 1993b. Estimation of regional effective soil hydraulic parameters by inverse modeling. In: D. Russo and G. Dagan (Eds.), Water Flow and Solute Transport in Soils, Advanced Series in Agricult. Sciences, 20, Springer Verlag, Berlin, pp. 211-233.

Feyen, J., D. Jacques, A. Timmerman and J. Vanderborgt. 1998. Modelling water flow and solute transport in heterogeneous soils: a review of recent approaches. J. Agric. Eng. Res., 70: 231-256.

Finsterle, S. and K. Pruess. 1995. Solving the estimation-identification problem in two-phase modeling. Water Resour. Res., 31: 913-924.

Franks, S., Ph. Gineste, K.J. Beven and Ph. Merot. 1998. On constraining the predictions of a distributed model: the incorporation of fuzzy estimates of saturated areas into the calibration process. Water Resour. Res., 34: 787-797.

Gribb, M.M. 1996. Parameter estimation for determining hydraulic properties of a fine sand from transient flow measurements. Water Resour. Res., 32: 1965-1974.

Griensven, A. van and W. Bauwens. 2001. Identification of distributed parameters in hydrologic models. Book of Abstracts, International Workshop on Catchment scale Hydrologic Modeling and Data Assimilation, Wageningen, The Netherlands, pp. 74-76.

Gupta, M.L. 1983. Groundwater conditions. Studies for the use of saline water in the command areas of irrigation projects, Haryana. Haryana State Minor Irrigation and Tubewells Corporation, Chandigarh, India, 98 p.

Gupta, H.V., S. Sorooshian and P.O. Yapo. 1998. Towards improved calibration of hydrologic models: multiple and noncommensurable measures of information. Water Resour. Res., 34: 751-763.

Hanson, J.D., K.W. Rojas and M.J. Shaffer. 1999. Calibrating the root zone water quality model. Agron. J., 91: 171-177.

Hollenbeck, K.J. and K.H. Jensen. 1998. Experimental evidence of randomness and nonuniqueness in unsaturated outflow experiments designed for hydraulic parameter estimation. Water Resour. Res., 34: 595-602.

Holman-Dodds, J. K., A. A. Bradley and P. L. Sturdevant-Rees. 1999. Effect of temporal sampling of precipitation on hydrologic model calibration. J. Geophy. Res., 104(D16): 19645-19654

Hopmans, J.H. and J. Simunek. 1999. Review of inverse estimation of soil hydraulic properties. In: M.Th. van Genuchten, F.J. Leij and L. Wu (Eds.), Characterization and Measurement of the Hydraulic Properties of Unsaturated Porous Media. University of California, Riverside, CA., pp. 643-659.

Isaaks, E.H. and R.M. Srivastava. 1989. An Introduction to Applied Geostatistics. Oxford University Press, New York, 561 p.

Israelsen, O.W. (1950). Irrigation Principles and Practices. 2nd Edition. John Wiley & Sons, Inc., New York, 160 p.

IWMI. 2000. Water issues for 2025: A research perspective. Research contribution to the World Water Vision. International Water Management Institute, Colombo, Sri Lanka.

Jensen, M.E. 1996. Irrigated agriculture at the crossroads. In: L.S. Pereira, R.A. Feddes, J.R. Gilley and B. Lesaffre (Eds.), Sustainability of Irrigated Agriculture. Kluwer Academic Publishers, The Netherlands, pp. 19-33.

Jhorar, R.K., W.G.M. Bastiaanssen, R.A. Feddes and J.C. van Dam. 2002. Inversely estimating soil hydraulic functions using evapotranspiration fluxes. J. Hydrol., 258: 198-213.

Kabat, P., R.W.A. Hutjes and R.A. Feddes. 1997. The scaling characteristics of soil parameters: from plot scale heterogeneity to subgrid parameterization. J. Hydrol., 190: 363-396.

Kim, C.P., J.N.M. Stricker and R.A. Feddes. 1997. Impact of soil heterogeneity on the water budget of unsaturated zone. Water Resour. Res., 33: 991-999.

Kool, J.B. and J.C. Parker. 1988. Analysis of the inverse problem for transient unsaturated flow. Water Resour. Res., 24: 817-830.

Kool, J.B., J.C. Parker and M.T. van Genuchten. 1987. Parameter estimation for unsaturated flow and transport models- a review. J. Hydrol., 91: 255-293.

Kumar, R. and J. Singh. 1994. Report advance training on integrated regional water management model: Sirsa irrigation circle. Indo-Dutch Project on Hydrological Studies, CCS Haryana Agricultural University, Hisar, India, 77 p.

Kumar, S., R.K. Jhorar and M.C. Agarwal. 1996. Reuse of saline irrigation water for cereal crops. Research Bulletin, Department of Soil Sciences, CCS Haryana Agricultural University, Hisar, India, 96 p.

Kustas, W.P., E.M. Perry, P.C. Doraiswamy and M.S. Moran. 1994. Using satellite remote sensing to extrapolate evapotranspiration estimates in time and space over a semiarid rangeland basin. Remote Sens. Environ., 49: 275-286.

Leij, F.J., W.J. Alves, M.T. van Genuchten and J.R. William. 1996. The UNSODA unsaturated soil hydraulic database. User's manual version 1.0. U.S. Salinity Laboratory, Riverside, California, 103 p.

Li, W., B. Li, Y. Shi, D. Jacques and J. Feyen. 2001. Effect of spatial variation of textural layers on regional field water balance. Water Resour. Res., 37: 1209-1219.

Manchanda, H.R. 1998. Management of saline irrigation. In: P.S. Minhas and N.K. Tyagi (Eds.), Agricultural Salinity Management in India, Central Soil Salinity Research Institute, Karnal, India, pp. 407-429.

Marquardt, D.W. 1963. An algorithm for least squares estimation of nonlinear parameters. J. Soc. Ind. Appl. Math., 11: 431-441.

Menenti, M., Azzali, S. and G. d'Urso. 1996. Remote sensing, GIS and hydrological modelling for irrigation management. In: L.S. Pereira, R.A. Feddes, J.R. Gilley and B. Lesaffre (Eds.), Sustainability of Irrigated Agriculture. Kluwer Academic Publishers, The Netherlands, pp. 453-472.

Minhas, P.S. and R.K. Gupta. 1992. Quality of irrigation water, assessment and management. Indian Council of Agricultural Research, New Delhi, 123 p.

Miller, R.W. and R.L. Donahue. 1990. Soils: an Introduction to Soil and Plant Growth. 6th edition. Prentice-Hall International Inc., 768 p.

Molden, D. 1997. Accounting for water use and productivity. SWIM Paper 1. International Water Management Institute, Colombo, Sri Lanka, 16 p.

Moran, M.S. and R.D. Jackson. 1991. Assessing the spatial distribution of evapotranspiration using remotely sensed inputs. J. Environmental Quality, 20: 725-737.

Navalawala, B.N. 1995. Water scenario in India. Yojana, October: 5-11.

Navalawala, B.N. 1999a. Improving management of irrigation resources. Yojana, January: 81-87.

Navalawala, B.N. 1999b. Water resources development and management. Yojana, July: 4-9, 28.

Olsthoorn, T.N. 1998. Groundwater modelling: calibration and the use of spreadsheets. PhD-thesis, Delft University, The Netherlands, 114 p.

Polubarinova-Kochina, P. YA. 1962. Theory of groundwater movement. Princeton University Press, Princeton, New Jersey, USA, 613 p.

Press, W.H., B.P. Flannery, S.A. Teukolsky and W.T. Vetterling, 1989. Numerical recipes in Fortran, the art of scientific computing. Cambridge University Press, 759 p.

Quintard, M. and S. Whitaker. 1988. Two phase flow in heterogeneous porous media: the method of large scale averaging. Transport Porous Media, 3: 357-413.

Raats, P.A.C. 1990. Characteristic lengths and times associated with processes in the rootzone. In: D. Hillel and D.E. Elrick (Eds.), Scaling in Soil Physics, Principles and Applications. SSA Special Publication No. 25, SSSA, Madison, WI, pp. 59-72.

Refsgaard, J.C. 1997. Parameterisation, calibration and validation of distributed hydrological models. J. Hydrol., 198: 69-97.

Reynolds, C.A., T.J. Jackson and W.J. Rawls. 2000. Estimating soil water holding capacities by linking the Food and Agriculture Organization soil map of the world with global pedon database and continuous pedotransfer functions. Water Resour. Res., 36: 3653-3662.

Rhoades, J.D., A. Kandiah and A.M. Mashali. 1992. The use of saline waters for crop production. FAO Irrigation & Drainage Paper 48, FAO, Rome, Italy, 133 p.

Richtmeyer, R.D. and K.W. Morton. 1967. Difference methods for initial-value problems. John Wiley& Sons, New York, 291 p.

Rijtema, P.E. and A. Abou Khaled. 1975. Crop water use. In: A. Aboukhaled, A. Arar, A.M. Balba, B.G. Bishay, L.T. Kadry, P.E. Rijtema and A. Taher (Eds.), Research on Crop water Use, Salt Affected Soils and Drainage in the Arabic Republic of Egypt. FAO Near East Regional Office, Cairo, pp. 5-61.

Roest, C.W.J., P.E. Rijtema, H.A. Abdel Khalek, D. Boels, S.T. Abdel Gawad and D.E. El Quosy. 1993. Formulation of the on-farm water management model FAIDS. Reuse Report 24, The Winand Staring Centre for Integrated Land, Soil and Water Research, now Alterra, Wageningen, The Netherlands, 118 p.

Romano, N. and A. Santini. 1999. Determining soil hydraulic functions from evaporation experiments by a parameter estimation approach: experimental verification and numerical studies. Water Resour. Res., 35: 3343-3359.

Rosema, A. 1990. Comparison of METEOSAT-based rainfall and evapotranspiration mapping in the Sahel region. Int. J. Remote Sens., 11: 2299-2309.

Russo, D. 1988. Determining soil hydraulic properties by parameter estimation: on the selection of a model for the hydraulic properties. Water Resour. Res., 24: 453-459.

Sakthivadivel, R., S. Thiruvegadachari, U. Amerasinghe, W.G.M. Bastiaanssen and D. Molden. 1999. Performance evaluation of Bhakra Irrigation system, India, using remote sensing and GIS techniques. Research Report 28. International Water Management Institute, Colombo, Sri Lanka, 22 p.

Saxton, K.E., W.J. Rawl, J.S. Romberger and R.I. Papendrick. 1986. Estimating generalized soil-water characteristics from texture. Soil Sci. Soc. Am. J., 50: 1031-1036.

Schaap, M.G. and F.J. Leij. 2000. Improved prediction of unsaturated hydraulic conductivity with Mualem-van Genuchten model. Soil Sci. Soc. Am. J., 64: 843-851.

Schmugge, T.J., T.J. Jackson, W.P. Kustas and J.R. Wang. 1992. Passive microwave remote sensing of soil moisture: Results from HAPEX, FIFE and MONSOON'90. ISPRS J. Photogram. Remote Sens., 47: 127-143.

Sijtsma, B.R., D. Boels, T.N.M. Visser, C.W.J. Roest and A.A.M.F.R. Smit. 1995. SIWARE user's manual. Reuse Report 27, The Winand Staring Centre for Integrated Land, Soil and Water Research, now Alterra, Wageningen, The Netherlands, 158 p.

Singh, J. 2000a. Groundwater status of Haryana. In: A.S. Dhindwal, M.S. Kuhad, V. Kumar and L.S. Suhag (Eds.), Management of Waterlogging Problems in Haryana. CCS Haryana Agricultural University, Hisar, India, pp. 1-13.

Singh, P. 2000b. Methods of irrigation in different crops. In: V. Kumar, A.S. Dhindwal, M.S. Kuhad and B.C. Sethi (Eds.), Efficient Management of Irrigation Water in Haryana. CCS Haryana Agricultural University, Hisar, India, pp. 41-54..

Smith, R.E. and B. Diekkrüger. 1996. Effective soil water characteristics and ensemble soil water profile in heterogeneous soils. Water Resour. Res., 32: 1993-2002.

Snow, V.O. and W.J. Bond. 1998. Inverse method to estimate mineralisation rate constants for nitrogen simulation models: interaction between sampling strategy and quality of parameter estimates. Aust. J. Soil Res., 36: 1-15.

Sood, S.K. 1969. A study of moisture retention characteristics of some soils irrigated by Bhakra canal. M.Sc. Thesis, Punjab Agricultural University, Hisar, India, 83 p.

Sorooshian, S. and F. Arfi. 1982. Response surface parameter sensitivity analysis methods for postcalibration studies. Water Resour. Res., 18: 1531-1538.

Stam, J.M.T., W. Zijl and A.K. Turner. 1989. Determination of hydraulic parameters from the reconstruction of alluvial stratigraphy. 4th International Conference on Computational Methods and Experiments, Capri, May 23-26, 1989.

Stewart, J.B., E.T. Engman, R.A. Feddes and Y. Kerr (Eds.). 1996. Scaling up in Hydrology using Remote Sensing, John Wiley and Sons, England, see Preface.

Tan, C.H. and S.F. Shih. 1997. Using NOAA satellite thermal infrared data for evapotranspiration estimation in South Florida. Soil Crop Sci. Soc. Florida Proc., 56: 109-113.

Taylor, S.A. and G.M. Aschroft. 1972. Physical Edaphology. Freeman and Co., San Franscisco, California, pp. 434-435.

Tyagi, N.K. 1996. Salinity management in irrigated agriculture. In: L.S. Pereira, R.A. Feddes, J.R. Gilley and B. Lesaffre (Eds.), Sustainability of Irrigated Agriculture. Kluwer Academic Publishers, The Netherlands, pp. 345-358.

Tyagi, N.K., S.K. Kamra, P.S. Minhas and N.T. Singh (Eds.). 1993. Irrigation in Saline Environment: Key Management Issues. Proc. Scientific Meeting-cum-Workshop on Sustainable Irrigation in Saline Environment, Karnal, India, February 17-19, 1993, 120 p.

Tyagi, N.K. and D.L.N. Rao. 1998. A perspective on research needs. In: P.S. Minhas and N.K. Tyagi (Eds.), Agricultural Salinity Management in India. Central Soil Salinity Research Institute, Karnal, India, pp. 509-519.

Van Dam, J.C. 2000. Field-scale water flow and solute transport: SWAP model concepts, parameter estimation and case studies. Ph.D. Thesis, Wageningen University, The Netherlands, 167 p.

Van Dam, J.C. and R.A. Feddes. 1996. Modeling of water flow and solute transport for irrigation and drainage. In: L.S. Pereira, R.A. Feddes, J.R. Gilley and B. Lesaffre (Eds.), Sustainability of Irrigated Agriculture. Kluwer Academic Publishers, The Netherlands, pp. 211-231.

Van Dam, J.C. and R.A. Feddes. 2000. Numerical simulation of infiltration, evaporation and shallow groundwater levels with the Richards'equation. J. Hydrol., 233: 72-85.

Van Dam, J.C., J.N.M. Stricker and P. Droogers. 1994. Inverse method to determine soil hydraulic functions from multi-step outflow experiments. Soil Sci. Am. J., 58: 647-652.

Van Dam, J.C., J. Huygen, J.G. Wesseling, R.A. Feddes, P. Kabat, P.E.V. van Walsum, P. Groenendijk and C.A. Diepen. 1997. Theory of SWAP version 2.0. Department of Water Resour., Report 71, Wageningen Agricultural University, Wageningen, The Netherlands, 167 p.

Van Genuchten, M.T.. 1980. A closed form equation for predicting the hydraulic conductivity of unsaturated soils. Soil Sci. Soc. Am. J., 44: 892-898.

Van Genuchten, M.T. and F.J. Leij. 1992. On estimating the hydraulic properties of unsaturated soils. In M.Th. van Genuchten, F.J. Leij and L.J. Lund (Eds.), Indirect Methods for Estimating Hydraulic Properties of Unsaturated Soils. Proc. Int. Workshop on Indirect Methods for Estimating Hydraulic Properties of Soils, Riverside, California, October 11-13, 1989, pp. 1-14.

Wagner, B.J. and S.M. Gorelick. 1986. A statistical methodology for estimating transport parameters: Theory and applications to one-dimensional advective-dispersive systems. Water Resour. Res., 22: 1303-1315.

Wahaj, R. 2001. Farmers actions and improvements in irrigation performance below the *Mogha*: How farmers manage water scarcity and abundance in a large scale irrigation system in South-Eastern Punjab, Pakistan. Ph.D. Thesis, Wageningen University, The Netherlands, 218 p.

Wallach, D., B. Goffinet, J.-E. Bergez, P. Debaeke, D. Leenhardt and J.-N. Aubertot. 2001. Parameter estimation for crop models, a new approach and application to a corn model. Agron. J., 93: 757-766.

Weiss, R. and L. Smith. 1998. Parameter space methods in joint parameter estimation for groundwater flow models. Water Resour. Res., 34: 647-661.

Wessolek, G., R. Plagge, F.J. Leij and M.Th. van Genuchten. 1994. Analysing problems in describing field and laboratory measured soil hydraulic properties. Geoderma, 64: 93-110.

Wildenschild, D. and K.H. Jensen. 1999. Numerical modelling of observed effective flow behaviour in unsaturated heterogeneous sands. Water Resour. Res., 35: 29-42.

Willardson, L.S., D. Boels and L.K. Smedema. 1997. Reuse of drainage water from irrigated area. Irrigation and Drainage Systems, 11: 215-239.

Wösten, J.H.M. and M.Th. van Genuchten. 1988. Using texture and other soil properties to predict the unsaturated soil hydraulic conductivity. Soil Sci. Soc. Am. J., 52: 1762-1770.

Wösten, J.H.M., P.A. Finke and M.J.W. Jansen. 1995. Comparison of class and continuous pedotransfer functions to generate soil hydraulic characteristic. Geoderma, 66: 227-237.

Wösten, J.H.M., A. Lilly and C.Le Bas. 1999. Development and use of a database of hydraulic properties of European soils. Geoderma, 90: 169-185.

Xevi, E., J. Gilley and J. Feyen. 1996. Comparative study of two crop yield simulation models. Agric. Water Manage., 30: 155-173.

Yadav, J.S.P. 1998. Sustainability issues associated with irrigation management. Souvenir, National Seminar on Water Management for Sustainable Agriculture- Problems and Perspectives for the 21st Century, April 15-17, 1998, IARI New Delhi, pp. 1-6.

Yan, J. and C.T. Han. 1991. Multiobjective parameter estimation for hydrologic models- weighting of errors. Trans. ASAE, 34: 135-141.

Yeh, W.W.G. and Y.S. Soon. 1981. Aquifer parameter identification with optimum dimension in parameterization. Water Resour. Res., 17: 664-672.

List of Symbols

The list of symbols is given in to two parts. Part I contains the main symbols used in the thesis. Part II contains symbols which are referred only to describe the model FRAME (Chapter 3)

I. List of main symbols

Symbol	Description	Dimension
B	Bias	L
$\boldsymbol{b}$	Vector containing parameters to be optimised	-
C	Differential soil water capacity	L^{-1}
CI	Confidence Interval	L
CV	Coefficient of Variation	-
D_{root}	Depth of the root zone	L
$\boldsymbol{E}[x_k]$	Expected value of water balance component x_k using inversely identified parameters	L
E_a	Actual soil evaporation rate	$L\ T^{-1}$
$\boldsymbol{E_a}$	Cumulative actual soil evaporation	L
E_{emp}	Soil evaporation rate according to an empirical function	$L\ T^{-1}$
E_{max}	Maximum soil evaporation rate according to Darcy's law	$L\ T^{-1}$
E_p	Potential soil evaporation rate	$L\ T^{-1}$
EC	Electrical conductivity of soil water	$L^3\ M^{-1}\ T^3\ I^2$
EC_{gw}	Electrical conductivity of groundwater	$L^3\ M^{-1}\ T^3\ I^2$
ET_a	Actual evapotranspiration rate	$L\ T^{-1}$
$\boldsymbol{ET_a}$	Cumulative actual evapotranspiration	L
ET_{ae}	Actual evapotranspiration rate incorporated with random error	$L\ T^{-1}$
ET_p	Potential evapotranspiration rate	$L\ T^{-1}$
ET_{RS}	Actual evapotranspiration rate as estimated from Remote Sensing	$L\ T^{-1}$
ET_{SIWARE}	Actual evapotranspiration rate as estimated by FRAME	$L\ T^{-1}$
F_i	Fraction of total area belonging to sub area i	-
h	Soil water pressure head	L
h_1	Pressure head below which roots start to extract water from the soil	L
h_2	Pressure head below which roots start to extract water optimally from the soil	L
h_{3h}	Pressure head below which roots cannot extract water optimally any more, at a high potential transpiration rate	L

Symbol	Description	Dimension
h_{3l}	Pressure head below which roots cannot extract water optimally any more, at a low potential transpiration rate	L
h_4	Pressure head below which no water uptake by roots is possible ('wilting point')	L
$\boldsymbol{I}$	Cumulative irrigation	L
k	Unsaturated soil hydraulic conductivity	L T^{-1}
k_{sat}	Saturated soil hydraulic conductivity of the unsaturated zone	L T^{-1}
LAI	Leaf Area Index	-
m	Empirical parameter in the Van-Genuchten model	-
n	Empirical parameter in the Van-Genuchten model	-
$n_{0,1}$	Random number with a mean of 0 and a variance of 1	-
n_{rr}	Number of random realizations	-
$\boldsymbol{P}$	Cumulative Precipitation /Rainfall	L
p	Relative error	-
$\boldsymbol{Q}_{deep}$	Cumulative deep percolation	L
q	Soil water flux density according to Darcy's equation	L T^{-1}
S_a	Actual soil water extraction rate by plant roots	T^{-1}
S_e	Relative saturation	-
S_p	Potential soil water extraction rate by plant roots	T^{-1}
S_y	Specific yield or drainable porosity of aquifer	-
SC	Soil cover fraction	-
sd	Standard deviation	L
T_a	Actual transpiration rate	L T^{-1}
$\boldsymbol{T_a}$	Cumulative actual transpiration	L
T_p	Potential transpiration rate	L T^{-1}
t	Time	T
v_i	Weighting function to account for the relative influence of each data point on the objective function	-
W	Water stored in soil profile	L
W_{rz}	Water stored in root zone	L
w_i	Weighting function to account for the relative influence of each evapotranspiration data point on the objective function	-
x	Horizontal coordinate	L
y	Spatial coordinate	L
z	Vertical coordinate	L

Symbol	Description	Dimension
Φ	Objective function	-
α	Empirical parameter in the Van-Genuchten model	L^{-1}
α_w	Reduction factor for water stress as used in SWAP	-
ϕ	Total porosity	-
λ	Empirical parameter in the Van-Genuchten model	-
θ	Volumetric soil water content	-
θ_{fc}	Volumetric water content at field capacity	-
θ_{res}	Residual volumetric water content	-
θ_{sat}	Saturated volumetric water content	-
θ_{wp}	Volumetric water content at wilting point	-
ρ_{scal}	Scale factor of similar media method	-

II. List of main symbols used in the model FRAME

Symbol	Description	Dimension
A_{Wi}	Wetted area per unit length of canal section *i*	L
A_{CCA}	Culturable Command Area	L^2
$A_{CCA,MCi}$	Culturable Command Area of Main Canal *i*	L^2
c	Solute concentration on volume basis	$M\ L^{-3}$
c_{in}	Solute concentration of incoming flux to a particular soil layer	$M\ L^{-3}$
c_{out}	Solute concentration of outgoing flux from a particular soil layer	$M\ L^{-3}$
d_i	Depth of water infiltrated along plot length during surface irrigation	L
d_{gw}	Depth of groundwater below soil surface	L
f_{in}	Incoming water flux to a soil layer	LT^{-1}
f_{out}	Outgoing water flux from a soil layer	LT^{-1}
$fp_{,CRi}$	Farmers' irrigation preference score value for crop *i*	-
H	Saturated thickness of aquifer	L
h	Hydraulic head in aquifer	L

Symbol	Description	Dimension
h_{gw}	Groundwater head in nodes of SGMP model	L
I_b	Basic infiltration rate	L T^{-1}
I_n	Net depth of irrigation per event	L
K	Saturated hydraulic conductivity of aquifer	L T^{-1}
$\boldsymbol{L}_{CU}$	Net leakage losses from a calculation unit	L
$\boldsymbol{L}_F$	Leakage losses from hypothetical shallow groundwater to the actual groundwater	L
$\boldsymbol{L}_{IC,CUi}$	Leakage losses from Internal Canal in Calculation Unit *i*	L
$\boldsymbol{L}_{MCi}$	Leakage losses from Main Canal *i*	L
L_{net}	Net recharge rate	L T^{-1}
$\boldsymbol{L}_{node}$	Leakage losses to a node	L
$\boldsymbol{L}_{Pi}$	Leakage losses from field Plot *i* during surface irrigation	L
$\boldsymbol{L}_{WCi}$	Leakage losses from Water Course *i*	L
M_d	Soil moisture deficit	L
N	Sink term in groundwater flow equation	L T^{-1}
$\boldsymbol{Q}$	Total water supply from canals, river and tubewells	L^3
$\boldsymbol{Q}_{CW}$	Available water supply from Canals and river	L^3
$\boldsymbol{Q}_{CW,CUi}$	Water supply allocated to Calculation Unit *i*	L^3
$\boldsymbol{Q}_{CW,MCi}$	Water supply allocated to Main Canal *i*	L^3
$\boldsymbol{Q}_{CRi}$	Water supply allocated to crop *I*	L^3
$\boldsymbol{Q}_{Fi}$	Water supply reaching field *I*	L^3
$\boldsymbol{Q}_{TW}$	Groundwater (TubeWells) extraction	L^3
$\boldsymbol{Q}_{TW,max}$	TubeWell installed capacity	L^3
q_0	On-farm stream discharge	L^3 T^{-1}
q_s	Leakage loss rate from water courses	L^3 T^{-1}
R_{cc}	Resistance against vertical flow	T
R_{pud}	Resistance of puddled soil layer for rice fields	T
R_r	Radial resistance to compute leakage losses from canals	T
S_y	Specific yield or drainable porosity of aquifer	-
s	Slope of the field plot	-
t_n	Net irrigation time	T
$\boldsymbol{WD}_{CRi}$	Deficit in water supply for crop *i* for a certain period	L^3
$\boldsymbol{WR}_{CRi}$	Water requirement for crop *i* for a certain period	L^3

Symbol	Description	Dimension
X_{pl}	Plot Length	L
X_{pw}	Plot width	L
X_{sl}	Canal section length	L
x_c	Critical distance at which infiltrated depth equals moisture deficit	L
y_i	Depth of flow in canal section *I*	L
Z_{cz}	Thickness of capillary zone	L
z_i	Thickness of soil layer *I*	L
α_{sm}	Reduction factor for water and salinity stress as used in FRAME	-
β	Fraction used to define readily available soil moisture	-
η_{man}	Manning's roughness coefficient	$L^{-1/3}$ T
θ	Volumetric water content	-
θ_{ASM}	Actual available Soil Moisture	L
θ_{fc}	Volumetric water content at field capacity	-
θ_{TAM}	Total Available soil Moisture	L
θ_{wp}	Volumetric water content at wilting point	-

Curriculum vitae

Raj Kumar Jhorar was born on January 4, 1965 in the village Saliwala in Rajasthan, India. After finalising his high school in 1982, he studied the Bachelor of Engineering program of Agricultural Engineering at the College of Technology and Agricultural Engineering, Udaipur in Rajasthan, India. He passed out his graduation in 1987. Thereafter he studied the Master of Technology in Agricultural Engineering with specialisation in Soil and Water Conservation Engineering at the Indian Institute of Technology, Kharagpur in West Bengal, India. Since 1992 he works as Assistant Professor in Soil and Water Engineering at Chaudhary Charan Singh Haryana Agricultural University, Hisar, India.